NOVEL SUPERACIDIC IONIC LIQUID CATALYSTS FOR ARENE FUNCTIONALIZATION

A Dissertation

Presented to

The Academic Faculty

By

Ernesto J. Angueira Batista

In Partial Fulfillment

Of the Requirements for the Degree

Doctor of Philosophy in Chemical Engineering

Georgia Institute of Technology

December, 2005

NOVEL SUPERACIDIC IONIC LIQUID CATALYSTS

FOR ARENE FUNCTIONALIZATION

Approved by:

Dr. Mark G. White, Advisor
School of Chemical and Biomolecular Engineering
Georgia Institute of Technology

Dr. Pradeep K. Agrawal
School of Chemical and Biomolecular Engineering
Georgia Institute of Technology

Dr. Christopher W. Jones
School of Chemical and Biomolecular Engineering
Georgia Institute of Technology

Dr. David Sherrill
School of Chemistry and Biochemistry
Georgia Institute of Technology

Dr. Peter J. Ludovice
School of Chemical and Biomolecular Engineering
Georgia Institute of Technology

Date Approved: August 9, 2005

DEDICATION

This thesis is dedicated to my mother, Ivette Collazo, and in memory of my grandmother Ana Angueira, they are the greatest inspiration in my life. Thanks to your hard work, dedication and motivation I am the person that I am and my achievements are a reflection of your encouragement. Also, this thesis is dedicated to the rest of my family, my loving wife Mayra, Dr. Mark White and his wife, and my friends; especially those who believe me and those who doubt me. To all of you, your unending love and support made this possible.

ACKNOWLEDGEMENTS

I would like to acknowledge Dr. Mark G. White for his continuous guidance and support during the past three years. Thank you for the opportunity and for believing in me. You helped me, not only to become a successful graduate student, but also to become a better person. I am so grateful to the other members of my thesis committee for their suggestions, assistance, critiques and encouragement. Also, I would like to thank Dr. Leslie Gelbaum (School of Chemistry and Biochemistry) for the guidance and support during the NMR studies. Last, but not least, to all my friends and colleagues for their support.

TABLE OF CONTENTS

LIST OF TABLES

LIST OF FIGURES

NOMENCLATURE

PTA - Purified terephthalic acid

PET - Polyethylene terephthalate

H^+ - Protons

ρ - Density (Kg/m^3)

x, X – Mol fraction

η - Viscosity (cP)

H_0 - Hammett acidity function

a_{H+} - Ion activity activity

γ_B - Activity coefficients of the unprotonated base

γ_{BH+} - Activity coefficients of the protonated base

O^+ - Organic cation

A^- - Inorganic anion

HOTf - Trifluoromethanesulfonic acid (Triflic acid)

k - rate constant

K - Equilibrium constant

F - Fractional conversion

H - Henry's law constant

ΔG^o_f - Gibbs free energy of formation (kcal/mol)

ΔH^o - Enthalpy(kcal/mol)

ΔS^o – Entropy (kcal/mol*K)

LUMO - Lowest unoccupied molecular orbital

HOMO - Highest occupied molecular orbital

R - Ideal gas constant

T - Temperature (K)

SUMMARY

There is a continuing interest in the subject of arene carbonylation, especially in strong acids and environmentally-benign alternatives are sought to HF/BF_3 and to $AlCl_3$ as conversion agents. Ionic liquids offer a powerful solvent for useful conversion agents such as aluminum chloride. The IL's permit $AlCl_3$ to be used at lower HCl partial pressures than with other solvents.

Simple equilibrium thermodynamics were used to identify the species in the IL, super acidic Brønsted ($ClHAl_2Cl_7^-$) and Lewis acidic ($Al_2Cl_7^-$) chloroaluminate anions that are responsible for the observed ultimate conversion of toluene to tolualdehyde. Modeling of the IL by semi-empirical methods showed that HCl could be placed in 3 different places in the IL and that the free energies of formation for these three structures were different.

^{27}Al NMR predictions helped us to have a better idea of the aluminum speciation in the ionic liquids and possible chemical environment. More specifically, the modeling studies suggested the existence of an aluminum-containing species having an unique structure not previously reported in the literature: the anion pair, $AlCl_3AlCl_4^-$, which appears to show ^{27}Al-NMR chemical shifts that are different from the dimer or the monomer. The ^{27}Al-NMR data of the IL before and after addition of HCl could be explained by a scheme that included this extra aluminum-containing species which apparently participates in an equilibrium with the anionic dimer $(Al_2Cl_7)^{-1}$ that has been reported in the literature. Only the anionic dimer is used in the reaction mechanism to initiate the carbonylation of toluene and to form an adduct with the product aldehyde thus

lowering the free energy of the reaction so that high conversions can be realized. This equilibrium between the two dimeric, aluminum-containing species is controlled by the structure of the organic cation as influenced by the length of the R-group ligand. The kinetically-controlled reactivity of this reaction apparently is related directly to the amount of the Brønsted super acid that was formed when HCl combines with the dimeric anion. The super acidity of the Brønsted species is the same when the Lewis acid is aluminum and for varying the R-group; however, IL's formed from $BMIM^+$ and MCl_3 show decreasing acid strengths as M is changed from Al to Ga to In, with the In IL being unreactive to arene carbonylation even though it shows activity towards some Friedel-Crafts alkylation reactions. Highest activity correlated with highest acidity of Lewis acid partner: Al > Ga >> In. Group V metal chlorides are inactive.

The length of the R-group in a family of organic cations apparently plays an important role in the chemistry of toluene carbonylation reaction. The activity for the toluene carbonylation reaction demonstrated a systematic decrease as the chain length in the cation was increased. In this work we showed that the variation in the reactivity as R was changed could not be correlated to the total amount of HCl absorbed in the ionic liquid since all of the IL's showed similar absorption amounts for HCl. The amount of CO dissolved in the IL's was apparently below the detection limit of the apparatus used here.

CHAPTER I

INTRODUCTION

The arene carbonylation reactions are important pathways to the synthesis of many building block chemicals used in different industries e.g., aryl aldehydes. Arenes are often functionalized with reactive groups in the course of multi-step synthesis, but arene aldehydes can be formed in a one-step synthesis by carbonylation in strong acids [1]. Aldehydes are desirable as functional groups since they can be easily reacted with amines, reduced to alcohols or oxidized to acids, as in terephthalic acid (Figure 1.1) [2].

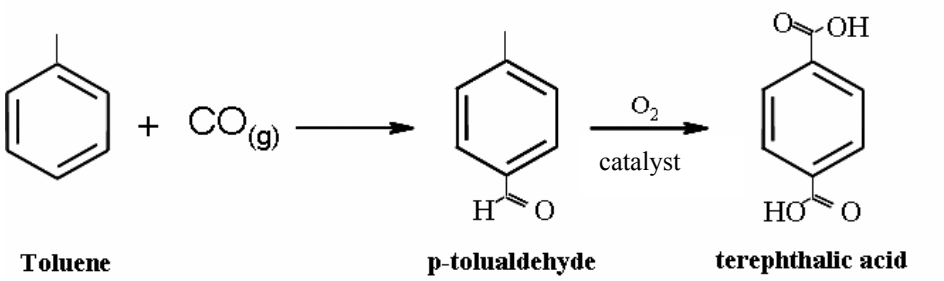

Figure 1.1. Terephthalic acid reaction.

Purified terephthalic acid (PTA) is the key raw material for the manufacture of polyester. It is used to make polyethylene terephthalate (PET), the primary container resin for applications such as carbonated beverage bottles and food containers.

The key advantages of using PET are:

a. Excellent transparency – its clarity enhances the presentation values of a product.
b. Lighter weight – reduces transportation costs and improves profit margins.
c. Outstanding physical properties that allows it to be processed reliably at high speeds.
d. Good impact resistance – strong and practically unbreakable.
e. Protective barrier in both directions – acts as an effective barrier for oxygen and carbon dioxide (for sparkling beverages).
f. Design freedom – features great design flexibility.
g. It can be recycled for other applications using a variety of recycling procedures.

Other derivatives of polyterephthalate provide dimensional stability, good heat resistance and durability for engineering applications. Polyester fibres based on PTA provide easy fabric care. Used both alone and in blends with natural and other synthetic fibres, polyester fibers are used in textiles, apparel and home furnishings. Polyester films are used widely in audio and video recording tapes, data storage tapes, photographic films, labels and other sheet material requiring both dimensional stability and toughness.

The formylation of arenes has attracted the commercial and scientific interests of scientist and engineer for over a hundred years. Acid-catalyzed reactions of hydrocarbons involve proton (H^+), and in some cases may also involve atoms or molecules, which act as electrophiles, in association with the protons [3]. This appears to

be the case with a superacidic homogeneous HF/BF_3 catalyst for the formation of benzene to form benzaldehyde. Other homogeneous superacids involve the pair of protic species, HX, and an aprotic electrophile such as $M^{n+}X_{(n/y)}{}^{y-}$, where M can be a post-transition element such as B, Sb, Al, *etc.* and X is usually a halide (F, Cl, Br or I).

Carbonylation of an aromatic compound can be carried out by a reaction generally referred to as the Gatterman-Koch reaction (Figure 1.2). Published in 1897, Gatterman and Koch described the direct carbonylation of various aromatic compounds by using high-pressure mixture of carbon monoxide and HCl together with a catalyst: mixture of cuprous chloride and aluminum chloride [4].

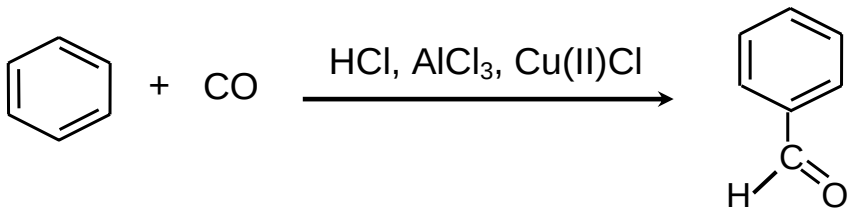

Figure 1.2. Gatterman-Koch reaction.

A metal atom, often functions in chemical reactions as a Lewis acid, accepting electron pair from molecules or ions**.** $AlCl_3$ is probably the most commonly used Lewis acid and also one of the most powerful. Aluminium chloride is a powerful Lewis acid, capable of forming stable Lewis acid-base adducts with even weak Lewis bases such as benzophenone or mesitylene [5]. Not surprisingly it forms $AlCl_4^-$ in the presence of chloride ion. In water, partial hydrolysis forms HCl gas or H_3O^+.

A general problem with the aluminum chloride "catalyst" is that it needs to be present in stoichiometric quantities in order for the reaction to go to completion, because it complexes strongly with the products. This makes it very difficult to recycle, so it must be destroyed after use, generating a large amount of corrosive waste. For this reason researchers are examining the use of more environmentally benign catalysts.

1.1 Other formylation catalysts

The reaction was subsequently "catalyzed" by other agents to include other Lewis acids [5]. Perfluoroalkanesulfonic acids were found to be equally powerful formylating agents that could be reused after a complicated regeneration process [6]. Trifluromethanesulfonic acid (triflic acid, CF_3SO_3H) has been identified as an effective homogeneous catalyst for electrophilic reaction since the triflate ion is an exceptional leaving group. With the synthesis of chloroaluminate ionic liquids, even more powerful acids were developed that could be used to carbonylate arenes and have been reported to be regenerated by a simple distillation process to remove the product aldehydes [5,7].

It has been observed that when a strong, Brønsted acid, such as HCl, was dissolved in acidic chloroaluminate ionic liquids, a superacid was created [8]. An arbitrary but widely accepted definition of a superacid is any system showing acidity greater than 100% sulfuric acid. These types of acidic, ionic liquids have been reported as conversion agents for arene carbonylation [7], alkylation of benzene with dodecene, [9] Friedel—Crafts sulfonylation [10], and Friedel—Crafts alkylations and acylations [11]. Reactivity data showed that increasing HCl partial pressure above the acidic,

chloroaluminate, IL increased the initial reactivity of the toluene carbonylation reaction [12].

1.2 Ionic Liquids

The development of ionic liquids dates to 1914. First research efforts involved the synthesis of ethylammonium nitrate [13]. Hurley and Wier at the Rice Institute in Texas, 1948, developed the first ionic liquids with chloroaluminate ions as bath solutions for electroplating aluminum [14]. These liquids have been studied primarily for their applications as electrolytes in electrochemistry technologies such as electroplating, batteries and alloy preparations.

An ionic liquid is a substance that is composed entirely of ions, and is a liquid at room temperature. Frequently the ionic liquid consists of organic cations and inorganic anions, although it is not limited to these combinations. While some people have said that the ionic liquid can have a high melting temperature such as in the case of the molten salt form of NaCl, the most commonly held understanding of this term is one that has a melting point of less than 100 ºC, more preferably less than 50ºC. For example, many preferred ionic liquids are liquid at room temperature, or less.

The cations of the ionic liquid include organic and inorganic cations. The cation used in this work is a dialkylimidazolium ion and this cation can be associated with a number of different anions (Figure 1.3). The anion includes organic and inorganic anions such as PF_6^-, $CF_3SO_3^-$, CF_3COO^-, *etc*. Some anions are Lewis acids such as $AlCl_3$, *etc*.

Many ionic liquids have been widely investigated with regard to applications other than as liquid solvents: such as electrolytes, phase-transfer reagents [15], surfactants [16], and fungicides and biocides [17,18].

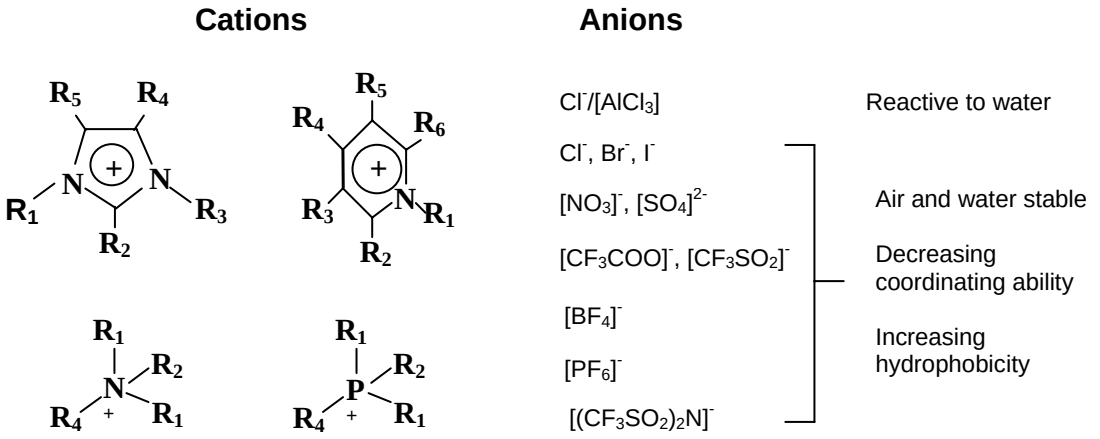

Figure 1.3. Examples of common cations and anion pairs used in the formation of ionic liquids, and general progression of changes in IL properties with anion type.

1.2.1 Properties of Ionic Liquids

The properties of ionic liquid that make them an attractive alternative solvent are: 1) low vapor pressure, 2) high thermal stability and 3) high polarity. In general, ionic liquids have low viscosity, essentially no vapor pressure, good heat transfer characteristics and are thermally stable.

The physical and chemical properties of ionic liquids can be varied over a wide range by the selection of suitable cations and anions. Some of the properties that depends

on the cation and anion selection includes: melting point, viscosity, density, acidity and coordination ability, solvation strength and solubility characteristics [19].

Changes in ion types, substitution, and composition produce new ionic liquid systems, each with an unique set of properties that can be explored. With the potential large matrix of both anions and cations, it becomes clear that it will be impossible to screen any particular reaction in all possible ionic liquids. Work is clearly needed to determine how properties of ionic liquids vary as functions of anion/cation and establish which, if any, properties change in a systematic way. Chloroaluminate ionic liquid systems are perhaps the most extensively studied.

1.2.1.1 Melting point

One of the most important properties for the evaluation of an ionic liquid is its melting point. The solid-liquid transition temperatures of ionic liquids can be below ambient temperature.

The dominant force in ionic liquids is Coulombic attraction between ions. Reports in the literature show that factors such as, low symmetry [20], weak intermolecular interactions (such as the avoidance of hydrogen bonding) [21, 22], and a good distribution of charge in the cation [23] are the main factors that influence the melting point of the salts, as generic classes. Within a similar series of salts, however, small changes in the shape of uncharged, covalent regions or the ions can have an important influence on the melting points of the salts (Table 1.1).

Table 1.1. Melting point of various chlorides.

Salt		Melting point (ºC)
NaCl		803
KCl		772
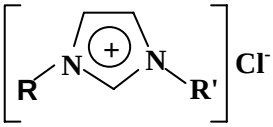	R=R' = methyl (MMIM)Cl	125
	R= methyl, R'= ethyl (EMIM)Cl	87
	R= methyl, R'= n-butyl (BMIM)Cl	65

Besides the cation , the anion influences the melting point, too. As the size of the anion increases, the melting point of the salt decreases (Table 1.2).

Table 1.2. Influence of different anions on the melting point of imidazolium salts.

Salt	Melting point (ºC)	Ref.
(EMIM)Cl	87	[24]
(EMIM)NO_2	55	[25]
(EMIM)NO_3	38	[25]
(EMIM)$AlCl_4$	7	[26]
(EMIM)BF_4	15	[27]
(EMIM)CF_3SO_3	-9	[21]
(EMIM)CF_3CO_2	-14	[21]

1.2.1.2 Density

The densities of the ionic liquids appear to be the physical property least sensitive to variations in temperature. The density of an ionic liquid depends on the type of cation and anion (Table 1.3). The density of comparable ionic liquids decreases as the bulkiness of the organic cation increases (Figure 1.4) [26]. Varying the anion results in more obvious effects in several cases. With bromoaluminate melts for example, it was possible to achieve densities unusual for normal organic solvents (Figure 1.5) [28].

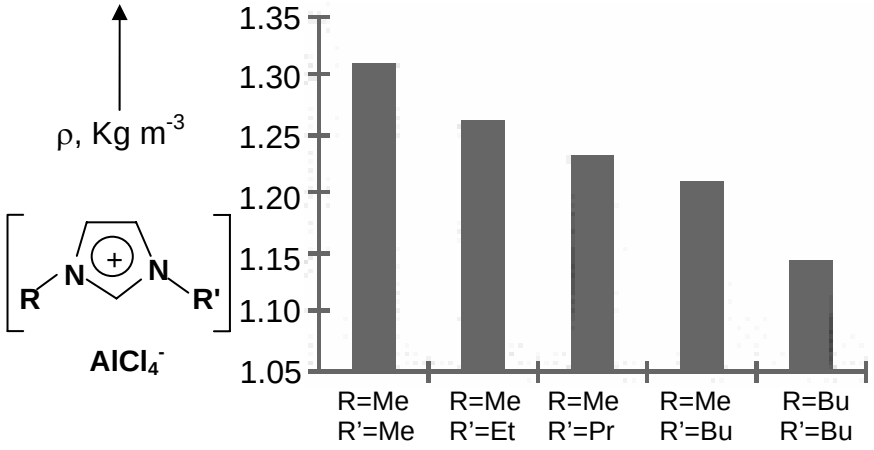

Figure 1.4. Dependence of density of 1,3-dialkylimidazolium chloride tetrachloroaluminate melts on the type of both alkyl groups; T=60ºC, $x_{AlCl3} = 0.5$.

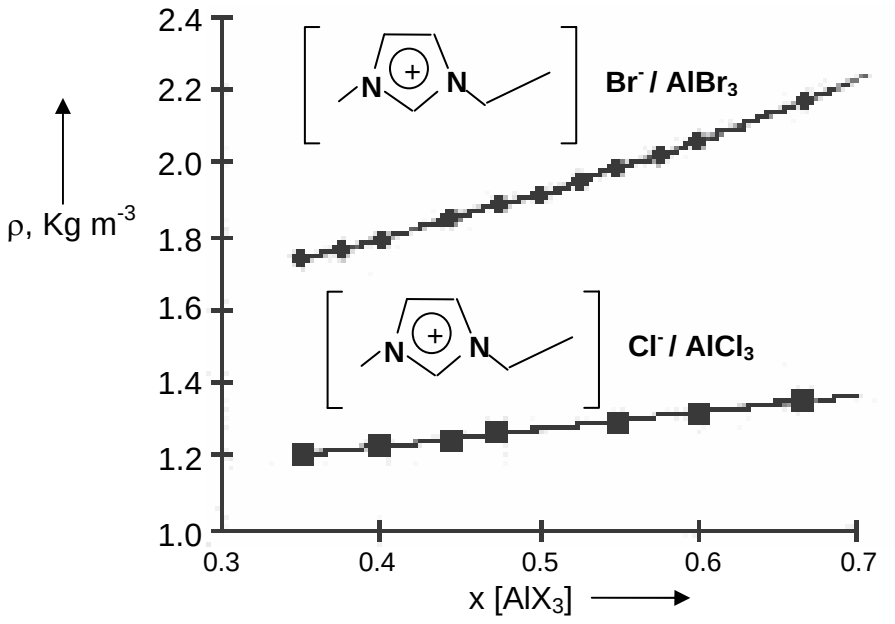

Figure 1.5. Dependence of density of two EMIM/tetrahaloaluminate melts on the mole fraction of aluminum trihalide at 60ºC.

1.2.1.3 Viscosity

The viscosity of a fluid arises from the internal friction of the fluid, and it manifest itself externally as the resistance of the fluid to flow. In ionic liquids the viscosity is determined by their tendency to form hydrogen bonding and by the strength of their van der Waals interactions and hydrogen bonding (Table 1.3) [21]. The viscosities of many ionic liquids are strongly dependent upon temperature.

The effect of hydrogen bonding becomes clear when, for example, the viscosity of chloroaluminate melts of different compositions are compared (Figure 1.6) [26]. The increase in viscosity of more than a factor of ten in ionic liquids with $x_{AlCl3} < 0.5$ is a result of the formation of hydrogen bonds between protons of the imidazolium cation and

the basic chloride ion. This conclusion is supported by IR [29] and X-ray spectroscopy [30], ROESY-NMR, and theoretical calculations [31]. When $x_{AlCl3} > 0.5$, the anions $AlCl_4^-$ and $Al_2Cl_7^-$ are present, in which the negative charge is much better distributed. This leads to the formation of weaker hydrogen bonds and a much lower viscosity. The different type of species as result of variation in the x_{AlCl3} will be discuss in the Acidity section.

Table 1.3. Density and Viscosity of ionic liquids.

Cation/Anion	Density (g/cm^3)	Viscosity (cP)	Ref.
EMIM/BF_4	1.279	32	[32]
EMIM/CF_3CO_2	1.285	35	[21]
EMIM/CF_3SO_3	1.390	45	[21]
BMIM/CF_3CO_2	1.209	73	[21]
BMIM/CF_3SO_3	1.290	90	[21]

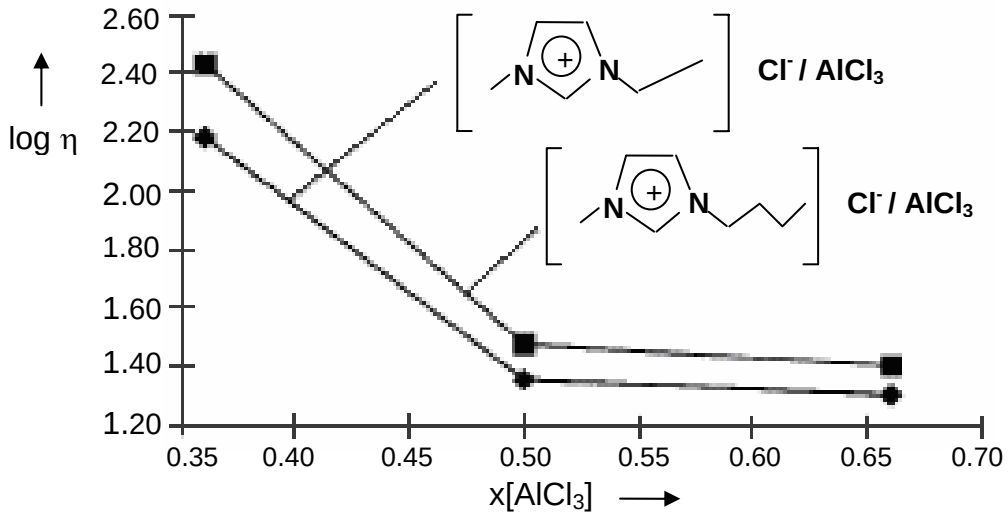

Figure 1.6. Dependence of the dynamic viscosity η (cP) of two 1,3-dialkylimidazolium tetrachloroaluminate melts on the mole fraction of aluminum trichloride at 25ºC.

1.2.1.4 Solubility in Ionic Liquids

By changing the nature of the ions present in an IL, it is possible to change the resulting properties of the IL. For example, the miscibility with water can be varied from complete miscibility to almost total immiscibility, by changing the anion from Cl- to $[PF_6]^-$ (Figure 1.3). The influence of the cation is shown by investigations of the solubility of 1-octene in different tosylate melts (Figure 1.7) [19]. By increasing the nonpolar character of the cation, the solubility of 1-octene in the melts increases markedly.

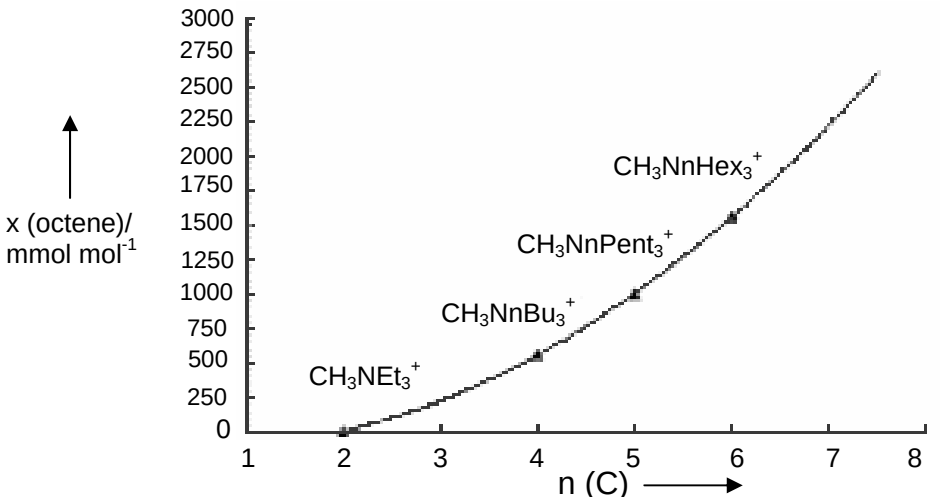

Figure 1.7. Solubility of 1-octene in four different tri-n-alkylmethylammonium tosylate melts at 80ºC, n (C) = number of C atoms of the alkyl residue.

1.2.1.5 Acidity of Ionic Liquids

The acidity and coordination properties of an ionic liquid are essentially determined by the nature of its anion. One property of interest for us is the acidity control by varying the imidazolium chloride to aluminum chloride ratio (Figure 1.8 - 1.9) [19]. The acidity and coordination properties are essentially determined by the nature of its anion. This variable acidity can be exploited in a process where high acidity is required for the conversion of substrate but where separation of product from IL is facilitated by low acidity.

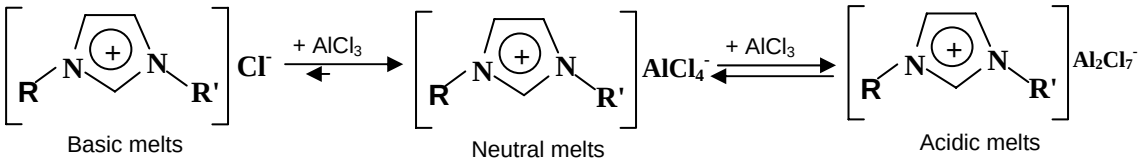

Figure 1.8. Control of the acidity of ionic liquids by the ratio of halide to Lewis acid.

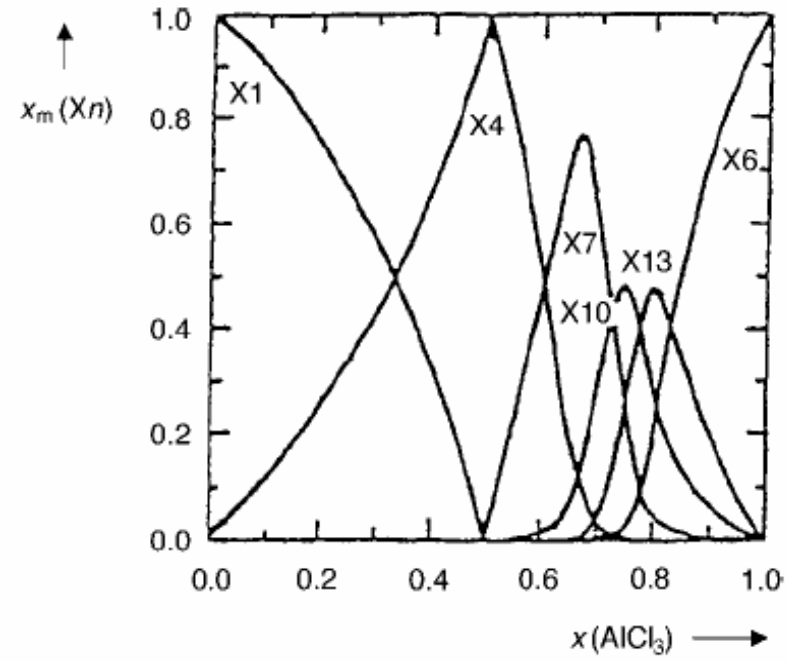

Figure 1.9. Mole fraction x_m of different anion species Xn in choroaluminates melts (X1=Cl^-; X4=$AlCl_4^-$; X7=$Al_2Cl_7^-$; X10=$Al_3Cl_{10}^-$;X13=$Al_4Cl_{13}^-$; X6=Al_2Cl_6).

The acidic nature of the ionic liquid can be attained by using an intrinsically acidic ionic liquid or by adding an acid to an ionic liquid. An ionic liquid can be made intrinsically acidic if the anion is a "combinable Lewis acid anion"; meaning that the Lewis acid is capable of combining with its anionic form to produce a non-coordinating polyanion, and the Lewis acid (*i.e.*, the anion precursor) is provided in molar excess to

the cation. For example $AlCl_3$ can combine with its anion $AlCl_4^-$ to form $Al_2Cl_7^-$, a powerful Lewis acid.

The strength of different acids is determined by comparing hydronium-ion concentrations of solutions having the same acid concentration. But in these superacids the hydronium-ion concentration is a poor indicatior of chemical reactivity due to the non-ideal liquid behavior. Therefore, the acidity of strong acids can be characterized by the Hammett acidity function (Figure 1.10) [33]. The Hammett acidity function is a scale that does include the effects of non-ideal liquids in this equilibrium: $H^+ + B \Leftrightarrow BH^+$. Hammett and Deyrup suggested a technique for measuring the degree of protonation of weakly basic indicators in acidic media by spectrophotometric methods. The Hammett acidity functions (H_0) is mathematically given by

$$H_0 = -\log_{10}\left[a_{H+}\left(\frac{\gamma_B}{\gamma_{BH+}} \right) \right] \qquad (1.1)$$

where the Hammett acidity function is directly proportional to the product of ion activity (a_{H+}) with the ratio of the activity coefficients of the unprotonated base (γ_B) to the protonated base (γ_{BH+}). However, Hammett acidity measurements have been recently performed on several solid acids such as sulfated zirconia and amorphous silica-alumina. Sulfuric acid has a Hammett acidity value H_0 -12. The more negative the value, the more acidic the composition.

The first superacids were the so-called Magic Acids (a mixture of fluorosulfonic acid and antimony pentafluoride, with varying concentrations of the two components)

[34]. These magic acids are capable of dissolving paraffin wax in the formation of a pentavalent carbonuim ion. Trifluromethanesulfonic acid (triflic acid, CF_3SO_3H) is one of the strongest simple protic acids known. The neat acid shows an H_0 of -14.1 [35, 36] which designates it as a superacid. Triflic acid and its conjugated base are stable when subjected to large thermal variations (up to 300ºC) and are quite resistant to oxidative and reductive cleavage. The fluoride ions of triflic acid are not released even in strongly nucleophilic media. Other simple superacids include fluorosulfuric acid (HSO_3F) which shows an H_0 value of -15.1 and it is the strongest known simple Brønsted acid.

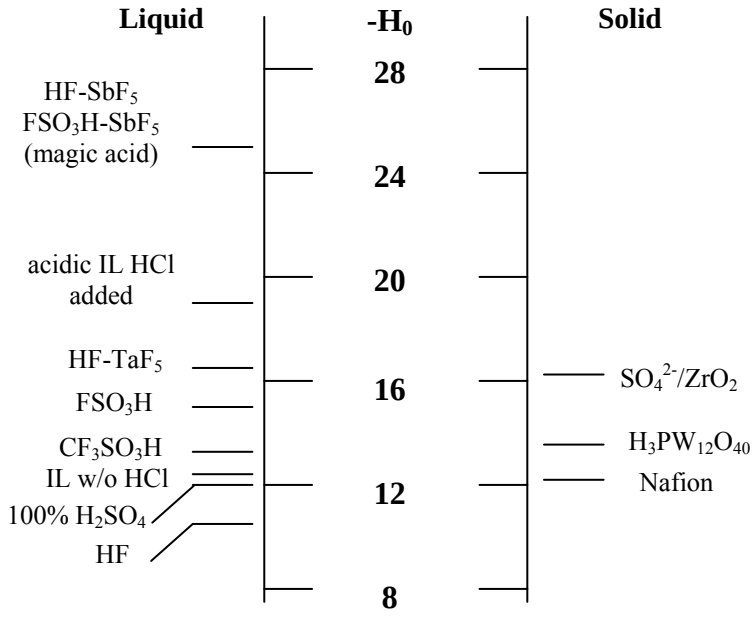

Figure 1.10. Hammett acidity value H_0 for familiar acids [19].

When a strong Lewis acid is added to a Bronsted acid the acidity of the medium usually increases. Recently, it was reported that strong, Brønsted acidity could be created

in the IL, $EMIM^+(Al_2Cl_7)^-$, upon exposure to dry, HCl gas [37]. Very strong acids can be produced by combining a Lewis acid with a Bronsted acid. One example is HF/BF_3. Others include $HCl/AlCl_3$; HF/TaF_3; HF/SbF_5. Preferably the ionic liquid stoichiometric with trace HCl has a Hammett acidity value H_0 -12, preferably acidic ionic liquid with HCl (1 atmosphere) with -18 or less [8]. It is known that protons are required to initiate the carbonylation reaction [38, 39]. Ma and Johnson [40] showed that carbocations were formed from selected arene hydrocarbons when combined with IL's derived from trimethylsulfonium bromide—$AlCl_3/AlBr_3$ and exposed to HBr gas. These results suggested to us that the combination of a Brønsted acid with the chloroaluminate IL might result in a potent conversion agent for reactions demanding high Brønsted acidity.

1.3 Goal and Organization of this Research

Environmental concerns dictate a need for the replacement of hazardous superacids with benign one. Commercial interest for arene carbonylation continues to be high even though one demonstrated process [41] uses the environmentally aggressive catalyst HF/BF_3. The very high vapor pressure of the HF/BF_3 system makes it an environmental threat and some researchers have sought low vapor pressure systems as an alternative. One of such is triflic acid [42, 43]. As a result of the desire to reduce the environmental threats, researchers seek a less aggressive agent for this reaction.

Ionic liquids offer a powerful solvent for useful conversion agents such as aluminum chloride. The IL's permit $AlCl_3$ to be used at lower HCl partial pressures than with other solvents [12].

The fundamental goal of this research is to determine the process conditions under which the reactivity of the IL system can be optimized from the standpoint of proper acidity, HCl and CO pressures needed and solubility to improve the reaction rates. The goal is to prepare ionic liquids having the acidity of trifluoromethanesulfonic acid (triflic acid, CF_3SO_3H) but without the deleterious reaction manifold to form ditolymethane and water. The ionic liquids showed almost no ditolymethane formed [44] and are an attractive alternative to the present technologies which utilize HF/BF_3 and similarly hazardous superacids.

Through mathematical modeling and prediction, it is hoped that we can use the knowledge of the effect of HCl upon the chloroaluminate speciation formation to produce a viable system at several different loadings of chloroaluminate anion to organic cation ratio and different the ligands R and R' in the organic cation.

The vast majority of work published to date on room-temperature ionic liquids relates to N-butylpyridinium and 1-ethyl-3-methylimidazolium (EMIM) tetrachloroaluminate systems. We speculate that changing the ligands R and R' in the organic cation may change the acidity of the resulting IL so as to to optimize the acidity of the system. An optimum acidity is one that can initiate the arene carbonylation at the lowest possible acidity level so that the tolualdehyde can be removed from the system by a low temperature evacuation. The regeneration of the IL is paramount to its use as a catalytic agent.

Provided that we can regenerate the IL and reuse it, then a simple 3-step process can be envisioned where the reaction occurs at modest pressure and temperature in the reactor, the fluid is continuously drawn off and flashed to a lower pressure vessel. Here,

the CO, HCl, and some toluene is drawn off to be recycled to the reactor and then the remaining liquid is flashed into a vacuum distillation tower where the tolualdehyde is removed from the ionic liquid and the IL is recycled back to the reactor.

This thesis is presented in five chapters. This chapter has provided an introduction to the topic. Details of the subsequent chapters follow:

Chapter 2 provides information about the arene carbonylation in acidic, chloroaluminates ionic liquids, including the effect of intrinsic acidity, Brønsted acidity, Al^{3+}/substrate ratio in the activity of the system.

Chapter 3 helps to understand the activity at the molecular level. This chapter includes modeling of thermodynamics and molecular properties to explained the formation of the ionic liquids, speciation of aluminum species: Al_nCl_{3n+1} as a function of HCl partial pressure, ^{1}H and ^{27}Al-NMR predictions and HCl host structure in ionic liquids.

In Chapter 4, we examined the effect of the cation and anion structures toward the system reactivity, including changing the length of the ligand in the cation, changing the Lewis acidity in the anion, and HCl total absorption predictions and experimental results.

Chapter 5 examines the molecular environment in acidic chloroaluminate IL's. We examined the different types of Al species, the kinetically-controlled reactivity of this reaction and suggested the existence of an aluminum-containing species having a unique structure not previously reported in the literature. The acidity of the IL's was determined using labeled acetone to reveal the presence and acid strength of protons (*via* the chemical shifts). Finally, Chapter 6 presents the major findings of this study and provides recomendatios for further investigation.

1.4 References

1. Booth, B. L., and El-Fekky, T.A., "A comparison of the effectiveness of sulfuric acid and trifluoromethanesulfonic acid in Koch carboxylation reactions ", J. C. S. Perkin I, p. 2441-6 (1979).

2. Komatsu, M., Ohta, T., Tanaka, T., Odu, R. and Takamizawa, Y., U.S. Patent 4,268,690.

3. Olah, G.A., Angew. Chem. Int. Ed. Eng., **32**, 767-788 (1993).

4. Gatterman and Koch, J. A., Chem. Ber., 30, 1622 (1897).

5. Olah, G.A., "Friedel-Craft and Related Reactions", John Wiley and Sons, New York, vol. 1 (1963).

6. Lalancette, J.M., Faurrier-Breault, M.J., and Thiffalut R., *Can. J. Chem.*, **52**, 589 (1974).

7. Saleh, R.Y., U.S. Patent 6,320,083, September 10, 1999.

8. Smith, G. P., Dworkin, A. S., Pagni, R. M., and Zingg, S. P., *J. Am. Chem. Soc.* **111**, 5075-5077 (1989).

9. Qiao, K., and Y. Deng, *J. Mol. Catal. A: Chemical*, **171** (2001) 81-4.

10. Nara, S. J., J. R. Harjani, M. M. Salunkhe, *J. Org. Chem.*, **66**, 8616-8620 (2001).

11. Boon, J. A., Levisky, J.A., Pflug, J.L., and Wilkes, J.S., *J. Org. Chem.* (1986), **51**, 480-3.

12. Iretskii, A. V., and White, M. G., *United States Provisional Patent* (2002).

13. Sugden S., Wilkins H., *J.Chem. Soc*. 1929, 1291-1298.

14. a) Hurley F.H., U.S Patent 2,446,331, 1948, b) Hurley F.H., Wier T.P., *J. Electrochem. Soc.*, 1951, 98, 207-212.

15. Albanese, D., Landini, D., Maia, A., and Penso, M., *J. Mol. Catal. A*, 1999, 150, 113.

16. Blackmore, E. S., Tiddy, G. J. T., *J. Chem. Soc., Faraday Trans*. 2, 1988, 84, 1115.

17. Pernak, J., Krysinski, J., Skrzypczak, A., *Pharmazie* 1985, 40, 570.

18. Pernak, J., Czepukowicz, A., Pozniak, R., *Ind. Eng. Chem. Res.* 2001, 40, 2379.

19. Wasserscheid, P. and Keim, W., *Angew. Chem. Int. Ed. 2000*, **39**, 3772-3789.

20. a) Seddon, K.R., *J. Chem. Tech. Biotechnol*. 1997, 68, 351-356; b) Seddon, K.R., *Kinet. Catal. Engl. Transl.* 1996, 37, 693-697.

21. Bonhôte, P., Dias, A.P., Papageorgiou, N., Kalyanasundaram, M., and Grätzel, M., *Inorg. Chem*., 1996, 35, 1168-1178.

22. Elaiwi, A., Hitchcock, P.B., Seddon, K.R., Srinivasan, N., Tan, Y.M., Welton, T., and Zora, J.A., *J. Chem. Soc. Dalton Trans.*, 1995, 3467-3472.

23. Stegemann, H., Rhode, A., Reiche, A., Schnittke, A., and Fullbier, H., *Electrochim. Acta*, 1992, 37, 379-383.

24. Wilkes, J.S., Levisky, J.A., Wilson, R.A., and Hussey, C.L., *Inorg. Chem.*, 1982, 21, 1263-1264.

25. Wilkes, J.S., and Zaworotko, M.J., *J. Chem. Soc. Chem. Commun.*, 1992, 965-967.

26. Fannin A.A. Jr., Floreani, D.A., King, L.A., Landers, J.S., Piersma, B.J., Stech, D.J., Vaughn R.L., Wilkes, J.S., and Williams, J.L., *J.Phys. Chem.*, 1984, 88, 2614-2621.

27. Holbrey, J.D., and Seddon, K.R., *J. Chem. Soc. Dalton Trans.*, 1999, 2133-2140.

28. Sander, J.R., Ward, E.H., and Hussey, C.L., *J. Electrochem. Soc.*, 1986, 133, 325-330.

29. Tait, S., and Osteryoung, R.A., *Inorg. Chem.*, 1984, 23, 4352-4360.

30. Dymek, C.J., Grossie, D.A., Fratini, A.V., and Adams, W.W, *J. Mol. Struct.*, 1989, 213, 25-34.

31. Mantz, R.A., Trulove, P.C., Carlin, R.T., and Osteryoung, R.A., *Inorg. Chem.*, 1995, 34, 3846-3847.

32. Noda, A., Hayamizu, K., and Watanabe, M., *J. Phys. Chem. B*, 2001, 105, 4603.

33. Hammett, L.P., and Deyrup, A.J., *J. Chem. Soc.*, **54**, 2721 (1932).

34. Olah, G.A., Prakash, G.K.S., and Sommer J., "Superacids", John Wiley and Sons, New York, 1st Ed., 42-46 (1985).

35. Grondin, J., Sagnes, R., and Commeyras, A., *Bull. Soc. Shim. Fr.* 1779 (1996).

36. Saito, S., Sato, Y., Ohwada, T., and Shudo, T., *J. Ame. Chem. Soc.*, **116**, 2312 (1994).

37. Booth, B. L. and El-Fekky, T. A., *J. Chem. Soc., Perkin Trans. 1*, 2441-6 (1979) P. Smith, A. S. Dworkin, R. M. Pagni, and S. P. Zingg, "Brønsted Superacidity of HCl in Liquid Chloroaluminate. $AlCl_3$-1-Ethyl-3-methyl-1*H*-imidazolium Chloride", *J. Am. Chem. Soc.,* 1989, **111**, 525.

38. Booth, B. L. and El-Fekky, T. A., *J. Chem. Soc., Perkin Trans. 1*, 2441-6 (1979).

39. Olah, G.A., Laali, K., Farooq, O. *J. Org. Chem*., 50, 1483-6 (1985).

40. Minhui Ma, and K. E. Johnson, "Carbocation Formation by Selected Hydrocarbons in Trimethylsulfonium Bromide—$AlCl_3$—$AlBr_3$—HBr Ambient Temperature Molten Salts", *J. Am. Chem. Soc.* (1995), **117**, 1508-13.

41. Effenberger, F. and Epple, G., Angew. Chem. Internat. Edn., (1972) **11**, 299, 300.

42. Sood, D. S., S. C. Sherman, A. V. Iretskii, J. C. Kenvin, D. A. Schiraldi, M. G. White, "Formylation of Toluene in Triflic Acid", *J. Catal.* **199**, 149 (2001).

43. Bo-Qing Xu, D. S. Sood, L. T. Gelbaum, and M. G. White, "Toluene Carbonylation Catalyzed by Mixtures of water and Trifluoromethanesulfonic Acid", *J. Catal* **186**, 345-352 (1999).

44. Angueira, E.J., and White, M.G., "Arene carbonylation in acidic, chloroaluminate ionic liquids" *J. Mol. Catal. A: Chemical*, 227 (2005) 51-58.

CHAPTER II

ARENE CARBONYLATION IN ACIDIC, CHLOROALUMINATE IONIC LIQUIDS[1]

There is a continuing interest in the subject of arene carbonylation, especially in strong acids such as trifluoromethanesulfonic acid [1] and environmentally-benign alternatives are sought to HF/BF_3 and to $AlCl_3$ as conversion agents. Moreover, it was of interest to explore the properties of the chloroaluminate/EMIM-Cl and chloroaluminate/BMIM-Cl IL's as a function of P_{HCl} and as a function of the n in the formula: $O^+[Al_nCl_{3n+1}]^-$ where O is either EMIM or BMIM. The probe reaction used for these characterizations is toluene carbonylation as it demands Brønsted acidity [1], and it was reported that strong, Brønsted acidity could be created in the IL, $EMIM^+(Al_2Cl_7)^-$, upon exposure to dry, HCl gas [2].

Chloroaluminate ionic liquids formed from either 1-ethyl-3-methyl-1*H*-imidazolium-chloride (EMIM-Cl) or 1-butyl-3-methy-1*H*-imidazolium chloride (BMIM-Cl) were examined as conversion agents for toluene carbonylation at room temperature and at pressures of 150 and 1100 psig. The effect was examined upon the toluene conversion and selectivity for changing the ratio of $AlCl_3$/EMIM-Cl or $AlCl_3$/BMIM-Cl from ½ to 2 mol/mol at a constant HCl partial pressure of 30 psig as well as the effect of changing the HCl partial pressure from 0 to 30 psig at a constant value of $AlCl_3$/EMIM-Cl or $AlCl_3$/BMIM-Cl = 2. The effect upon reactivity was also determined for changing

[1] Material in this chapter has been previously published in the following article: Angueira, E.J., and White, M.G., "Arene carbonylation in acidic, chloroaluminate ionic liquids" *J. Mol. Catal. A: Chemical*, 227 (2005) 51-58.

the Al^{3+}/toluene ratio at a constant value of $AlCl_3$/EMIM-Cl = 2 when the P_{HCl} was 30 psig for pressures of 150 and 1100 psig.

2.1 Experimental

2.1.1 Chemicals

The imidazolium compounds were obtained from Sigma Aldrich and used without further purification. Aluminum chloride (99.99%), obtained from Sigma Aldrich, was sublimed under a vacuum before use. Toluene (anhydrous, 99.8%) was obtained from Sigma Aldrich and used without further purification. Carbon monoxide, CP grade, and HCl (anhydrous, 99+ %) were obtained from Airgas and Sigma Aldrich, respectively.

2.1.2 Preparation of IL's—chloroaluminates/EMIM-Cl and chloroaluminates/BMIM-Cl

The weighing instrument, chemicals, and material transfers for $AlCl_3$, either EMIM-Cl or BMIM-Cl were placed in an AtmosBag filled with dry Ar. $AlCl_3$ is weighed; either EMIM-Cl or BMIM-Cl is added to obtain the desired $AlCl_3/O^+$ ratio.

2.1.3 Reaction studies—Low pressure

1. Low pressure reactions were carried in a Fisher Porter glass tube. A dried Fisher Porter tube with a stirring magnet was placed in the AtmosBag.
2. The chloroaluminate/EMIM-Cl IL or chloroaluminate/BMIM-CL IL was weighed into the Fisher Porter tube.
3. Toluene was added to obtain the desired Al^{3+}/toluene ratio.
4. The reactor was sealed, removed from the AtmosBag and purged with HCl gas before HCl gas was added to the desired partial pressure and then this mixture was stirred for 30 minutes at room temperature.
5. Carbon monoxide was then added to give a total pressure of 150 psig. The reaction temperature was room temperature and the CO pressure was monitored to verify CO consumption.
6. Previous experiments with HOTf showed that a stirring rate of 800 rpm was sufficient to overcome mass transfer resistance. Since the conversion rate in the IL is similar to that for HOTF (*vide infra*) when the acid/substrate = 10 mol/mol, we will use a similar stirring rate of 1000 rpm.
7. After the reaction was completed, the reactor was slowly vented and purged with Ar.
8. The mixture was poured into a separatory funnel filled with an ice/distilled water mixture so as to dilute the acidic components.

9. The organic layer was collected after it was neutralized with a saturated sodium bicarbonate solution.

2.1.4 Reaction studies—High pressure

1. The high pressure experiments were completed using the same procedure described in the low pressure experiments, but we used a Parr Instrument Co. (Moline, IL) stirred autoclave (50 cm^3) lined with Hastalloy C.
2. The stirring rate was adjusted to 1000 rpm.
3. The post-reaction work-up of the products after the high pressure runs was the same as that described for the low pressure runs.
4. After the addition of HCl, carbon monoxide was added to a total pressure of 1100 psig,

2.1.5 Analytical

1. Organic products were analyzed in a HP-5890 Series II Plus GC equipped with a HP-5972 mass spectrometer. High purity helium (99.995, Airgas) was the carrier gas and the column was 15 m long, 0.25mm i.d., and 0.25 μm film thickness obtained from Supelco (SPB-5 24032).
2. An analytical method was developed to separate all the liquid-phase

products using the following GC oven protocol: initial temperature = 35ºC, hold for 5 minutes, then increase temperature 10ºC per minute, and finally hold temperature at 180ºC for the final 5.50 minutes.

2.2 Results

2.2.1 Activity versus intrinsic acidity

Five IL's, $O^+[Al_nCl_{3n+1}]^-$, were prepared for which n = ½, 1, 1.11, 1.5, and 2 when O^+ was 1-ethyl-3-methyl-1*H*-imidazolium (EMIM) cation and three more IL's for which n = 1.11, 1.5 and 2 when O^+ was 1-butyl-3-methyl-1*H*-imidazolium (BMIM) cation. These IL's were used as conversion agents for the low-pressure, carbonylation of toluene at room temperature using an amount of IL that would give 1 mol Al^{3+}/mol of toluene. One additional IL was prepared by the action of HCl gas contacting 3-Me-imidazole at room temperature [3]. The product of this reaction is 3-Me-imidazolium chlorohydrogenate and this IL represents the case where n = 0. BMIM-Cl or EMIM-Cl was not used for this case since both form solids upon reaction with HCl at room temperature. We began each of these tests with the same amount of toluene. The gas phase contained HCl gas at 30 psig and the balance was CO for a total pressure of 150 psig and the reaction was stopped after 16 h. From the literature [4], it was expected that only the acidic IL's, *i. e.*, n > 1, should be active for this carbonylation and we did observe this trend (Figure 2.1). Even with HCl added to the gas phase at 30 psig, no reaction product, *p*-tolualdehyde, was observed for the three IL's for which n = 0, ½, or

1; however, increasing toluene conversion was observed for the three IL's having n = 1.11, 1.5 and 2 derived from either BMIM-Cl or EMIM-Cl. Previous authors have characterized these IL's as intrinsically acidic when n > 1 and our results appear to confirm this characterization when the probe reaction is toluene carbonylation, which is known to demand strong acidity.

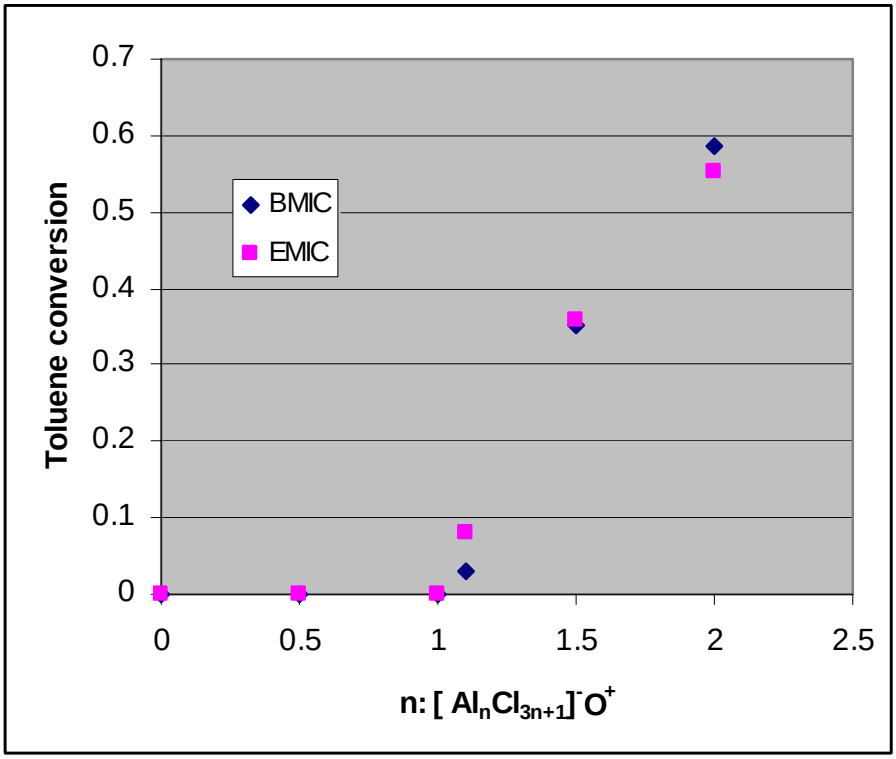

Figure 2.1. Toluene conversion as a function of n: $[Al_nCl_{3n+1}]^-O^+$.

These results also suggest that the IL's derived from either EMIM-Cl or BMIM-Cl were equally active for the toluene carbonylation reaction when the value of n was set. BMIM-Cl was reliably dry from the source whereas some batches of the EMIM-Cl were

contaminated with water. Accordingly, we used BMIM-Cl as the organic cation in many of the remaining parts of this chapter.

2.2.2 Activity *versus* Brønsted acidity

We were interested to know if the intrinsic acidity of the acidic chloroaluminate IL could be increased by adding a Brønsted acid, as suggested by the results of others [2, 5]. The Brønsted acid was HCl gas and the acidic chloroaluminate system was $EMIM^+/Al_2Cl_7^-$. This choice of HCl as the Brønsted acid follows from 1) the fact that its concentration in the IL can be adjusted reversibly by changing the partial pressure of HCl above the IL and 2) the acidity of the resulting IL was claimed to be super acidic [2, 5, 6]. For these tests the Al^{3+}/substrate ratio was 1 mol/mol and the dissolved HCl concentration in the IL phase was adjusted by changing the HCl gas partial pressure [6] (0, 5, 15, & 30 psig) while the partial pressure of the CO was adjusted so that the total pressure remained constant at 150 psig. All tests were completed at room temperature for varying durations from 15 minutes to 21 hours.

Even the IL not treated with HCl gas showed some low activity for toluene carbonylation (Figure 2.2, ~12% toluene conversion in 4 h); however, when HCl was added to the gas phase in little as 5 psig, the toluene conversion at 4 h was > 30%. Other runs for the HCl partial pressure was $\geq$ 15 psig showed about 40-45% toluene conversion at 4 h. Apparently, the reactivity of the IL system for this Brønsted-initiated reaction appears to be greatly enhanced with the addition of HCl in the gas phase even at modest partial pressures. These results are consistent with the findings of others who claimed that

HCl gas was absorbed by the acidic, chloroaluminate IL's developed from $EMIM^+$ as the organic cation [2, 7].

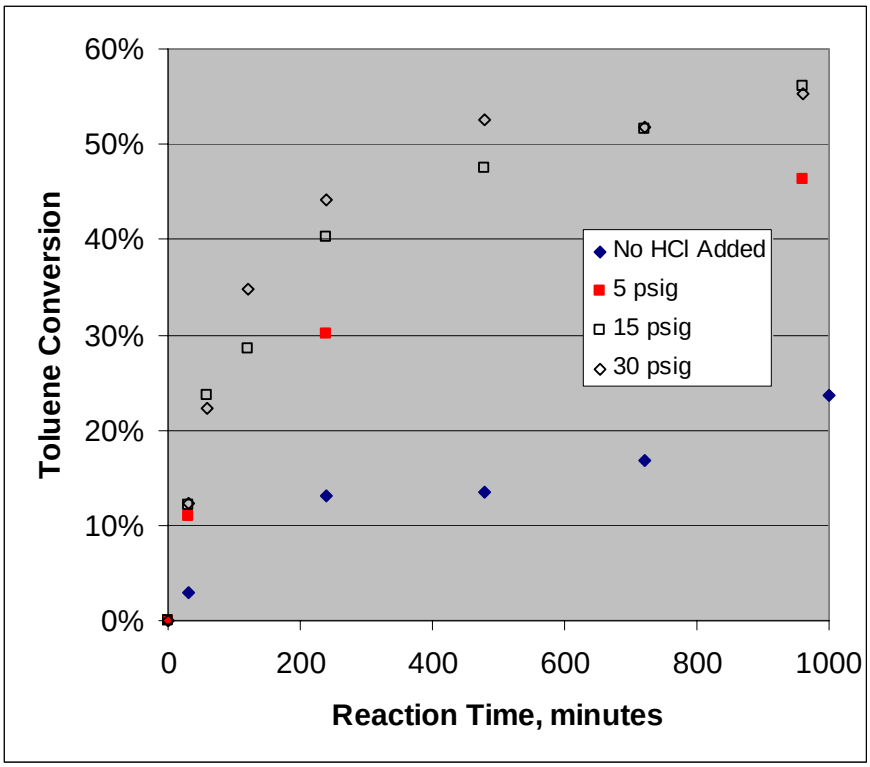

Figure 2.2. Effect of HCl pressure upon reactivity.

2.2.3 Activity *versus* Al^{3+}/substrate ratio

The effect of changing the Al^{3+}/substrate ratio has been reported for the Gatterman-Koch, $AlCl_3$-mediated carbonylation of benzene at high pressure (~1,000 psig) [8]. They showed that the benzene conversion *versus* time curves were higher for a series of reaction isotherms in which the Al^{3+}/substrate increased from ½ to 1. We were curious if this same result could be observed for the chloroaluminate IL's. In

determining the effect of changing Al^{3+}/toluene, we must be mindful of the findings of Campbell and Johnson [6] who showed the [HCl] dissolved in the IL also depended upon the intrinsic acidity of the IL (*i. e.,* the $Al^{3+}/EMIM^{+}$ ratio). Accordingly, batch reactor data were collected at room temperature and for HCl partial pressure equal to 30 psig when the total pressure was adjusted to either 150 or 1100 psig by adding dry CO. Each run contained an acidic chloroaluminate IL [$(Al_nCl_{3n+1})^{-}/EMIM^{+}$] for which $\underline{n} = 2$, but the initial amounts of IL were increased at constant initial amount of toluene so that the Al^{3+}/toluene ratio was ½, 1, 1.5 or 2 mol/mol. The transient results are shown in Figure 2.3 for each value of Al^{3+}/toluene. These data show transients in the conversion versus time that are similar to the earlier work [8] for the benzene carbonylation in $AlCl_3$. For each ratio of Al^{3+}/toluene, the toluene conversion increased rapidly at short reaction times, then, the conversion changed little at long reaction times. The ultimate toluene conversion appears to increase with increasing value of Al^{3+}/toluene at low (150 psig) and high total pressures (1100 psig). The rate of approach to ultimate conversion is higher for the runs operated at 1100 psig than those completed at 150 psig. When Al^{3+}/toluene = ½, the ultimate conversion was 28% for both low and high pressure runs. For the 1100 psig run, Al^{3+}/toluene = 1, the conversion at 15 minutes (50%) was nearly equal to the ultimate conversion observed for this run (51%) and for the lower pressure run (~50%). When the Al^{3+}/toluene ratio was 1.5, only one run was completed for which the conversion was 79% at 21 hours for the high pressure run. For the runs at Al^{3+}/toluene = 2, the ultimate conversion was 97.2% at 1100 psig (~4 h) and 87.2% at 150 psig (16 h). If the reaction had been allowed to run at these conditions for a longer

time, the ultimate conversion would be nearly complete. Taken together, these data suggest that Al^{3+} is the limiting reagent in these runs.

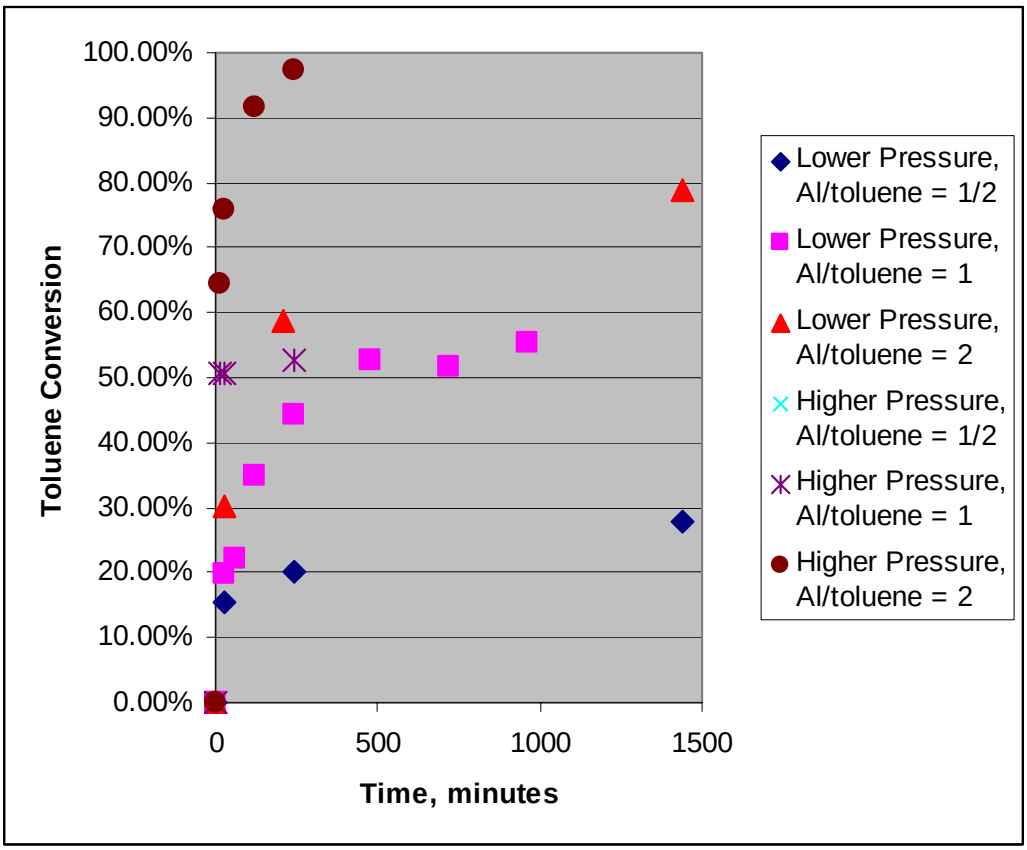

Figure 2.3. Toluene conversion for changing the Al^{3+}/toluene ratio.

The ultimate conversion of toluene increased linearly with increasing values of the Al^{3+}/toluene ratio, Figure 2.4, showing a slope of ~½ and an intercept near zero. Holloway and Krase [8] observed a similar result for benzene carbonylation over $AlCl_3$ at 1000 psig and room temperature although the slope of their data, when plotted on the same figure, was higher (~0.64 mol converted/mol $AlCl_3$) also with an intercept near zero. For the runs where the toluene conversion < 0.8, the reaction products remained as

a liquid; however, when the conversion exceeded a value of 0.8 a slurry was formed. The data at the low and high pressure formed a single line when the conversion was less than 0.8; however, for the data at higher conversion, the data collected from the lower pressure run did not obey this same relationship. Mass transport effects could be influencing the lower pressure data at the higher conversions when the slurry was formed.

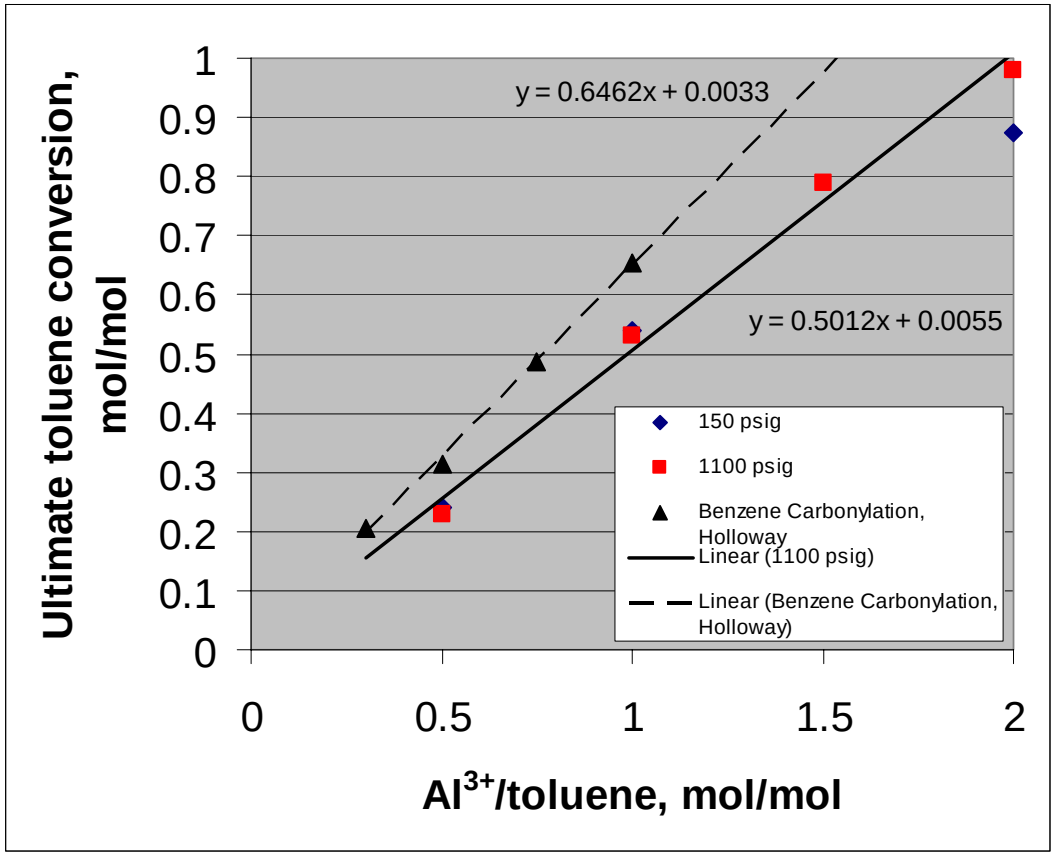

Figure 2.4. Ultimate toluene conversion *versus* Al^{3+}/toluene.

2.2.4 Selectivity

The regio-selectivity to the three isomers (*p*-tolualdehyde, *o*-tolualdehyde, *m*-tolualdehyde in all of these tests was 90%/7%/3% at conversions approaching 100%. There was no substantial effect upon this distribution of regio-isomers for varying the HCl partial pressure, the Al^{3+}/EMIM-Cl ratio, the Al^{3+}/toluene ratio, or the P_{CO} when the toluene conversions of the tests were similar. The selectivity to the *para*-isomer approached 95% at lower toluene conversions. The chemical selectivity was less than <3% to the only other products: di- and tri-tolymethanes. These regio- and chemical-selectivity's for the IL systems are very similar to those we reported for the triflic acid system when the acid/substrate ratio > 6 mol/mol [1].

An additional test was completed to address the issue of isomerization of tolualdehyde after its formation. *p*-tolualdehyde was added to an acidic IL (n = 2) in the ratio of one mole of aldehyde per mole of Al in the IL and HCl gas was contacted with this IL at a pressure of 30 psig for ½ h. The HCl was vented and this mixture was stirred at room temperature for 9 h. The products were worked up per the usual procedure and analyzed by GC/MS. No other isomers of tolualdehyde were observed to form in this mixture. Apparently, the IL does not promote the isomerization of *p*-tolualdehyde at these conditions.

2.3 Discussion

It appears that acidic, chloroaluminate, IL's formed from either BMIM-Cl or EMIM-Cl is equally strong acids that can initiate the toluene carbonylation reaction at even modest pressures. In our laboratory, [1] it was observed, initial toluene conversion rates of 2 h^{-1} in triflic acid, when the acid/substrate ratio was 10 for a total pressure of 1100 psig at room temperature. This conversion rate in triflic acid can be compared to the data from the IL (2.6 h^{-1}) having Al^{3+}/toluene = 2 also at 1100 psig and room temperature. Considering that these initial reaction rate data are free from mass transport effects, it becomes obvious that the acidic chloroaluminate IL's described here have activities that are similar to or greater than that of the triflic acid system for the toluene carbonylation reaction. One final comparison from the old literature is appropriate. Holloway and Krase [8] showed that benzene could be carbonylated in CO (1000 psig) at room temperature using a molar equivalent of $AlCl_3$. Under the proper conditions, the initial benzene conversion rate was 2.4 h^{-1} which was only slightly smaller than what we report here for the initial toluene carbonylation rate in the acidic chloroaluminate/EMIM-Cl IL's (2.6 h^{-1}).

Chloroaluminate IL's, $O^{+}[Al_nCl_{3n+1}]^{-}$, prepared with $\underline{n} \leq 1$ and derived from either BMIM-Cl or EMIM-Cl are not active (Figure 2.1) for the toluene carbonylation reaction even when HCl is added to the gas phase at a partial pressure of 30 psig. HCl is absorbed [6] by these basic or neutral IL's in concentrations greater than the intrinsically acidic IL's; however, the HCl does not produce Brønsted acids as indicated here and as speculated by others [6]. These authors represent HCl absorption by IL's as follows:

$$HCl_{(g)} + O^+A^- \leftrightarrow O^+\left[H(ClA)\right]^- \qquad (2.1)$$

where O^+ is the organic cation (BMIM-Cl or EMIM-Cl), A^- is the chloroaluminate anion and its speciation depends upon the value of $\underline{n}$ in the formula: $O^+[Al_nCl_{3n+1}]^-$. When $\underline{n}$ = 1; then they suggest that the anion A^- is the monomeric chloroaluminate anion, $AlCl_4^-$, and the proton in the resulting species $[HCl(AlCl_4)]^-$ is not labile and therefore cannot act as a Brønsted acid. Moreover, when $\underline{n}$ is less than 1, say ½ then, A = $AlCl_4^-$ and the HCl absorption can be modelled as:

$$HCl_{(g)} + O^+Cl^-O^+AlCl_4^- \leftrightarrow O^+\left(HCl_2\right)^-O^+\left[AlCl_4\right]^- \qquad (2.2)$$

The anionic species $(HCl_2)^-$ also is very unlikely to surrender a labile proton. If we use this model for this system of IL's, then it becomes obvious that no carbonylation activity will result from the basic or even neutral chloroaluminate IL's notwithstanding that HCl is present in the system. The genesis of labile protons in the acidic chloroaluminate IL's will be discussed below.

The effect of $\underline{n}$ upon the formation of Brønsted acidity with the addition of HCl can also be related to its effect upon the speciation of the Al in the IL [9]. That is, when $\underline{n}$ > 1, a fraction of the total aluminum in the IL is a dimer, $[Al_2Cl_7]^-$ and a trimer, $[Al_3Cl_{10}]^-$. We speculate that both multimeric chloroaluminate species can form protons by interacting with HCl *via* a mechanism shown below.[2]

[2] Chandler and Johnson express this equation for n = 2 by the following formalism:

$$HCl(gas) + \mathcal{O}^+[Al_2Cl_7]^- = \mathcal{O}^+[ClHAl_2Cl_7]^-$$

For the sake of clarity in the discussion here, we will use the formalism found in references 6 and 9.

$$HCl_{(g)} + O^{+}\left(Al_nCl_{3n+1}\right)^{-} \leftrightarrow H^{+}\left[AlCl_4\right]^{-} + O^{+}\left[Al_{(n-1)}Cl_{(3n-2)}\right]^{-} \qquad (2.3)$$

An alternative formalism has been recently described by Chandler and Johnson [10]. This reaction can proceed further to form additional labile protons such that when n = 3 originally, then two moles of protons could be produced. The toluene conversion data could be correlated with the mol fraction of the total Al^{3+} that can produce protons and weighted these mole fractions according to their reaction stoichiometry to produce protons: number protons = $\Sigma_i^n(i\text{-}1)X_i$; where X_i = mole fraction of chloroaluminate of nuclearity = i. That is, when i = 1, the chloroaluminate anion is a monomer, when i = 2, it is a dimer, *etc*. The result, Figure 2.5, shows a linear relationship between the toluene conversion and the weighted mole fraction of the Al species [9] that are capable of forming protons when HCl is added to the IL: $\Sigma_i^n(i\text{-}1)X_i$. This result should not be a surprise in view of the reports reported by Campbell and Johnson who showed that the proton concentration in the same IL does change linearly with the fraction of the Al that was initially present as a dimmer [6].

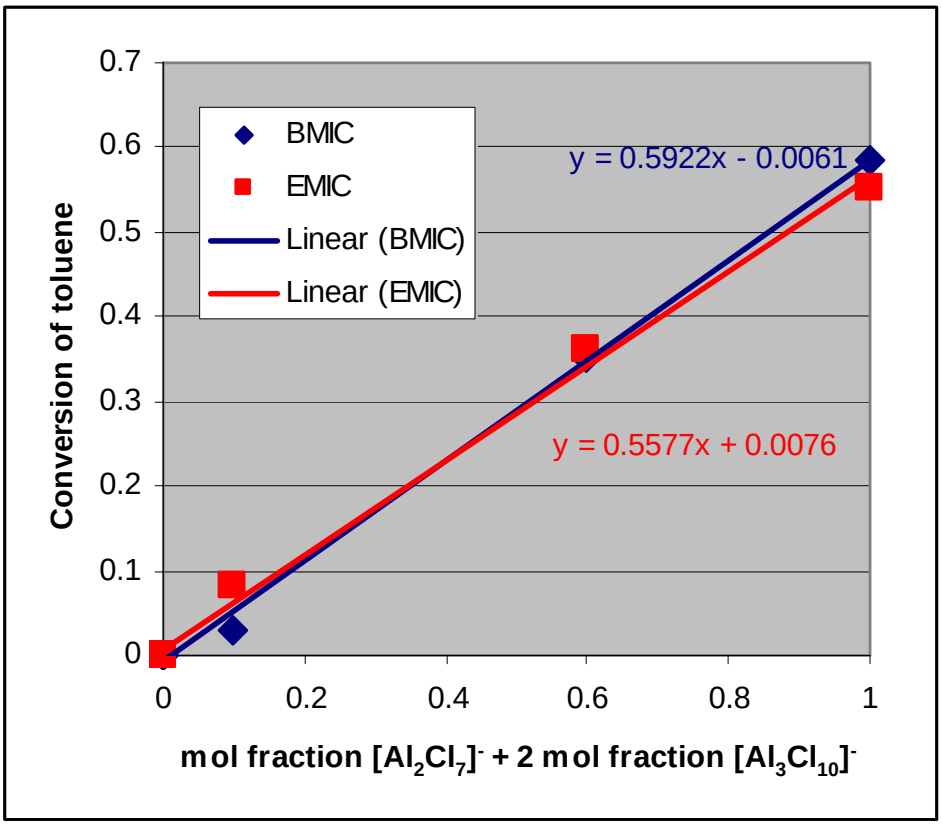

Figure 2.5. Toluene conversion *vs*. mol fraction $[Al_2Cl_7]^-$ + 2 mol fraction $[Al_3Cl_{10}]^-$.

Consider further the finding that the slope of these curves is ~ 0.57. The conversion of toluene is limited by the amount of Al^{3+} present initially here at 1 mol Al^{3+}/mol toluene. In other tests, *vide supra*, the ultimate conversion was 0.97 for a starting mixture having 2 mol Al^{3+}/mol toluene when the value of $\underline{n} = 2$. Using this final conversion of 0.97 instead of a value of 0.58, slope now becomes (0.57 x 0.97/0.58 = 0.95). This slope suggests that one mole of toluene is converted for every mole of protons that are formed by the reaction of HCl with the Al species in the IL.

The mechanism [11] for the toluene carbonylation reaction was reported to be a Brønsted-mediated reaction by electrophilic substitution of an aryl ring hydrogen. *Para-*

selectivity is favored by this mechanism which is reported to proceed by a carbocation intermediate. For the triflic acid system, the source of the proton is obvious; however, for the chloroaluminate IL's the genesis of the protons must be examined further. Consider the data and subsequent interpretation of their data by Campbell and Johnson [6] who speculated that the HCl gas became absorbed in the IL by a mechanism shown below.

$$HCl_{(g)} + O^{+}\left(Al_2Cl_7\right)^{-} \leftrightarrow H^{+}\left(AlCl_4\right)^{-} + O^{+}\left(AlCl_4\right)^{-}; K_1 \qquad (2.4)$$

They speculated that the proton associated with the chloroaluminate anion, $(AlCl_4)^-$, was labile and thus could function in the role normally associated with a labile proton. Consider now the role of this labile proton in the reaction mechanism normally advanced for arene carbonylation:

$$CO_{(g)} + H^{+}\left(AlCl_4\right)^{-} + O^{+}\left(AlCl_4\right)^{-} \leftrightarrow HCO^{+}\left(AlCl_4\right)^{-} + O^{+}\left(AlCl_4\right)^{-}; K_2 \qquad (2.5)$$

$$Arene + HCO^{+}\left(AlCl_4\right)^{-} + O^{+}\left(AlCl_4\right)^{-} \rightarrow AreneHCOH^{+}\left(AlCl_4\right)^{-} + O^{+}\left(AlCl_4\right)^{-}; k_3 \qquad (2.6)$$

$$AreneHCOH^{+}\left(AlCl_4\right)^{-} + O^{+}\left(AlCl_4\right)^{-} + H_2O \rightarrow AreneCHO + aqueous\_phase; k_4 \qquad (2.7)$$

Here the labile proton is associated with one monomeric chloroaluminate anion whereas the organic cation (O^+ = $BMIM^+$ or $EMIM^+$) in the IL is associated with the other chloroaluminate anion. For this mechanism, the absorption of HCl and its association with the IL species was assumed to be reversible under equilibrium constant K_1 and that the formation of the formyl cation is also reversible and governed by equilibrium constant, K_2. The electrophilic substitution reaction is presumed to be the rate-determining step under rate constant k_3. The product can be freed from the carbocation

intermediately upon contact with water. This step is not reversible because the formed hydronium ion, H_3O^+, is of too low acidity to catalyze the reverse step in the toluene carbonylation reaction [1]. The data shown in Figures 2.3 and 2.4 made it necessary to derive a rate equation assuming that the Al^{3+} species was the limiting reagent. One rate law derived from this mechanism for which the chloroaluminate species is the limiting reagent is as follows

$$Rate = KP_{CO}\left[Al^{3+}\right]_0^{\,2}\left[H^+\right](1-f)\left(M-\frac{1}{2}f\right) \tag{2.8}$$

where, $M = N^o_{tol}/(N^o_{Al3+})$ and f is the fractional conversion of Al^{3+}. Integration of this rate law according to the isothermal, batch design equation leads to the following equation:

$$\left[\frac{1}{M-0.5}\right]\ln\left[\frac{M-\frac{1}{2}f}{M(1-f)}\right] = \frac{K}{2}\left[Al^{3+}\right]_0 P_{CO}\left[H^+\right]t;\ for M > \frac{1}{2} \tag{2.9}$$

$$\frac{f}{1-f} = \frac{K}{2}\left[Al^{3+}\right]_0 P_{CO}\left[H^+\right]t;\ for M = \frac{1}{2} \tag{2.10}$$

The conversion of the Al^{3+} species, f, is directly related to the toluene conversion using the stoichiometry revealed in Figure 2.4: ½ mol of toluene is used in the conversion of 1 mol of Al species. The toluene conversion data (Figure 2.2) were fit to equations 2.9 and 2.10, using this stoichiometry for varying P_{HCl} when M = 1 and the total pressure was 150 psig (Figure 2.6). The slopes of these curve-fits are the product: k

$[Al^{3+}]_o P_{CO}[H^+]$. For these tests P_{CO} and the temperature was nearly constant. Thus, the variation of the slope is proportional to the $[H^+]$ in the IL.

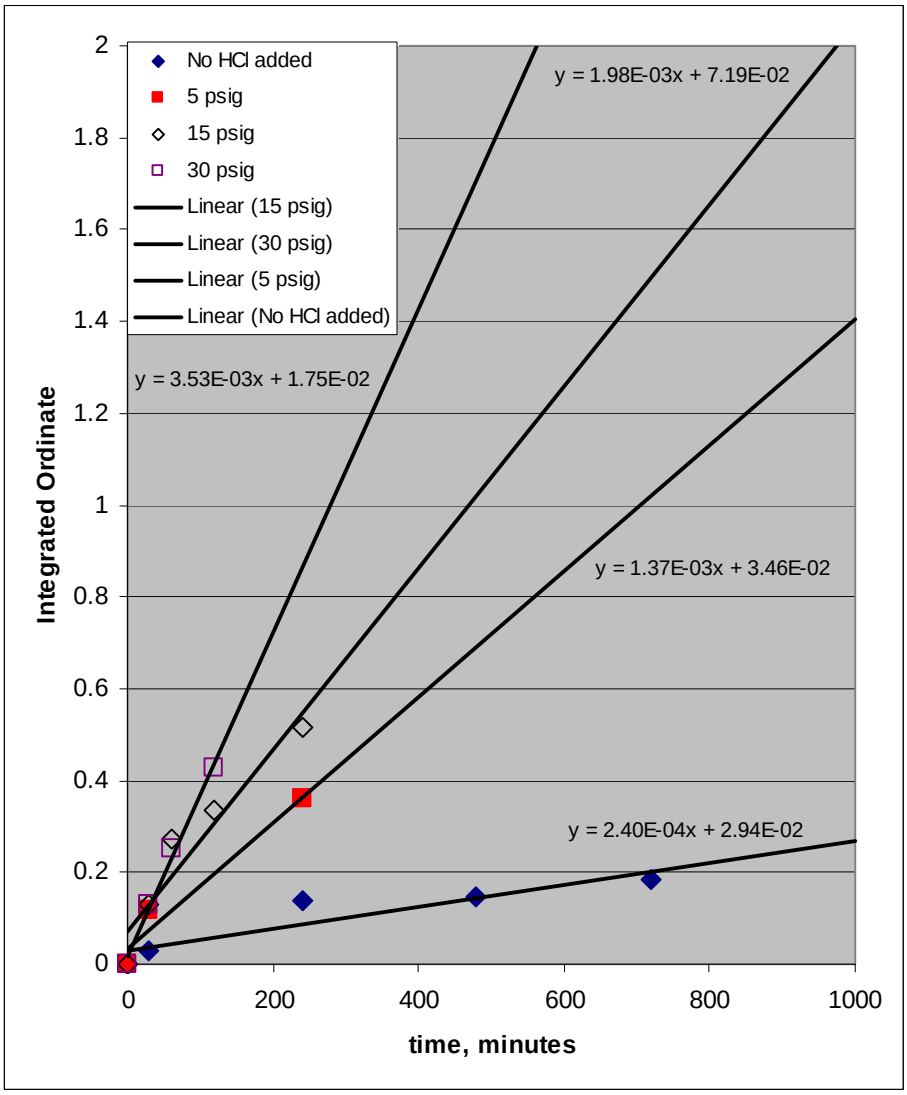

Figure 2.6. Effect of P_{HCl}: integrated rate plot.

Next, these slope data were plotted, Figure 2.6, *versus* the absolute partial pressure of HCl (psia) to determine how the product $k[Al^{3+}]_o P_{CO}[H^+]$ responded to increasing partial pressure of HCl (Figure 2.7). These results show almost a linear

increase in the slopes of Figure 2.6 with increasing partial pressure of HCl, when expressed as an absolute pressure. Since k, $[Al^{3+}]_o$ and P_{CO} are nearly constant in these tests, we conclude that the $[H^+]$ in the IL increases linearly with increasing partial pressure of HCl gas above the IL. A linear relationship of $[H^+]$ with HCl pressure was also reported earlier by Campbell and Johnson [6] who showed that the concentration of $[H^+]$ in an acidic, EMIM-Cl/chloroaluminate IL varied with P_{HCl} as follows:

$$[HCl], mM = \{1.3 \times 10^3 - 1.43 \times 10^3 X_{AlCl3}\} P_{HCl} \quad (2.11)$$

where P_{HCl} was expressed in atmospheres and X_{AlCl3} is the mole fraction of $AlCl_3$ in the IL which equalled 2/3 for these data.

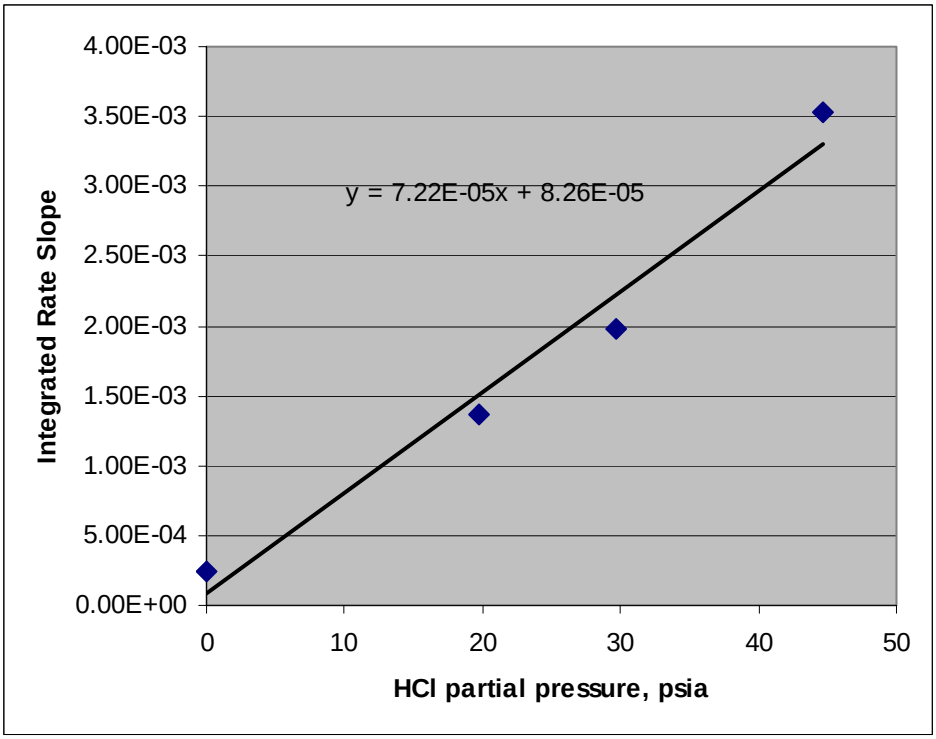

Figure 2.7. Effect of HCl partial pressure upon $[H^+]$ in IL.

The finite but small [H^+] concentration in the run without HCl added to the gas phase may be an artifact introduced by the less-than-perfectly-dry, AtmosBag in which the reagents were prepared. Others reported the finding of water in the room-temperature melts in concentrations of 7.5-20 mM [12]. This adventitious water vapour [8] can react with dry $AlCl_3$ to form HCl gas that can then combine with other dry $AlCl_3$ to form a strong Brønsted acid. Holloway and Krase [8] actually added up to 1 cm^3 of water per every 60 grams of $AlCl_3$ to obtain a maximum activity in their results. As with our experience [13] in other systems that have high affinity for water vapor, such as KO_2, the attainment of nearly zero water partial pressure in a dry box is never realized.

Consider now the effect that the Al^{3+}/toluene ratio has upon the reactivity of the system. We speculate that the reaction stops when ½ of the Al^{3+} cations initially in the mixture become associated with the product tolualdehyde molecules to form the complex $CH_3(C_6H_4)CHOH^+AlCl_4^-$ since the other ½ of the Al^{3+} species are needed to form the IL with the organic cation. The solid formed at high conversion could be related to this association of the chloroaluminate anion with the tolualdehyde carbocation. Holloway and Krase [8] also reported the formation of a solid during benzene carbonylation over $AlCl_3$. Their system being simpler than ours, suggests that the solid formed could also be the result of the association of the benzaldehydeH^+ with $AlCl_4^-$.

The linear relationship of the ultimate, fractional, toluene conversion with the ratio of mol Al^{3+}/mol toluene, initially in mixture, suggests that the reaction is not catalytic and from a consideration of the slope (mol toluene converted/mol Al^{3+}) we conclude that at least two aluminum cations are needed for each toluene converted. A similar [1] result was observed for toluene carbonylation in the presence of triflic acid,

except the slope of those data suggested that 10 triflic acid molecules were required for every tolualdehyde produced.

From the forgoing we believe that the reaction mechanism often cited for the triflic acid mediated arene carbonylation also explains well the data for the acidic, chloroaluminate IL system. The selectivity of the IL-based system is similar to the triflic acid system. Moreover, the way in which the Al^{3+} species limits the reactivity of the IL system is very similar to what has been observed for the Gatterman-Koch $AlCl_3$ system, even to the formation of solid products. It is plausible that the IL does not use any unusual chemistry for the arene carbonylation conversion. Therefore, we can *speculate* that the higher reactivity of the IL system is a direct consequence of it being a superior solvent for the reactants (arene and CO) and for the catalyst: H^+. Consider a compilation of data (Figure 2.8) for arene carbonylation in triflic acid, acidic-chloroaluminate IL's, and $AlCl_3$. Here, data of initial arene conversion rate (h^{-1}) were plotted versus P_{CO} for reactions completed at room temperature. The data for benzene carbonylation in $AlCl_3$ (Al^{3+}/benzene = 1) shows conversion rates of 0.5-0.7 h^{-1} over the range of pressures from 500 to 1000 psig. These data were larger than the conversion rates for the triflic acid system where the acid/substrate ratio was 2 (0.1-0.4 h^{-1}) but less than the conversion rate data for triflic acid in large excess (10 mol acid/1 mol substrate) where the conversion rate was 2 h^{-1}. Data for the IL system showed conversion rates of 0.4 – 1 when Al^{3+}/toluene = 1 and the conversion rates were 0.6 to 2.6 h^{-1} when the Al^{3+}/toluene = 2. The increased reactivity of the IL systems could be a direct result of the superior solvation power normally attributed to IL's in that the reactant CO and the source of protons, HCl, are readily dissolved in the IL. The reason for this better solvation power

(*e. g.*, higher acidity) cannot be ascertained from the data presented here, although sparse data in the literature suggests that the acidic chloroaluminates derived from EMIM-Cl are very strong acids showing Hammett acidity functions near -18 [2, 4, 14]. The high solubility of HCl gas and its formation of protons in the IL would directly influence the reactivity of these arene carbonylations.

The regioselectivity to form the isomers of tolualdehyde apparently changes little with conversion level. Moreover, it appears that p-tolualdehyde does not isomerize under reaction conditions in the IL. Sood observed the same result with triflic acid [1]. By inference, it is assumed that the other isomers of tolualdehyde do not isomerize in the IL. Thus, the regioselectivity is determined by the reaction(s) that form the tolualdehyde isomers, initially.

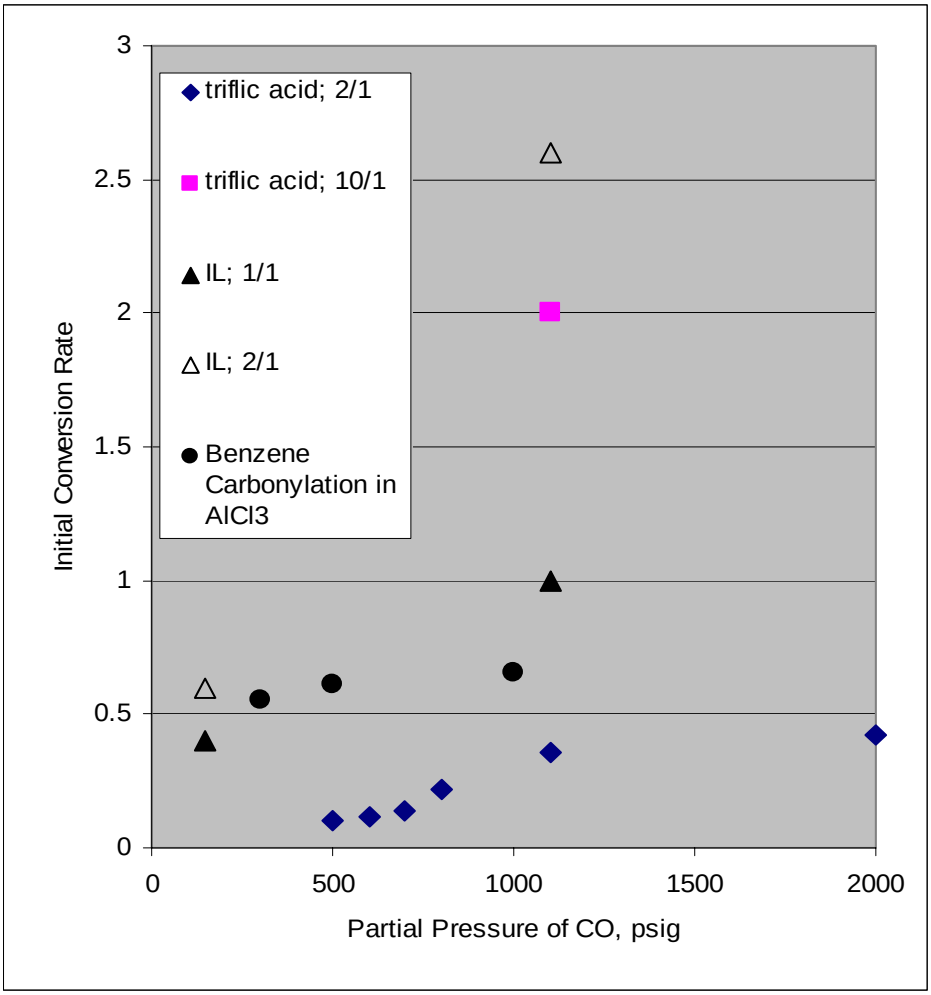

Figure 2.8. Arene conversion rate for room temperature carbonylations.

2.4 Summary

The Al^{3+} species in acidic chloroaluminate IL's interact with HCl gas to form protons and chloroaluminate species that can harbor the product aldehydes. As such, the Al^{3+} species are co-reactants with the arene and CO. The formed protons are probably very highly acidic such that the absorption of CO is favored even at modest pressures and

the formation of formyl cation takes place rapidly. The role played by the proton in the IL system is not unlike that observed for protons in the perfluoroalkanesuflonic acid systems. The Al^{3+} species that are not directly associated with the organic cation in the IL system are free to sequester the product aldehydes much the same way as has been observed for $AlCl_3$. The superior reactivity demonstrated by acidic, chloroaluminate IL's is probably due to their enhanced solvation power for HCl and CO.

2.5 References

1. Xu, B., Sood, D.S., Gelbaum, L.T., and White, M.G., "Toluene Carbonylation Catalyzed by Mixtures of water and Trifluoromethanesulfonic Acid", *J. Catal* **186**, 345-352 (1999); Sood, D. S., Sherman, S.C., Iretskii, A.V., Kenvin, J.C., Schiraldi, D.A., and White, M.G., "Formylation of Toluene in Triflic Acid", *J. Catal.* **199**, 149 (2001).

2. Smith, P., Dworkin, A. S., Pagni, R. M., and Zingg, S. P., "Brønsted Superacidity of HCl in Liquid Chloroaluminate. $AlCl_3$-1-Ethyl-3-methyl-1*H*-imidazolium Chloride", *J. Am. Chem. Soc.,* 1989, **111**, 525.

3. Driver, G., and Johnson, K.E., "3-Methylimidazolium bromohydrogenates(I): a room-temperature ionic liquid for ether cleavage", *Green Chemistry*, (2003), **2**, 163-9.

4. Karpinski, Z. J., and Osteryoung, R.A., *Inorg. Chem.* (1984), **23**, 1491-4; Kbdul-Sada, A. A. K., Greeway, K.R., Seddon, K.R., and Welton, T., *Org. Mass Spectrom.* (1993), **28**, 759-65.

5. Zingg, S.P., Dworkin, A.S., Sørlie, M., Chapman, D.M., Buchanan, A.C., III, and Smith, G.P., "Reactivity of Anthacene in Liquid $SbCl_3$-$AlCl_3$-N-(1-Butly)Pyridinium Chloride Mixtures", *J. Electrochem. Soc.*, **131**, #7, 1602-8 (1984).

6. Campbell, J.L.E., and Johnson, K.E., "The Chemistry of Protons in Ambient-Temperature Ionic Liquids - Solubility and Electrochemical Profiles of HCl in HCl-IMCl-$AlCl_3$ Ionic Liquids As a Function of Pressure (295K)", *J. Am. Chem. Soc.*, **117,** 7791 (1995).

7. Qiao, K., and Deng, Y., "Alkylations of benzene in room temperature ionic liquids modified with HCl", *J. Mol. Catal. A: Chemical*, **171** (2001) 81-4.

8. Holloway, J.H., and Krase, N.W., "Synthesis of Benzaldehyde from Benzene and Carbon Monoxide under Pressure", *Ind. & Eng. Chemistry*, **25**, No. 5, 497, (1933).

9. Wasserscheid, P., and Keim, W., "Ionic Liquids—New "Solutions" for Transition Metal Catalysis" *Angew. Chemie (Int. Ed.)*, (2000) **39**, 3772-89.

10. Chandler W.D., and Johnson, K.E., "Thermodynamic Calculations for Reactions Involving Hydrogen Halide Polymers, Ions, and Lewis Acid Adducts. 3. Systems Constituted from Al^{3+}, H^{+} and Cl^{-}", *Inorg. Chem.* (1999), **38**, 2050-6.

11. Olah, G.A., and Kuhn, S.J., "Friedel-Crafts and Related Reactions", ed. By G. A. Olah, Wiley Intersciences: New York, 1964; vol III, Chapter XXXVIII; B. L. Booth, and T. A. El-Fekky, *J. Chem. Soc., Perkin Trans. 1*, 2441-6 (1979); Olah, G. A., Laali, K., and Farooq, O., *J. Org. Chem.* **50**, 1483-6 (1985).

12. Sahami, S., and Osteryoung, R.A., *Anal. Chem.*, **55**, 1970, (1983).

13. Stull, J.O., and White, M.G., "Hyperbaric Kinetics of the Simple Hydration and Potassium Superoxide," *O.E.D.* Vol. **11**, "Current Practices and New Technology in Ocean Engineering," pp. 325-342 (1986); Poehlein, S., and White, M.G., "Hyperbaric Kinetics for the Reaction of Potassium Superoxide with Water and Carbon Dioxide," *A.S.M.E. Ocean Engineering Division*, Vol. **12**, "Current Practices and New Technology in Ocean Engineering," pp. 55-61 (1987).

14. Smith, G.P., Dworkin, A.S., Pagni,, R.M., and Zingg, S.P., "Quantitative study of the acidity of hydrogen chloride in a molten chloroaluminate system (aluminum chloride/1-ethyl-3-methyl-1H-imidazolium chloride) as a function of HCl pressure and melt composition (51.0-66.4 mol% $AlCl_3$)" *J. Am. Chem. Soc.* **111**, 5075-7 (1989).

CHAPTER III

MODELING OF THERMODYNAMICS AND MOLECULAR PROPERTIES[1]

The results of simulation studies can help to understand the properties of a complex mixture by examining the structures, thermodynamics and interactions at the molecular level. A recent text showed the results of such simulations studies for ionic liquids [1]. Equilibrium thermodynamics were used to predict the composition of an EMIM-Cl/chloroaluminate IL [2] and we extended this earlier work to model, the acidic, chloroaluminate ionic liquid (IL) derived from the combination of 1-R-3-methyl-imidazolium-chloride (RMIM-Cl, R = ethyl, *n*-butyl, *n*-hexyl, *n*-octyl, *n*-dodecyl, or benzyl) and aluminum chloride complex ($AlCl_3$) in contact with HCl gas using quantum mechanics software to determine the thermochemical and molecular properties of these fluids. The principles of equilibrium thermodynamics of chemically reacting systems were employed to calculate the concentrations of species in the IL's so as to understand better the reactivity of arene formylations in these IL's. The molecular properties determined were the bond lengths, ^{1}H-, and ^{27}Al-NMR chemical shifts.

[1] Material in this chapter has been accepted for publication in the following article: Angueira, E.J., and White, M.G., "Predicting the Composition of Acidic, Ionic Liquids in Contact with HCl Gas" in press *AIChE Jourmal*, and has been previously published in the following article: Angueira, E.J., and White, M.G., "Ionic liquid structure effect upon reactivity of toluene carbonylation: 1. Organic cation structure" *J. Mol. Catal. A: Chemical*, 238 (2005) 163-174.

3.1 Modeling Macroscopic Properties

For our attempt at modeling the macroscopic properties of the IL's, we borrow the approach used by Chandler and Johnson [2] who modeled basic, neutral, and Lewis acidic chloroaluminate IL's using a collection of 22 elementary reactions to describe the species present in these materials. They did not attempt to model the trinuclear, or tetranuclear Al compounds that were reported by others (see Figure 1.9 page 14). For the sake of simplicity, we will only include mono and dinuclear Al species in our modeling. They predicted the free energies of formation for species appearing in the elementary reactions using semi-empirical and higher-level quantum mechanical calculations. From these free energies of reaction they estimated the equilibrium constants for all 22 elementary reactions. The scope of this present investigation was limited to Lewis and Brønsted acidic IL's and thus only a maximum of six reactions were needed to model the chemical equilibria over a range of $[AlCl_3/O^+]^o$ ratios of 1 to 3 mol/mol where O^+ = $EMIM^+$.

(1) $Cl^- + AlCl_3 \Leftrightarrow AlCl_4^-$, $K_1 = 6.7 \times 10^{51}$

(2) $AlCl_3 + AlCl_4^- \Leftrightarrow Al_2Cl_7^-$, $K_2 = 1.0 \times 10^{19}$

(3) $2\ AlCl_3 \Leftrightarrow Al_2Cl_6$, $K_3 = 3.0 \times 10^{15}$

(4) $HCl\ (g) + AlCl_3 \Leftrightarrow HAlCl_4$, $K_4 = 5.05$

(5) $HCl\ (g) + AlCl_4^- \Leftrightarrow ClHAlCl_4^-$, $K_5 = 0.133$

(6) $HCl\ (g) + Al_2Cl_7^- \Leftrightarrow ClHAl_2Cl_7^-$, $K_6 = 0.1$

Subsets were used of these six reactions and the corresponding equilibrium constants [2] to model the IL under the desired conditions. For example, when no HCl was added to the system, then only the first three reactions were used when $[AlCl_3/O^+]^o$ ratio was >2 and only the first two reactions were needed for the case when $1 < [AlCl_3/O^+]^o < 2$. For the case when $[AlCl_3/O^+]^o < 1$, Chandler and Johnson established a set of equations to model the basic ionic liquid; whereas we used only equation 1. When HCl was added and when $1< [AlCl_3/O^+]^o < 2$, reactions 1, 2, 4, 5 & 6 were employed; whereas, when HCl was present and when $[AlCl_3/O^+]^o$ ratio >2 all six reactions were used.

A system of algebraic equations was developed to establish the equilibrium compositions from a consideration of the atom balances shown below and the equilibrium criteria.

Atom balances:

$$[AlCl_3] = [AlCl_3]^0 - [AlCl_4^-] - [HAlCl_4] - [ClHAlCl_4^-] - 2([Al_2Cl_6] + [Al_2Cl_7^-] + [ClHAl_2Cl_7^-]) \quad (3.1)$$

$$[Cl^-] = [Cl^-]^0 - [AlCl_4^-] - [Al_2Cl_7^-] - [ClHAlCl_4^-] - [ClHAl_2Cl_7^-] \quad (3.2)$$

Equilibrium criteria restraints:

$$\frac{[AlCl_3][Cl^-]}{[AlCl_4^-]} - \frac{1}{K_1} = 0; \frac{[AlCl_3][AlCl_4^-]}{[Al_2Cl_7^-]} - \frac{1}{K_2} = 0; \quad (3.3)$$

$$\frac{[AlCl_3]^2}{[Al_2Cl_6]} - \frac{1}{K_3} = 0; \frac{[AlCl_3][HCl]}{[HAlCl_4^-]} - \frac{1}{K_4} = 0; \quad (3.4)$$

$$\frac{[AlCl_4^-][HCl]}{[ClHAlCl_4^-]} - \frac{1}{K_5} = 0; \frac{[HCl][Al_2Cl_7^-]}{[ClHAl_2Cl_7^-]} - \frac{1}{K_6} = 0 \quad (3.5)$$

These equations and the equilibrium constant data from Chandler and Johnson [2] were committed to a spreadsheet environment and the option "Solver" was used to establish mathematical solutions. It was found that uniform convergence was not possible in all cases, and therefore it was necessary to appeal to our knowledge of the IL chemistry to choose the correct solution from among the possible mathematical solutions. As an example, it is known from the chemistry of the chloroaluminate IL's that the chloride anion appears in significant concentrations only in basic IL's therefore mathematical solutions in acidic IL's were discarded that showed significant concentrations of this anion. Also, it is known, that dimeric Al_2Cl_6 appears in significant concentrations only when $[AlCl_3/O^+]^o > 2$. By these means, only those mathematical solutions that were consistent with the known phase diagram of the acidic IL's were accepted. Shown below are our efforts to model these systems and use the predictions to interpret results from reaction studies. For the interpretation of the predictions, it was necessary to complete a selected number of experiments so as to verify some of the assumptions inherent to the modeling. These experiments include the titration of the ionic liquids with a Lewis base (p-tolualdehyde) so as to confirm the stoichiometry of the final product of toluene carbonylation with the ionic liquid Lewis acid component.

3.2 Experimental

3.2.1 Chemicals

The imidazolium compounds were obtained from Sigma Aldrich and used without further purification. Aluminum chloride (99.99%), obtained from Sigma Aldrich, was sublimed under a vacuum before use. Toluene (anhydrous, 99.8%) was obtained from Sigma Aldrich and used without further purification. HCl (anhydrous, 99+%) was obtained from Sigma Aldrich.

3.2.2 Preparation of IL's—chloroaluminates/EMIM-Cl

The weighing instrument, chemicals, and material transfers for $AlCl_3$, and EMIM-Cl were placed in a AtmosBag filled with dry Ar. $AlCl_3$ is weighed; and EMIM-Cl is added to it so as to obtain the desired $AlCl_3/O^+$ molar ratio.

3.2.3 Titration studies

1. One equivalent of *p*-tolualdehyde per mol of Al in the sample was added to separate IL's which were prepared having the Al/O^+ ratio of ½, 1/1, 1.5/1 and 2/1.
2. The amount of base and Al was the same in each sample, whereas, the amount of EMIM-Cl was varied to develop the desired Al/O^+ ratio.

3. The mixture of *p*-tolualdehyde and IL was slowly heated up to 413 K and placed under a vacuum (200 milliT = 26.7 Pa) for ½ hour so as to remove the weakly absorbed base.
4. The vaporized base was condensed into a trap held at 77 K.
5. The amount of base remaining in the IL was determined by weighing the amount of base found in the trap and subtracting this amount from the initial mass of base placed in the IL.

3.3 Results

3.3.1 EMIM-Cl chloroaluminate IL without HCl added

The first attempt at modeling was to reproduce Figure 13 in the publication by Chandler and Johnson [2]: the phase diagram for Al speciation over the range of $0 < [AlCl_3/O^+]^o < \infty$ in the absence of HCl gas above the liquid. This result is shown in Figure 3.1 where only the first three reactions were used for the modeling. These predictions agree with those shown in the manuscript by Chandler and Johnson and therefore, we believe that our mathematical routine is correct. That is, basic IL's ($0 < [AlCl_3/O^+]^o < 1$) show Cl^- and $AlCl_4^-$ as the dominate species and no $AlCl_3$ or Al_2Cl_6 is present in these mixtures. The Cl^- concentration decreases to a value of 0 as $[AlCl_3/O^+]^o$ approaches 1 (*i. e.*, $[AlCl_3/(AlCl_3 + O^+]^o = ½$] where the concentration of $AlCl_4^-$ reaches a maximum value of unity. For $1 < [AlCl_3/O^+]^o < 2$ the concentration of $AlCl_4^-$ decreases from its maximum value of unity to a value of 0 while the concentration of $Al_2Cl_7^-$

reaches a maximum value = 1. For values of $[AlCl_3/O^+]^o > 2$, the concentration of $Al_2Cl_7^-$ decreases as the concentration of Al_2Cl_6 increases. The following shows a simulation on the effect of adding HCl gas to the Lewis acidic IL's.

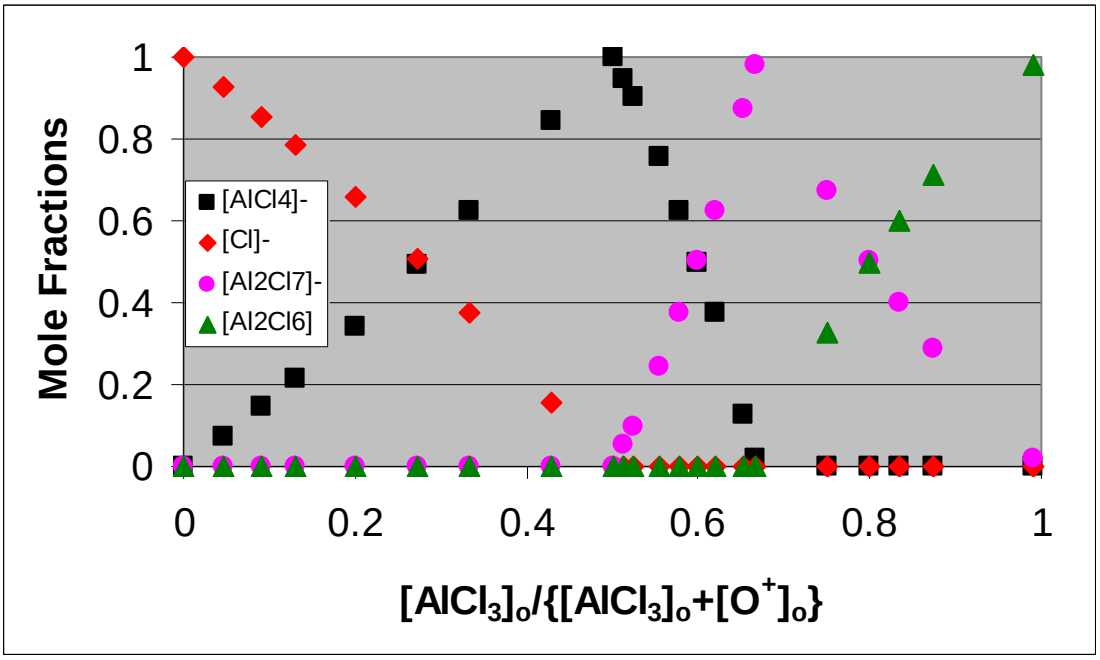

Figure 3.1. Modeling the EMIM-Cl IL Speciation Diagram.

3.3.2 Effect of adding HCl to an Acidic IL: $[AlCl_3/O^+]^o = 2$

Thermodynamic calculations were completed for an IL at 298 K where the value of $[AlCl_3/O^+]^o$ was 2 mol/mol and for HCl gas pressures from 0 to 500 psia (3.45 MPa) using reactions numbered 1 – 6 to simulate the formation of the IL. The goal of this modeling was to determine how HCl gas changed the equilibrium composition, if at all, and to determine what species were formed as HCl was introduced into the system. The results of the earlier modeling, Figure 3.1, show that the composition of the IL agrees

with that predicted by Chandler and Johnson when no HCl was present in the IL: mole fraction of $Al_2Cl_7^-$ = 1, all other species = 0. As the HCl partial pressure was increased, the mole fraction of the Brønsted super acidic, chloroaluminate anion, $ClHAl_2Cl_7^-$, increased rapidly at first and then its mole fraction appeared to approach an asymptote (Figure 3.2). The mole fraction of the Lewis acid, chloroaluminate anion ($Al_2Cl_7^-$) decreased monotonically for increasing partial pressure of HCl; whereas the mole fraction of the monomeric chloroaluminate anion, $AlCl_4^-$, remains constant at nearly 0 except at the highest HCl partial pressure where its mole fraction is 0.04. Finally, the mole fractions of the acidic chloroaluminate species, $HAlCl_4$ and $ClHAlCl_4^-$ (not shown), are small when the HCl pressure is less than 100 psia (0.69 MPa) and their mole fractions become significant (0.01) only when the HCl partial pressure is nearly 500 psia (3.45 MPa). No chloride anion (not shown) was formed in significant quantity which agrees with the fact that the melt was acidic. These results show that only the super acidic chloroaluminate anion ($ClHAl_2Cl_7^-$) was formed in significant amounts when HCl gas was added to this acidic IL. If this result is true, then this IL under HCl should catalyze the toluene carbonylation reaction which is known to proceed only in super acidic media [3]. Moreover, the strong Lewis acid, $Al_2Cl_7^-$, is also present and it should play a role in the arene carbonylation by forming an adduct with the weak Lewis base: tolualdehyde [4].

We were also interested to learn the effect of adding HCl gas to a system where Al_2Cl_6 was also present. This condition was met when the $[AlCl_3/O^+]^o > 2$, (*e. g.*, see Figure 3.1).

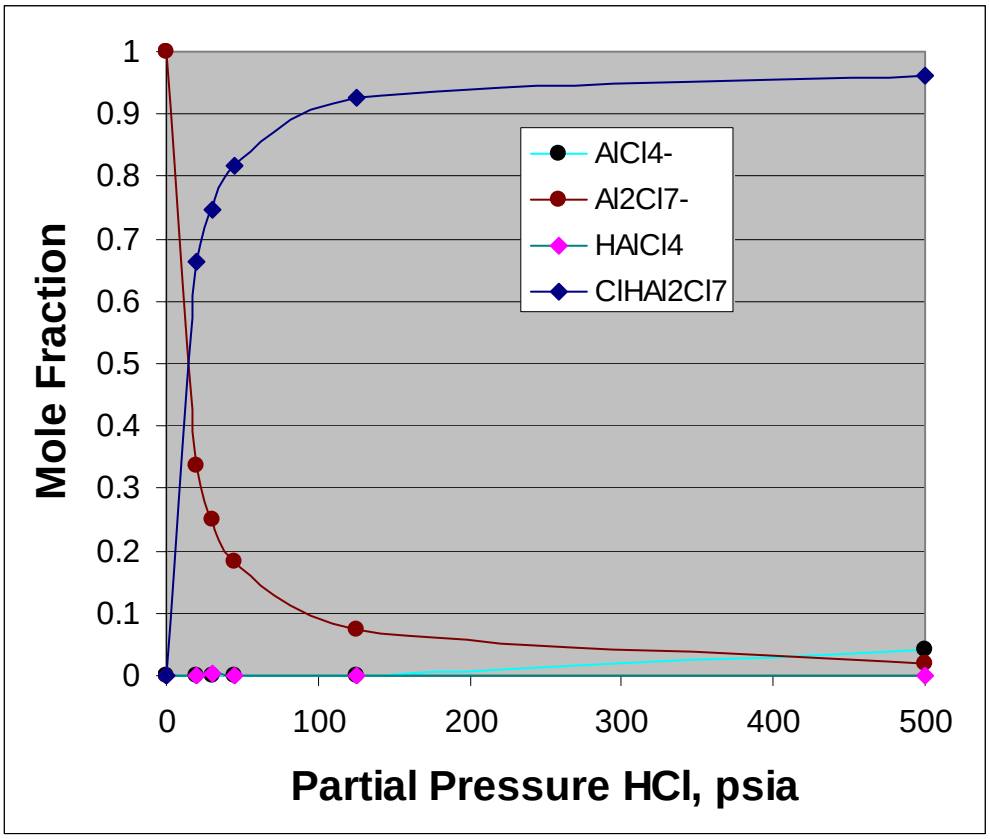

Figure 3.2. Equilibrium Composition of IL as P_{HCl} Changes for $[AlCl_3/O^+]^o = 2$.

3.3.3 Acidic IL: $[AlCl_3/O^+]^o = 3$

The IL phase diagram [5] shows that when $[AlCl_3/O^+]^o$ equals 3, a precipitate of $AlCl_3$ forms in equilibrium with a liquid composed of a mixture having $[AlCl_3/O^+]^o < 3$. This mixture was prepared to confirm the partial solubility of Al_2Cl_6 in the IL at room temperature when $[AlCl_3/O^+]^o = 3$ (*vide infra*). When additional organic cation was placed in this mixture to the extent that the final mixture shows $[AlCl_3/O^+]^o = 2$, then a single phase was formed. Calculations were repeated for the case where the value of

$[AlCl_3/O^+]^o = 3$ in an attempt to determine if HCl can be an agent to alter the solubility of Al_2Cl_6 in the IL at room temperature, Figure 3.3.

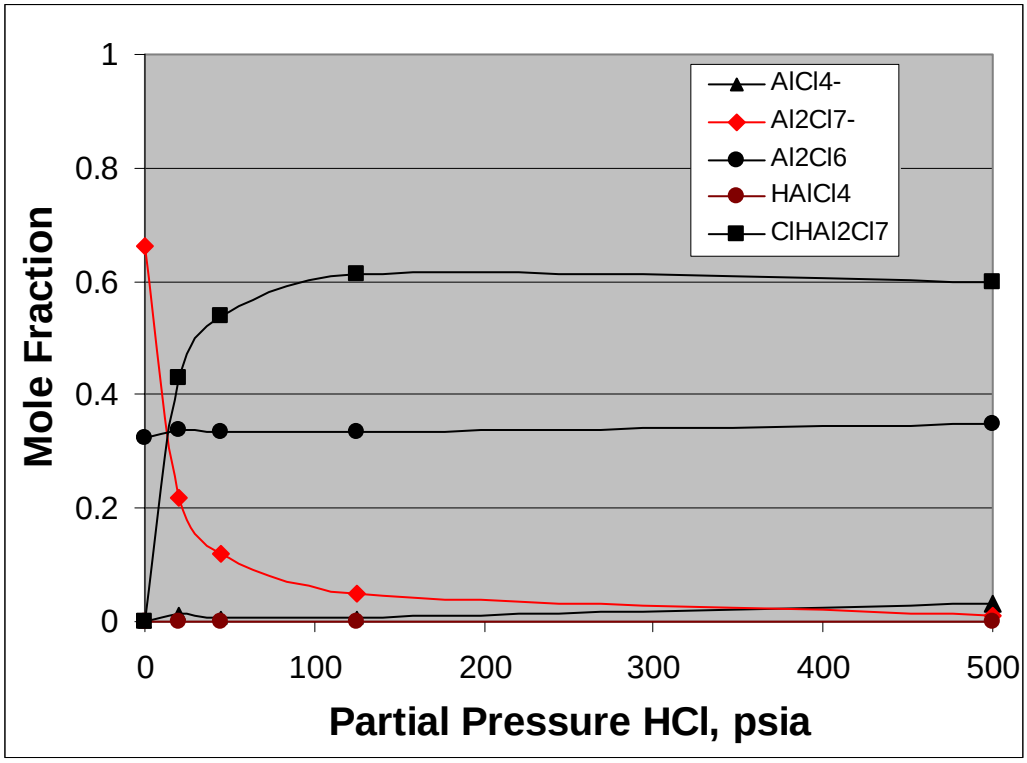

Figure 3.3. Equilibrium mixture composition for $[AlCl_3/O^+]^o = 3$.

The predicted composition of this IL with $[AlCl_3/O^+]^o = 3$ shows that the addition of HCl in the gas phase to the extent of 19.7 psia (135 kPa) does not cause the Al_2Cl_6 mole fraction to change much (0.32→0.34) while the mole fraction of $Al_2Cl_7^-$ decreases from 0.67 to 0.22. At the same time, the mole fraction of super acidic chloroaluminate increased from zero to 0.61 while the mole fraction of the monomeric $AlCl_4^-$ increased from 0 to 0.01. The acidic $HAlCl_4$ and $ClHAlCl_4^-$ species appears only in very low mole fractions (<0.01) at all levels of HCl partial pressures < 500 psia (3.45 MPa). These

simulations show that adding HCl gas to the system does not change the mole fraction of Al_2Cl_6 very much. Experimental verification of these predictions was sought by a visual inspection of an IL in a low pressure cell having $[AlCl_3/O^+]^o = 3$ was contacted with HCl gas at room temperature for which the pressure was adjusted from 0 to 150 psia, 1.03 MPa, (Figures 3.4-a and 3.4–b). The single phase system (Figure 3.4-a, $[AlCl_3/O^+]^o = 2$) did not show any solid formation when HCl was added to the gas phase at 298 K.

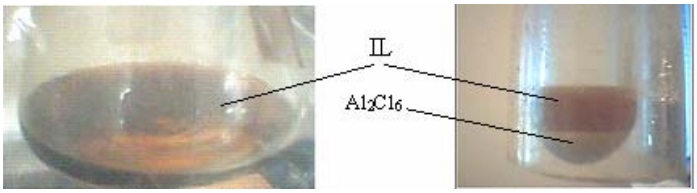

Figure 3.4-a. EMIM-Cl/$AlCl_3$ = 1/2. Figure 3.4-b. EMIM-Cl /$AlCl_3$ = 1/3.

No significant change was observed in the amount of precipitate in the IL ($[AlCl_3/O^+]^o = 3$) upon application of increasing HCl partial pressures at 298 K.

3.3.4 Summary of HCl effects

Shown in Figure 3.5 is a compilation of these calculations as a function of the HCl partial pressure ($0 < P_{HCl} < 44.7$ psia, 0.31 MPa) for a range of $[Al/O^+]^o$ ratios of 1 to 100. The mole fractions of $AlCl_4^-$ and Al_2Cl_6 in these mixtures depend only upon the initial fraction of Al in the mixture and these mole fractions do not depend upon the HCl partial pressure. Some recent literature citations [6] suggest that HCl interacts with the

IL to alter the proportional of monomeric aluminum anion to dimeric aluminum anion by the following equilibrium:

$$O^+Al_2Cl_7^- + HCl \Leftrightarrow H^+\{O^+[(AlCl_4)^-]_2\} \qquad (3.6)$$

The conclusion based upon this report apparently is different from our predictions. We shall comment more on these findings.

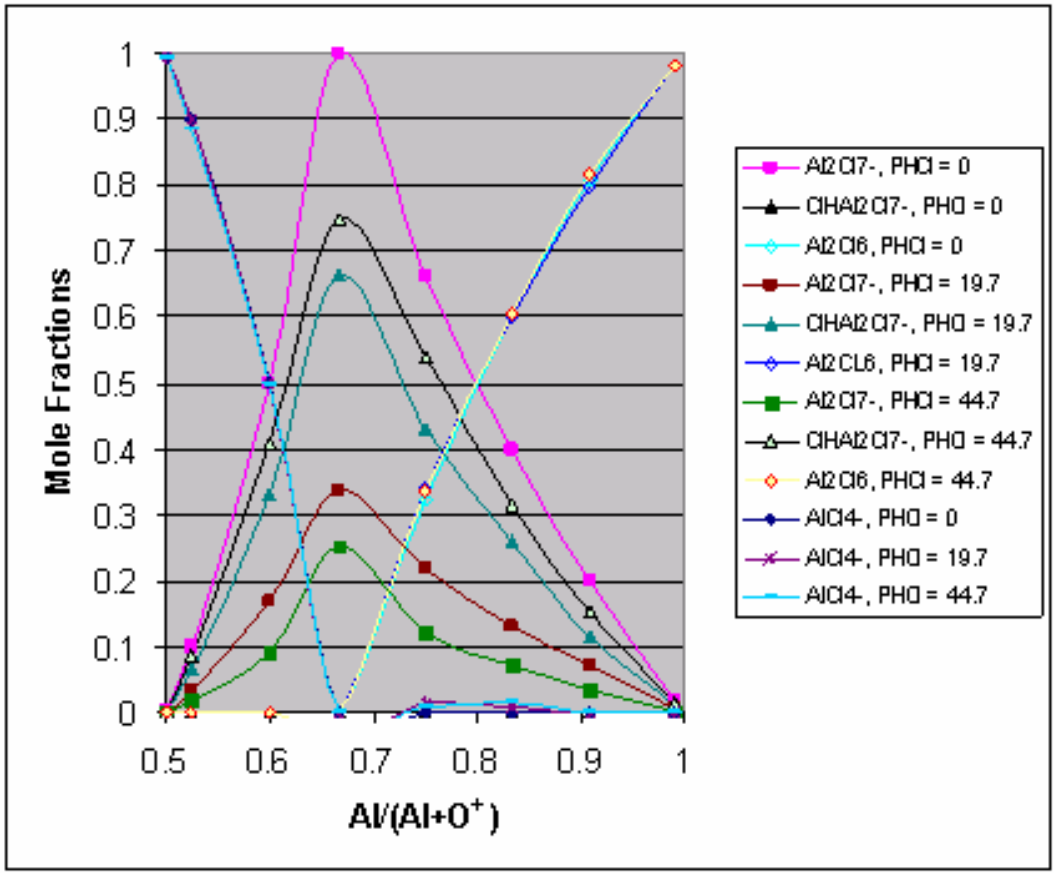

Figure 3.5. Summary of Equilibrium Calculations on Acidic IL in Contact with HCl.

On the other hand, the mole fractions of the Lewis and Brønsted acids ($Al_2Cl_7^-$ and $ClHAl_2Cl_7^-$) depend upon the composition of the initial mixture and the partial pressure of HCl above the IL. Notice how the mole fraction of the Brønsted acid increases with increasing partial pressure of HCl and that the mole fraction of the Lewis acid decreases, proportionally, with increasing partial pressure of HCl over the range of $[AlCl_3/O^+]^o$ ratios from 1 to 100. Thus, the trend suggested for the cases where $[AlCl_3/O^+]^o = 2$ and 3 appears to describe also the behavior of the species found in the IL's having a wider range of $[AlCl_3/O^+]^o$ ratios.

3.3.5 Effect of HCl on Brønsted and Lewis acids

The simulations of the chemical equilibria that were used to summarize the effect of adding HCl gas to the acidic chloroaluminate IL's (Figure 3.5) can be examined in more detail to describe the effect upon the molar amounts of $ClHAl_2Cl_7^-$, Figure 3.6, when the partial pressure of HCl in the gas phase was 0, 19.7 (135 kPa) and 44.7 psia (0.31 MPa) and when $1 < [AlCl_3/O^+]^o < 2$. When no HCl was added, there was no super acidic chloroaluminate anion formed; however, when HCl was present at 19.7 (135 kPa) or 44.7 psia (0.31 MPa), super acidic anion was formed. Moreover, the molar amount of super acidic anion appears to increase linearly with increasing ratio of $[AlCl_3/O^+]^o$ when the partial pressure of HCl was either 19.7 (135 kPa) or 44.7 psia (0.31 MPa). Certainly, this species would be directly involved in the initiation of the toluene carbonylation reaction and these results suggest that the conversion of toluene would be proportional to the ratio: $[AlCl_3/O^+]^o$.

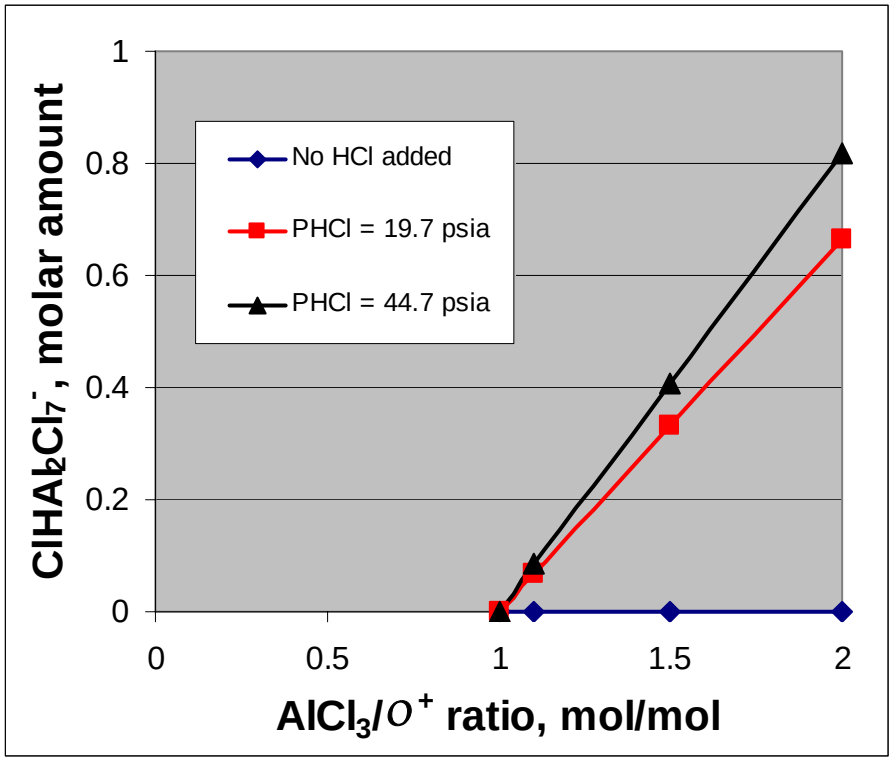

Figure 3.6. Effect of HCl upon super acidic chloroaluminate anion, $ClHAl_2Cl_7^-$.

Our predictions, Figure 3.7, show that the chloroaluminate anion has the highest molar amount for the case when no HCl was added to the gas phase which is in keeping with the hypothesis that the acidic chloroaluminate anion arises from the chloroaluminate anion by reaction with dissolved HCl. Increasing the partial pressure of HCl above the IL causes a dramatic decrease in the chloroaluminate anion.

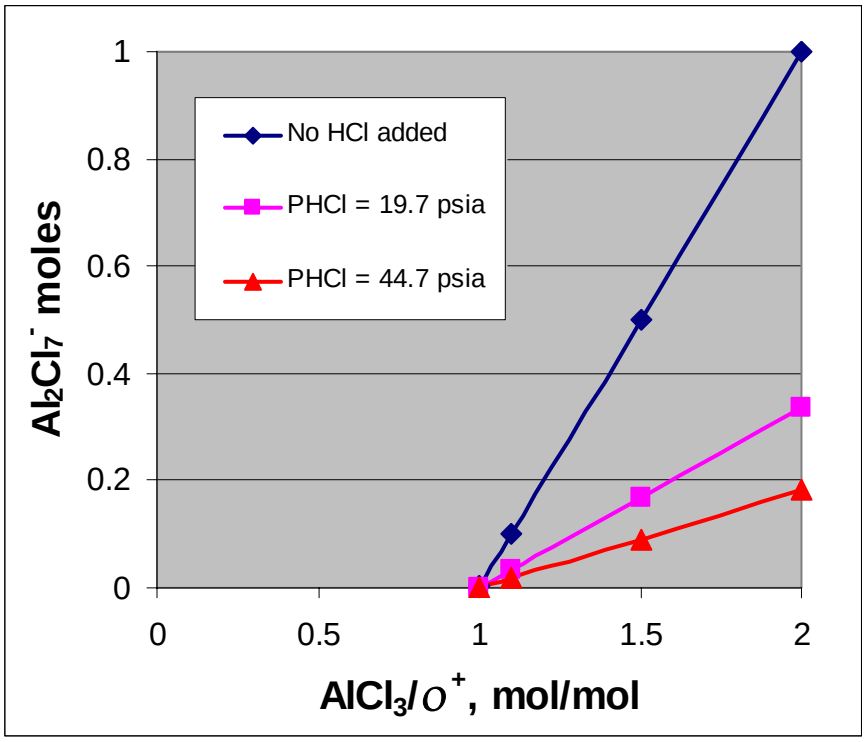

Figure 3.7. Estimates of Lewis acidic chloroaluminate anion $Al_2Cl_7^-$.

For all partial pressures of HCl, the chloroaluminate anion molar amount increases linearly with the ratio $[AlCl_3/O^+]^o$.

3.3.6 Correlation of Toluene Conversion Data

The next step is to properly use these equilibrium predictions to simulate our results from the formylation of toluene in acidic chloroaluminate IL's [7, 8]. The *ultimate* conversion of toluene to form tolualdehyde increased linearly [7, 8] with increasing ratio of $[AlCl_3/O^+]^o$ at a constant partial pressure of HCl at 44.7 psia (0.31 MPa) over the room temperature IL. The toluene formylation is equilibrium limited

owing to its slightly positive, free energy of reaction (~ 8 kcal/mol, 34 kJ/mol) [9] unless an agent is present to sequester the product so that the reverse reaction cannot occur. It was observed this same effect with the triflic acid system so that the ultimate conversion of toluene to tolualdehyde depended upon the formation of an adduct with the product aldehyde so as to shift the chemical equilibrium to its product [10]. Thus, the final conversion of reactant was determined by the amount of acid present initially in the reaction mixture. The reaction becomes a stoichiometric reaction rather than a catalytic reaction because the "catalyst" cannot be regenerated *in situ*. Thus, it is possible to predict the ultimate toluene conversion knowing only the composition of the starting mixture [10]. We speculate that this same chemistry may be observed for the reaction completed in the acidic, chloroaluminate IL's. Thus, it is appropriate to examine species in the IL that may form an adduct with the product aldehyde. One such species is the super acidic chloroaluminate anion ($ClHAl_2Cl_7^-$) as it plays the same role in the IL system as triflic acid plays: a) a catalyst to initiate the reaction mechanism and b) the same species becomes an agent to sequester the aldehyde against the back reaction by forming a carbocation and/or an oxonium ion. We believe that the strong Lewis acid, $Al_2Cl_7^-$, can also sequester the aldehyde by forming an adduct with the aldehyde. The stoichiometry for adduct formation will be discussed below.

The reaction can only be initiated by a super acidic species; therefore, no reaction will be observed if no super acidic species is present. This condition is met when the ratio $[AlCl_3/O^+]^o = 1$ for *all values of the HCl partial pressure*. Therefore, we expect that no toluene carbonylation will be observed when $[AlCl_3/O^+]^o = 1$ and that is what we observed [7, 8]. When $[AlCl_3/O^+]^o > 1$ and for HCl present in the gas phase, the

thermodynamic predictions show that a) the super acidic, chloroaluminate anion ($ClHAl_2Cl_7^-$) is present to initiate the reaction and to sequester part of the tolualdehyde and b) the Lewis acidic chloroaluminate anion ($Al_2Cl_7^-$) is also present to sequester the remaining amount of tolualdehyde. The ultimate conversion of toluene will be governed by the sum of the species that can sequester the aldehyde: $ClHAl_2Cl_7^- + Al_2Cl_7^-$. We may now speculate on the stoichiometry by which the tolualdehyde is sequestered by these two species. From the literature of triflic acid [11] and its hydrates, the water molecules can form adducts with triflic acid, CF_3SO_3H n H_2O, with n = ½, 1, 2, and 4. Water is a weak Lewis base in that it shows lone pairs of electrons on the oxygen that can be donated into a Lewis acid and or can be protonated by a strong Brønsted acid. In this manner water is similar to tolualdehyde in its interaction with strong Lewis and Brønsted acids and thus we expect that tolualdehyde may form an adduct with $ClHAl_2Cl_7^-$ with a stoichiometry of ½, 1, 2 or 4. We speculate that the Lewis acidic chloroaluminate anion can sequester at most 1 tolualdehyde molecule. The predicted toluene conversion is n x moles of $ClHAl_2Cl_7^-$ + 1 x moles of $Al_2Cl_7^-$ for values of n = ½, 1, 2, or 4. Accordingly, the observed toluene conversion per mole of $AlCl_3$ present initially in the system was plotted *versus* the fraction of Al originally present as super acidic chloroaluminate anion and the chloroaluminate anion weighted by the stoichiometry of n tolualdehyde molecules/super acid and 1 tolualdehyde molecule/Lewis acid (Figure 3.8). Only when n = 1, did the predicted toluene conversion agree with the observed toluene conversion for the cases $[AlCl_3/O^+]^o$ = 1.0, 1.1, 1.5, and 2. A slope of one suggests that the assumed stoichiometries for binding the tolualdehyde molecules were true and that the toluene conversion data were correlated with the predicted species amounts. These results

suggest that the toluene formylation reaction under added HCl gas can be correlated from the results of a simple chemical equilibrium theory. The ultimate conversion to the product aldehyde is predicted well from a consideration of the distribution of super acidic Brønsted ($ClHAl_2Cl_7^-$) and Lewis acid ($Al_2Cl_7^-$) chloroaluminate anions in the IL under HCl gas.

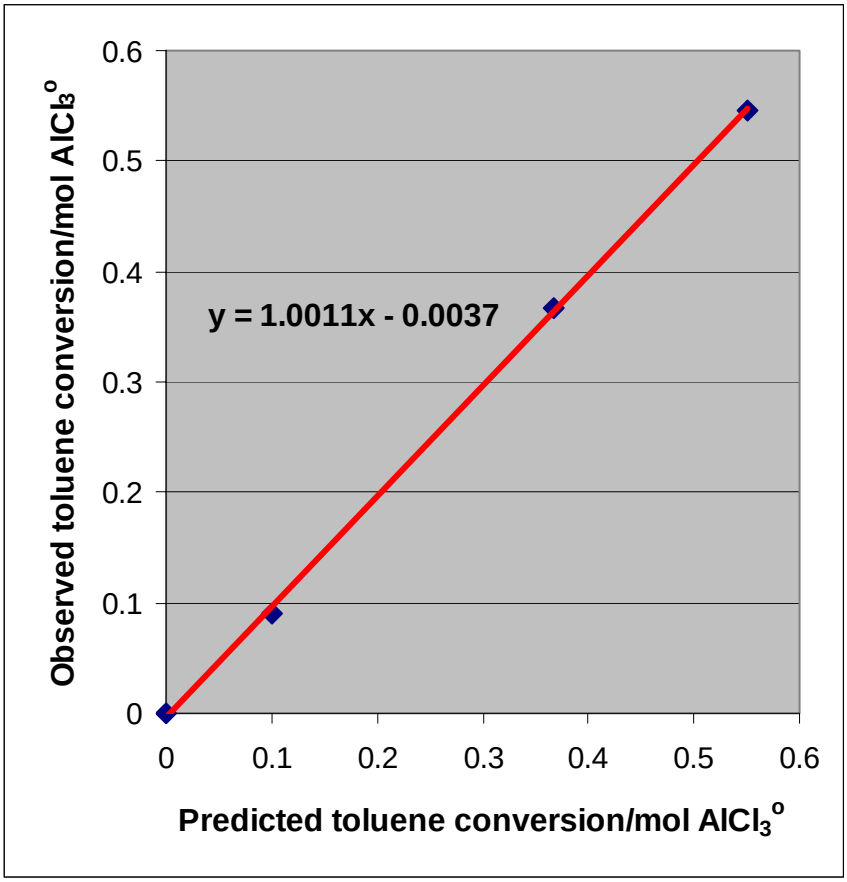

Figure 3.8. Correlation of Toluene Conversion with Predicted Amounts of Brønsted and Lewis Acids in IL.

These thermodynamic estimates of the superacidic Brønsted chloroaluminate anion molar amounts can also be used to correlate data of toluene conversion versus reaction time in a batch reactor for varying partial pressures of HCl. Data [7, 8] at low

conversion could be correlated with reaction time to produce initial slopes that were equal to the product: $k[CO][ClHAl_2Cl_7^-][AlCl_3]^o$ where [CO] is the concentration of CO dissolved in the IL. This dissolved CO concentration depends upon the partial pressure of CO above the IL, P_{CO}, the temperature, and the Brønsted acidity of the liquid [12]. Since the slope data were extrapolated to zero conversion, the concentration of product aldehyde is zero and therefore the Lewis acidic chloroaluminate anion ($Al_2Cl_7^-$) was assumed to play no role in the chemistry under these "extrapolated" conditions. Accordingly, we seek to fit the slope data to the molar amount of super acidic Brønsted chloroaluminate anion (Table 3.1).

Table 3.1. Correlation of slope data from integrated rate plot [8].

HCl Partial Pressure, psia	$ClHAl_2Cl_7^-$, moles	$k[CO][ClHAl_2Cl_7^-]$
0	0	0.0000826
19.7 (135 kPa)	0.663	0.00151
29.7 (204 kPa)	0.748	0.00223
44.7 (308 kPa)	0.817	0.00331

These data could be correlated on a semi-log plot (Figure 3.9) with the equation shown below:

$$\log_{10}\{k[CO][ClHAl_2Cl_7^-]\} = 1.94[ClHAl_2Cl_7^-] - 4.09 \qquad (3.7)$$

therefore

$$k = 10^{(-4.09)} \text{ and } [CO] = HP_{CO} = 10^{\{1.94[ClHAl2Cl7-]\}}/[ClHAl_2Cl_7^-] \qquad (3.8)$$

From a consideration of these correlations, we suggest that the IL not in contact HCl shows a rate constant for this reaction equal to $10^{-4.09}$ and the effect of HCl on the reactivity of this IL can be correlated directly with the super acidic Brønsted chloroaluminate anion molar amount, predicted from equilibrium thermodynamics, and indirectly through the effect of this super acid on the solubility of the CO in this IL through the effective Henry's law constant, *H*, equation (3.8).

Data from the literature of arene carbonylation by trifluoromethane sulfonic acid shows that the CO solubility depends upon the acid strength of the media [12]. That is, CO is much more soluble in triflic acid ($-H_o = 14.1$) than it is in concentrated sulfuric acid ($-H_o = 12$) at the same temperature and CO partial pressure. This observation is consistent with our correlation where the value of the Henry's Law constant depends upon the molar amount of super acidic Brønsted chloroaluminate anion in the IL. The effect of the super acidic Brønsted chloroaluminate anion concentration in the IL upon the CO solubility in the IL is quite significant. When the HCl partial pressure was increased from 19.7 (135 kPa) to 44.7 psia (0.31 MPa), the "apparent" dissolved CO concentration increased by 61% (Eq. (3.8)); whereas, the predicted amount of super acidic Brønsted chloroaluminate anion in the IL increased by only 24%. Measurements of dissolved CO and ($ClHAl_2Cl_7^-$) concentrations in the IL as a function of HCl partial pressure will be necessary to elaborate further the ideas described here.

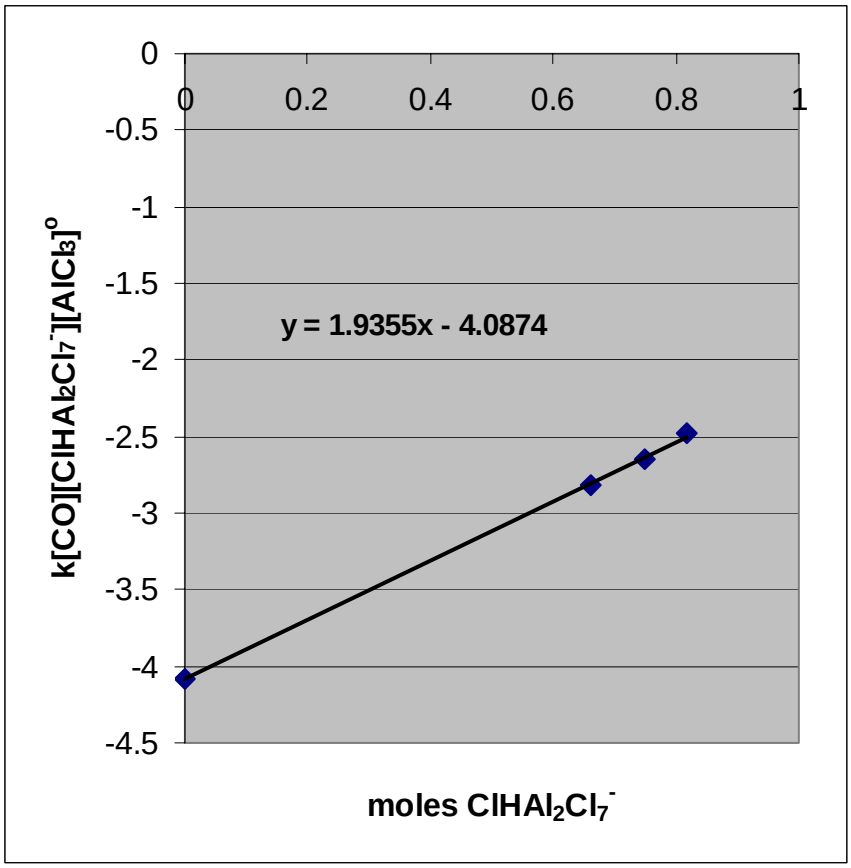

Figure 3.9. Correlation of integrated rate data.

3.3.7 Titration of IL with a Lewis base

It is possible to confirm the assumed stoichiometry of one aldehyde sequestered for every $Al_2Cl_7^-$ by a simple titration experiment. One equivalent of *p*-tolualdehyde per mol of Al in the sample was added to separate IL's which were prepared having the Al/O^+ ratio of ½, 1/l, 1.5/1 and 2/1. Since no HCl was added to this system, we presume that very little Bronsted acid was present. The amount of base and Al was the same in each sample; whereas, the amount of EMIM-Cl was varied to develop the desired Al/O^+ ratio. These first two IL's were basic, and neutral (Al/O^+ = ½, 1/1); whereas, the last two

were acidic (Al/O^{+} = 1.5/1 and 2/1). The mixture of *p*-tolualdehyde and IL was heated to 413 K and placed under a vacuum (200 milliT, 26.7 Pa) for ½ hour so as to remove the weakly absorbed base. The vaporized base was condensed into a trap held at 77 K. The amount of base remaining in the IL was determined by weighing the amount of base found in the trap and subtracting this amount from the initial mass of base placed in the IL. These results are shown in Figure 3.10.

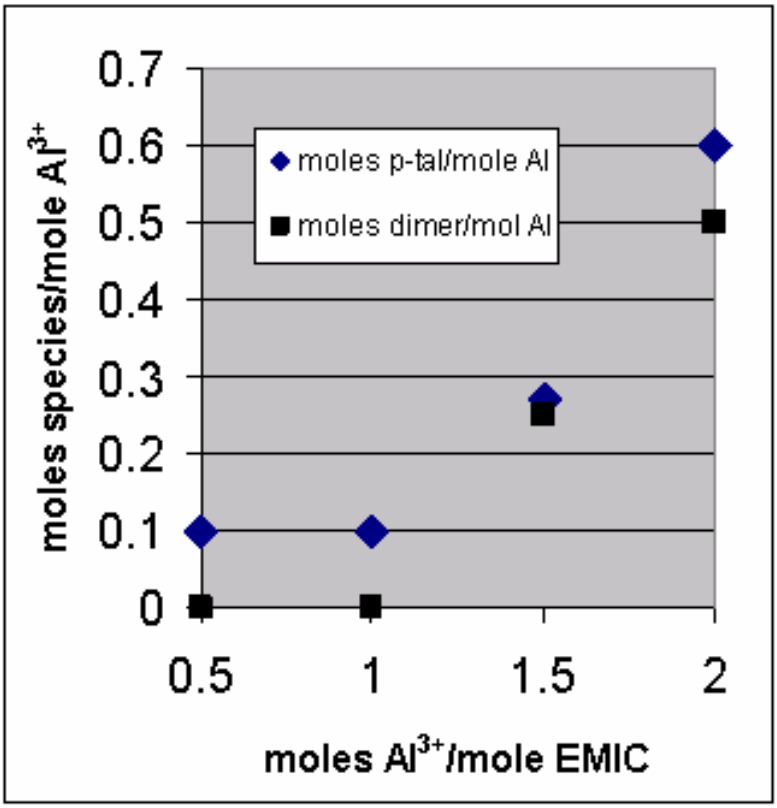

Figure 3.10. Titration of IL by a Lewis Base.

For the basic and neutral IL's, the amount of *p*-tolualdehyde not found in the LN2 trap was ~ 10% of the amount of Al in the system. One might expect that these two IL's would not retain any of the aldehyde as a result of their intrinsic chemistry and this

expectation could be realized if 1) all of the base vaporized from the IL was found in the LN2 trap and 2) the IL's were dry and had not reacted with adventitious water vapor. We speculate that the small amounts of aldehyde not found in the LN2 trap may be explained by a combination of these two reasons. The amount of *p*-tolualdehyde estimated to be retained in the IL increased when increasing the Al/O^+ ratio above unity. On the same figure we show the predicted moles $Al_2Cl_7^-$/mol Al in the IL. Notice that the amount of *p*-tolualdehyde retained in the sample was always slightly greater than the amount of $Al_2Cl_7^-$ predicted to be in the sample. Again, we speculate that a combination of loss of base and/or adventitious moisture may account for the unexpectedly larger amount of base retained in the IL. From the trend with increasing amount of Al in the sample, we conclude that $Al_2Cl_7^-$ does sequester *p*-tolualdehyde in the proportion of 1 mol of aldehyde for every 1 mol of $Al_2Cl_7^-$ (slope of Figure 3.10 = ½ mol p-tolualdehyde / ½ mol of $Al_2Cl_7^-$). This finding suggests a stoichiometry of 1 mol of the aldehyde for every mole of $Al_2Cl_7^-$ in the IL and it confirms our use of this stoichiometry (*vide supra*) in predicting the ultimate conversion of toluene.

3.4 Modeling Molecular Properties

The previous work was aimed at modeling the macroscopic properties of the ionic liquids for the purpose of predicting the concentration of species that may be present in the IL when HCl was added to the gas phase above the IL. It is appropriate to use the quantum mechanics approach to predict also the molecular structures of these ionic liquids so that one can understand the molecular properties of the species present such as

proton and ^{27}Al-NMR chemical shifts. These predicted chemical shifts can be compared to the observed chemical shifts so as to determine the structure of the IL's.

3.4.1 Modeling of the IL's for HCl solubility

Semi-empirical methods (AM-1, PM3 and MNDO) from the Cerius and Spartan '02 software suites were used to 1) optimize the geometry of species in the IL's such as 1-R-3-Me-imidazolium cation, $AlCl_4^-$, $Al_2Cl_7^-$, and $HAl_2Cl_8^-$, and 2) calculate the thermodynamic properties of these equilibrium structures. Although some earlier investigators speculated on the formation of monomeric, Al Brønsted acidic species ($HAlCl_4$), Zawodzinski showed that molecular HCl could be detected in acidic $AlCl_3$-EMIM-Cl [13], and our previous modeling showed that $HAlCl_4$ and $HAlCl_4^-$ were not present in these IL's when the HCl pressure was less than 30 atm. These results may be placed in the context of the older literature where Brown showed that HCl does not react with $AlCl_3$ to form $HAlCl_4$ [14] and thus suggested that this substance only exists as ion pairs at the conditions of their measurements.

Preliminary modeling began by constructing the IL with the following species: $AlCl_3$, $AlCl_4^-$, HCl, and $EMIM^+$. The optimized geometry (PM3) depended upon the initial starting positions of these species which was determined by a MM2 preliminary geometry optimization (Figure 3.11).

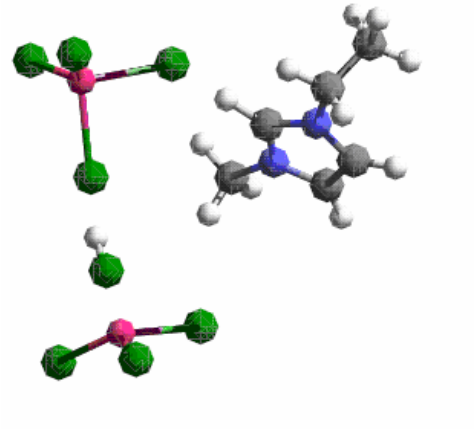

Figure 3.11 - a (-428.7 kcal/mol)

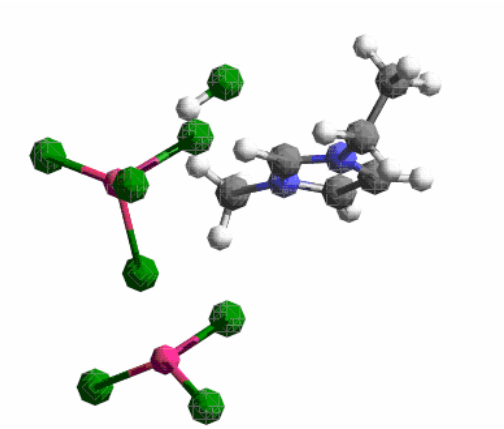

Figure 3.11 - b (-427.7 kcal/mol)

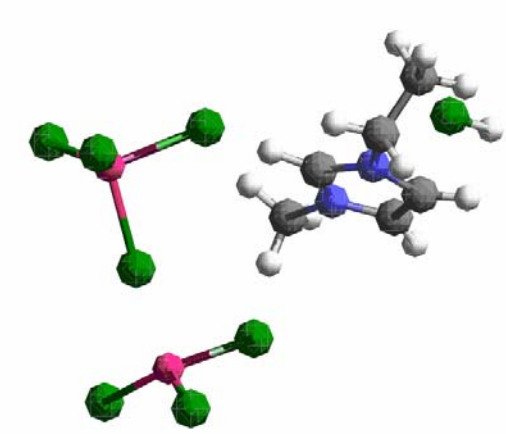

Figure 3.11 - c (-425.1 kcal/mol)

Figure 3.11. Sites for the HCl in the Ionic Liquids.

In every case, the $AlCl_3$ and $AlCl_4^-$ associated to form a pair with a short distance between the coordinately unsaturated site of the $AlCl_3$ and a Cl from either the $AlCl_4^-$ or the Cl of the bridging HCl. The HCl was located in three distinctive structures: 1) between the $AlCl_3$ and $AlCl_4$ anion to form structure 3.11-a (ΔG^o_f = -428.7 kcal/mol); 2) between the anion and cation (structure 3.11-b; ΔG^o_f = -427.7 kcal/mol), or 3) associated with the cation (structure 3.11-c; ΔG^o_f = -425.1 kcal/mol). Since the aluminum species always appeared as a pair, and since earlier modeling work by Chandler and Johnson [2] supports a dimeric Al species as the structured favored in acidic, chloroaluminates, subsequent modeling efforts will examine the dimeric anion $Al_2Cl_7^-$ as the building block for the anionic species in these acidic IL's and these results will be compared to the free energies of the optimized geometries for these structures with the free energies of formation that were developed from monomeric chloroaluminate species so as to determine the structure(s) of the thermodynamically-favored, chloroaluminate species in equilibrium with HCl.

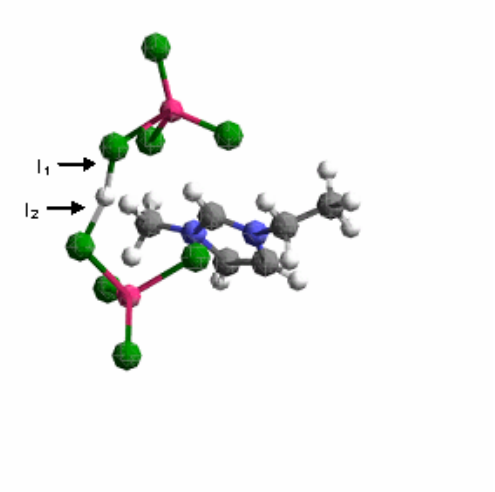

3.12-a. ClHCl bridging ($AlCl_3$) polyhedra

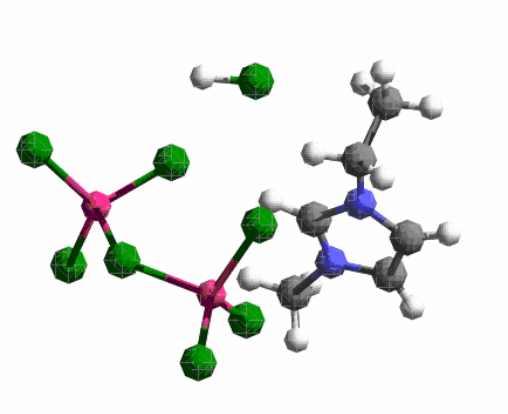

3.12-b. HCl between anion & cation

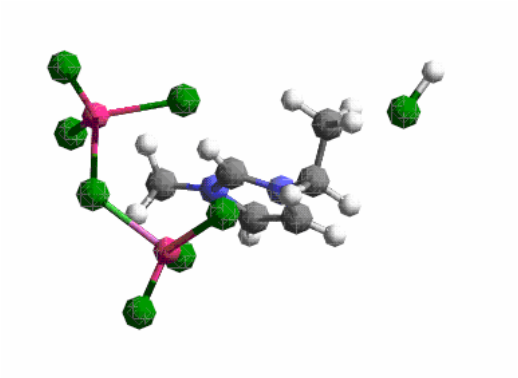

3.12-c. HCl near cation

Figure 3.12. Three Structures for Siting of HCl in $EMIM^+$-$Al_2Cl_7^-$ Ionic Liquid.

The modeling of the IL by semi-empirical methods revealed three possible optimized structures, Figure 3.12, that developed upon absorption of HCl gas at room temperature. As an example, consider the results from the PM3 model which shows the HCl inserted into the $Al_2Cl_7^-$ anion to form a bridging species (Figure 3.12-a). In the second structure, HCl was associated with the $Al_2Cl_7^-$ anion through a terminal Cl and

also associated with the imidazolium cation through the C-2 proton (Figure 3.12-b) (See Figure 3.14 for carbon identification). The third structure shows the HCl species involved with the cation only (Figure 3.12-c). The free energies of formation for each of these three species at 298 K were as follows: 3.12-a, -428.93 kcal/mol; 3.12-b, -430.59 kcal/mol; and 3.12-c, -427.26 kcal/mol. These free energies of formation were lower for the chloroaluminate species appearing as the anionic dimer ($Al_2Cl_7^-$) rather than as the pair of species ($AlCl_3/AlCl_4^-$). The dimer structures were favored by 0.23 kcal/mol (3.12-a vs. 3.11-a), 2.9 kcal/mol (3.12-b vs.3.11-b), and 2.2 kcal/mol (3.12-c vs. 3.11-c). Considering the accuracy of the predictions (± 4.0 -5.0 kcal/mol) [15] the dimers (Figure 3.12) would appear to show a free energy of formation similar to the corresponding structures in Figure 3.11. For HCl placed between the anion and cation, changes in either the cation or the anion would affect the amount of HCl absorption into the IL and thus could have a direct influence of the reactivity of the IL for Brønsted-demanding reactions. On the other hand, HCl attached to structure 3.12-a would be largely influenced by the type of anion metal chloride; whereas, HCl absorption in structure 3.12-c would influenced mainly by changes in the structure of the imidazolium cation. One can interrogate the degree of influence these structural changes in the cation might have on the HCl absorption equilibria by calculating the free energy change associated with the following equation to model HCl absorption:

$$\{RMIM^+ Al_2Cl_7^-\} + HCl \Leftrightarrow \{RMIM^+ HCl\ Al_2Cl_7^-\} \qquad (3.9)$$

We show here the free energies of formation for the three structures of the absorbed species as R was changed using three semi-empirical quantum mechanical programs: AM-1, PM3, and MNDO (Tables 3.2-3.4).

Table 3.2. $\Delta G_{Absorption}$ for HCl into $RMIM^{+}$-$Al_2Cl_7^{-}$ IL and HCl bond length (AM-1).

Alkyl group, R	$\Delta G_{Absorption}$, kcal/mol			HCl bond length, Å (gas phase = 1.28 Å)			
Structure→	12-a	12-b	12-c	12-a (I_1)	12-a (I_2)	12-b	12-c
Ethyl	11.7	3.4	2.8	1.53	1.63	1.32	1.29
Butyl	11.9	5.5	4.6	1.55	1.61	1.32	1.29
Benzyl	11.4	4.2	6.2	1.53	1.63	1.32	1.29
Hexyl	13.8	3.3	7.1	1.56	1.61	1.32	1.29
Octyl	12.6	3.6	7.4	1.53	1.63	1.32	1.29
Dodecyl	18.4	4.0	8.3	1.53	1.64	1.32	1.29

Table 3.3. $\Delta G_{Absorption}$ for HCl into $RMIM^{+}$-$Al_2Cl_7^{-}$ IL and HCl bond length (PM3).

Alkyl group, R	$\Delta G_{Absorption}$, kcal/mol			HCl bond length, Å (gas phase = 1.27 Å)			
Structure→	12-a	12-b	12-c	12-a (I_1)	12-a (I_2)	12-b	12-c
Ethyl	2.3	0.7	4.0	1.53	1.52	1.35	1.27
Butyl	-0.8	1.1	2.7	1.53	1.51	1.35	1.27
Benzyl	4.7	1.7	4.6	1.53	1.51	1.35	1.27
Hexyl	2.8	0.9	6.8	1.52	1.52	1.34	1.28
Octyl	-0.4	0.3	1.2	1.53	1.50	1.34	1.28
Dodecyl	4.9	0.5	6.6	1.53	1.52	1.34	1.28

Table 3.4. $\Delta G_{Absorption}$ for HCl into $RMIM^{+}$-$Al_2Cl_7^{-}$ IL and HCl bond length (MNDO).

Alkyl group, R'	$\Delta G_{Absorption}$, kcal/mol			HCl bond length, Å (gas phase = 1.35 Å)			
Structure→	12-a	12-b	12-c	12-a (I_1)	12-a (I_2)	12-b	12-c
Ethyl	15.4	3.0	3.0	1.60	1.62	1.35	1.35
Butyl	16.6	4.0	3.8	1.60	1.61	1.35	1.35
Benzyl	15.3	2.4	1.4	1.60	1.60	1.352	1.35
Hexyl	17.1	2.1	2.5	1.60	1.63	1.36	1.35
Octyl	18.9	2.8	2.2	1.60	1.62	1.35	1.35
Dodecyl	18.2	1.2	2.3	1.60	1.61	1.35	1.35

Two of three models (AM-1, and MNDO) predicted the highest values of the free energies of absorption for HCl absorption at the 3.12-a site. The PM3 predictions show that no one site for the HCl is favored for each and every cation. If one considers the inaccuracy in these predictions for the free energy (± 4.0 -5.0 kcal/mol) [15], siting of HCl at the 3.12-b and 3.12-c sites show about the same free energy of absorption from the predictions of the MNDO model. The AM-1 model shows similar ΔG absorption for structures 3.12-b and 3.12-c for all R. The PM3 predictions show the same $\Delta G_{absorption}$ for the 3.12-b, 3.12-c sites only for the cations ethyl, butyl, benzyl and octyl.

The H-Cl bond length can be estimated using the semi-empirical models and all three models (AM-1, PM3, and MNDO), show that the HCl bond length depends upon the structure (3.12-a, 3.12-b, 3.12-c) but a systematic change in the bond length was not observed for changing R. All 3 models showed that structure 3.12-a exhibit similar HCl bond length (1.52 – 1.60 Å), and this bond is I_1 in Figure 3.12-a. For most cases of R, AM1 and MNDO predicted that bond I_2 was longer than I_1 (1.59-1.63 Å) while PM3 predcited I_2 to be the similar to I_1 (1.51-1.53). The three models demonstrated that the H-Cl bond length for the 3.12-c structure was the shortest, often very similar to the bond length predicted for the isolated gas phase molecule by the same model (1.284 Å for AM1, 1.268 Å for PM3, and 1.348 Å for MNDO). Predicted values for the H-Cl bond lengths in structure 3.12-b were 1.32 Å for AM1, 1.34 – 1.35 Å for PM3, and 1.35 Å for MNDO. From these predictions, one might infer that the H-Cl bond length may depend upon its environment, being longest when associated with the chloroaluminate anion, shortest when associated with the cation, and of some intermediate bond length when associated with both anion and cation as in the structure 3.12-b. HCl bond length may be

significant as it relates to the reactivity of the H-Cl species for protonation and reaction in the toluene carbonylation reaction. In a control experiment where no IL was present, no conversion of toluene was observed after 18 h of reaction in HCl and CO at the conditions that produced significant conversion to *p*-tolualdehyde when the IL was present.

When this system without the IL was modeled with AM-1, PM3, or MNDO the HCl would associate with the toluene (Figure 3.13) and the H-Cl bond length was no longer than that predicted for the gaseous, isolated HCl molecule by each model. This result shows that the bond length of the H-Cl molecule predicted from the semi-empirical methods may be used in conjunction with the reactivity of the reference system to estimate the relative reactivity of the unknown systems containing the IL. That is, we suggest that HCl sited in the 3.12-c structures are likely to be unreactive towards catalyzing the toluene carbonylation reaction from a consideration of the predicted H-Cl bond lengths being similar to the HCl bond length in the isolated molecule; whereas the HCl sited in the 3.12-a and 3.12-b structures could be reactive towards toluene carbonylation owing to the longer H-Cl bond lengths predicted for these structures. These predictions suggest that at least three absorption sites could be developed when HCl contacts the IL's described here and that the reactivity of the HCl may depend upon its location in the IL structure. Subsequent predictions of ^{1}H-NMR chemical shifts may shed further light on the effect of HCl siting at its potential to become a very strong Brønsted acid.

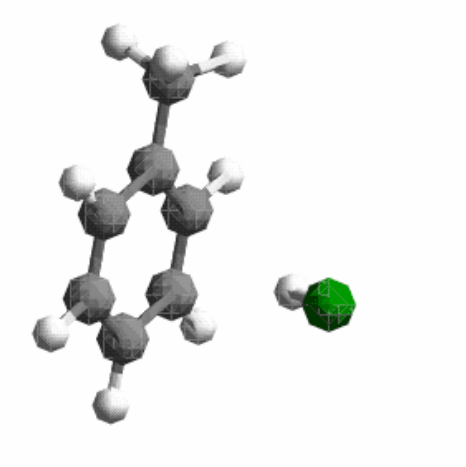

Figure 3.13. Model of HCl in toluene.

3.4.2 ^{1}H and ^{27}Al NMR predictions

NMR probes the environment of the nucleus by assaying the energy required to change the nuclear spin for a species residing in a strong magnetic field. NMR has been used to discover the molecular structure of liquids which are not amenable to the usual technique for elucidating structure: x-ray diffraction. The knowledge of structure and species developed in the IL can help us to understand the reactivity results. For example, the chemical shift of protons in liquids and solids has been used to correlate the intrinsic Brønsted acidity in these systems [16, 17]. In as much as NMR probes the nuclear environment of the proton, one can relate the downfield chemical shift of the proton (*i. e.*, "deshielding" of the nucleus by reduced electron density), it is possible to relate this chemical shift to the charge on the proton and thus infer its acid strength. Such chemical shifts are helpful in interrogating for different proton acid strengths that may be present in a material.

^{1}H-NMR, ^{13}C-NMR and ^{27}Al-NMR data were calculated using HF wave function method with a basis set of 3-21G* orbitals [18]. Some of the geometries were developed from *ab initio* methods using the same basis set whereas other geometries were developed from a PM3 semi-empirical calculation. Others predicted the ^{27}Al-NMR spectra of Al complexes and they showed quite large discrepancies between predicted and observed chemical shifts [19]. Thus, we must rely upon the trends in these calculations to help us establish peak assignments in the NMR spectra.

Significant efforts have been reported by some researchers to understand the molecular environment of the organic cations in the melt, such as the dialkylimidazolium cations. These researchers demonstrated that the chemical shifts of the ring protons on the dialkylimidazolium cations of the melts are highly dependent on the concentrations of aluminum chloride and organic chloride in the melt, whereas the chemical shifts of the protons on the two, alkyl groups (R, R') show little or no composition dependence [20]. Apparently, only some of the cation protons are influenced by the intrinsic acidity of the melt. We attempted to reproduce these results using the Cerius software package resident in the School of Chemical and Biomolecular Engineering and using Spartan '04 molecular modeling package.

3.4.2.1 Predicting Proton NMR in the IL

It was found that the largest downfield peak in the ^{1}H-NMR spectrum is the proton residing on the C-2 carbon which is between the two nitrogens (Figure 3.14). The

predicted and observed chemical shifts are shown in Table 3.5 for the protons on C-2, 4, and 5 carbons in neutral (n = 1) and acidic (n=2) ionic liquids.

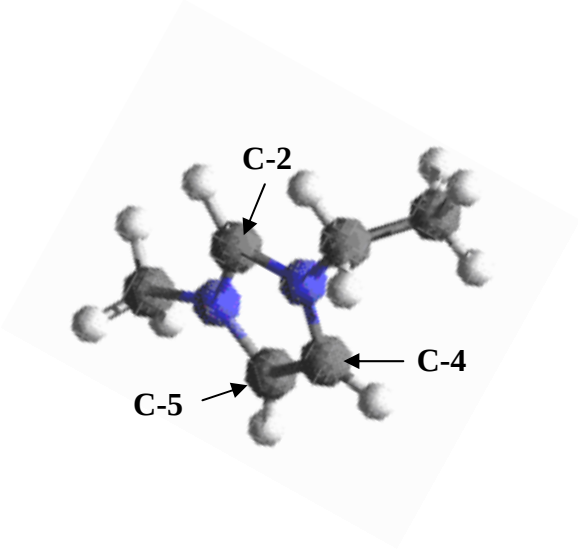

Figure 3.14. Identification of carbons in the organic cation.

Table 3.5. Predicted and Observed ^{1}H-NMR Chemical Shifts in $O^{+}Al_nCl_{3n+1}$.

EMIM	Chemical Shift, ppm from DMSO				
Proton on Carbon Number	Predicted for the structures of			Observed data [20]	
	$AlCl_4^-$	$AlCl_3AlCl_4^-$	$Al_2Cl_7^-$	n = 1	n = 2
2	7.079	14.696	7.106	6.05	6
4	4.741	5.555	4.747	5.05	5.05
5	4.779	5.617	4.784	5.05	5.05

DoMIM	Chemical Shift, ppm from DMSO				
Proton on Carbon Number	Predicted for the structures of			Observed data	
	$AlCl_4^-$	$AlCl_3AlCl_4^-$	$Al_2Cl_7^-$	n = 1	n = 2
2	4.935	8.498	14.54	NA	NA
4	5.701	7.081	5.86	NA	NA
5	5.646	5.692	5.64	NA	NA

A neutral ionic liquid was modeled with n = 1 with either the $(EMIM)^+$ cation or the $(DoMIM)^+$ cation. The predicted ^{1}H-NMR for this structure having the $AlCl_4^-$ anion and the $EMIM^+$ cation shows a chemical shift of 7.08 ppm from DMSO (9.6 ppm from TMS), this without HCl added. For a neutral ionic liquid with the $(DoMIM)^+$ cation, the downfield peak was at 4.94 ppm from DMSO, which is slightly upfield from the proton resonance where the cation was EMIM-Cl. It seems, the longer the chain ligand donates some electron density on this proton which resides on the C-2 carbon of the imidazolium ring in keeping with the classical ligand effect of alkyl groups. The effect of changing R upon the protons residing on the C-4 and C-5 protons was just the opposite. That is, the chemical shifts were shifted 1 ppm downfield when the R-group was changed from ethyl to dodecyl. Data from the open literature could be used to compare with these predictions when R = ethyl when n = 1. The predicted chemical shifts were predicted to be slightly higher for the C-2 proton (by 1 ppm) and for the C-4, 5 protons (0.3 ppm).

Consider next the predicted proton NMR spectrum for the acidic $EMIM^+$ and $DoMIM^+$ IL's where n = 2. We have shown that two different models for the anion can be used to describe the acidic IL: the anion pair ($AlCl_3AlCl_4^-$) and the dimer ($Al_2Cl_7^-$). In Table 3.5 we show the proton chemical shifts for these two models of the anion. For the $EMIM^+$ cation, the anion pair model produces a C-2 protons with a large chemical shift downfield (~14 ppm from DMSO) whereas with the dimer the predicted chemical shift for this proton is ~7 ppm from DMSO which is similar to that predicted for the neutral IL. The observed chemical shift for the acidic IL is 6 ppm from DMSO and one could conclude that the predictions from the dimer model for the anion are more accurate or that very little of the anion pair is present in the actual IL. Consider next, the modeling of

the IL having R = dodecyl. Here the C-2 proton for the anion pair shows a chemical shift of 8.5 ppm from DMSO; whereas the prediction with the dimer model is 14.5 ppm from DMSO. This modeling of the IL without HCl added suggests that the neutral species is modeled well by the software as confirmed by the observed proton NMR. Modeling results for the acidic IL's can be reconciled with the observed chemical shifts when one permits the Al speciation to change with the structure of the cation (i. e., with R). This result must be confirmed by direct observation of the ^{27}Al-NMR.

3.4.2.2 Proton NMR of IL when HCl is added

The predicted proton NMR spectrum of isolated HCl gas shows a single resonance at 1.68 ppm from TMS. The NMR spectrum of the HCl proton can be predicted when it was added to an intrinsic acidic ionic liquid (EMIM-Cl/$AlCl_3$). When HCl was placed between the Al's of the anion pair, it showed a downfield peak at 15.3 and 17.2 ppm from TMS. The peak at 15.7 ppm is the proton in HCl and the peak at 17.2 is the proton on the C-2 carbon (Table 3.6). The introduction of HCl into this structure caused the C-2 to experience a chemical shift from 9.6 to 17.2 ppm and therefore become very acidic as a result of the addition of HCl to the aluminum anion. This increased acidity of the C-2 proton seems highly unlikely. When the HCl was place between the anion and cation the proton resonances for HCl and C-2 proton are 14.3 and 17.7 ppm. Resonance of the HCl proton is about 1 ppm upfield from that shown when HCl was placed between the anion pair. For the HCl placed on the cation, the proton resonance was 2.6 ppm, which is only 0.8 ppm downfield from the resonance in isolated, gaseous

HCl. We may infer, based on the chemical shifts that this proton in less acidic when the HCl was sited near the cation rather than when located near the anion. Also shown in Table 3.6 are the predictions for the ^{1}H-NMR chemical shifts when the dimer model for the aluminum species is used and R = ethyl. Notice that the chemical shifts predicted for the HCl protons are similar to those predicted using the anion pair model for the aluminum species. Thus, the choice of anion model does not appear to influence the chemical shift predicted for the HCl proton.

Table 3.6. Predicted ^{1}H-NMR Chemical Shifts in RMIM-HAl_2Cl_8 IL's.

Proton NMR Resonance	ppm downfield from TMS	
In the model	Al EMIM	Al DoMIM
3.11 (a) pair	15.3	15.3
3.11 (b) pair	14.3	14.4
3.11 (c) pair	2.50	2.70
3.12 (a) dimer	15.4	15.5
3.12 (b) dimer	14.4	10.6
3.12 (c) dimer	2.60	2.40

The same calculations were repeated for the case when R = dodecyl. The results of these calculations suggest that the size of the R-group does not influence the chemical shift of the HCl proton.

Thus, we conclude that the three sites for HCl in the IL show different acidities and that the most acidic site is that where the HCl resides in the anion. The predicted ^{1}H-NMR chemical shifts mirror the predicted bond lengths between the H-Cl atoms; *i. e.*, the largest chemical shift downfield of TMS corresponds to the longest H-Cl bond length.

This prediction must be confirmed by experiment. Moreover, these predictions suggest that the proton residing on the C-2 carbon can be quite acidic; depending upon the presence of HCl in the mixture and this unexpected prediction must be examined by experiment.

3.4.2.3 Predicting ^{27}Al-NMR chemical shifts in the IL

^{27}Al NMR predictions demonstrated a more complicated picture in that the aluminum species may be monomeric (e. g., $AlCl_4^-$), dimeric ($Al_2Cl_7^-$) or the anion pair ($AlCl_3AlCl_4^-$) and the concentrations of these species in the IL depends upon the ratio of the organic cation and inorganic anion. In our effort, we used aqueous $Al(NO_3)_3$ as an external reference for both the predictions and the observations. The predicted chemical shift was 72.4 ppm downfield from aqueous aluminum nitrate for $AlCl_4^-BMIM^+$, which is our model for the neutral ionic liquid. It is generally accepted in the literature that the $AlCl_4^-$ anion is the predominant species in the neutral (n=1) IL (Figure 3.15).

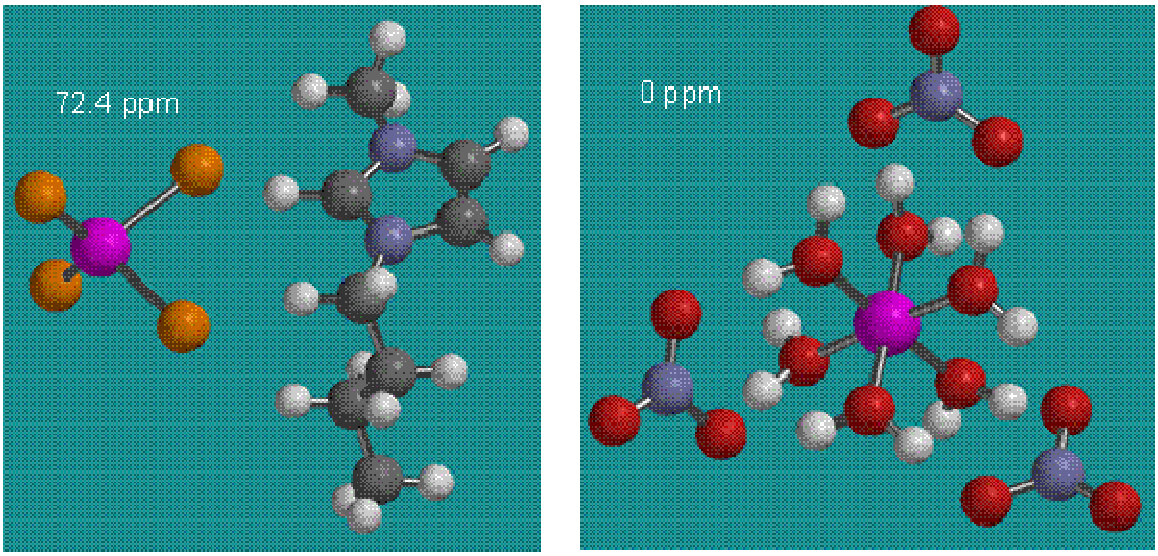

a - Monomeric $AlCl_4^-BMIM^+$ b- Aqueous $Al(NO_3)_3$ External Reference

Figure 3.15. ^{27}Al NMR prediction for a neutral ionic liquid.

For an intrinsically acidic ionic liquid the phase diagram [5] demonstrated more than one type of aluminum species. It was of interest to model the formation of these species when n = 2 in the ionic liquid formation using Transition State Geometry Optimization (Figure 3.16). We assumed that the IL contained initially the species shown in scheme I: the dialkylimidazolium chloride and Al_2Cl_6. These species were placed in the program as the reactants and the program was initiated to give the geometry of the optimized transition state. It was observed that the symmetry of Al species has been lowered and that the distance of the C-Cl bond was lengthened. Two possible products can be obtained upon coming out of this transition state. Product 1 is the dimeric anion $Al_2Cl_7^-$, which is generally accepted as the structure of this anion in an intrinsic acidic ionic liquid. The two aluminums are in similar chemical environment and show chemical shifts of 69.8 and 69.7 ppm, approximately 2.6 and 2.7 ppm upfield from

the predicted chemical shift of the monomeric aluminum anion $AlCl_4^-$. Product 2 is the anion pair, $AlCl_3$ $AlCl_4^-$, and this species has not been proposed in the open literature. The two aluminums are in different chemical environment and they show chemical shifts at 62.7 and 60 ppm, even more upfield of the neutral monomeric species, than the dimeric anion $Al_2Cl_7^-$. The free energies of formation are nearly the same (~100 kcal/mol) for these two species and therefore these two products have equal opportunities to be formed. Moreover, since the free energies of formation are the same for these two species, appeal to thermodynamics cannot arbitrate between presences in actual IL's. Some other characterization must be used in this arbitration and it appears that ^{27}Al-NMR chemical shifts might be useful.

Scheme I

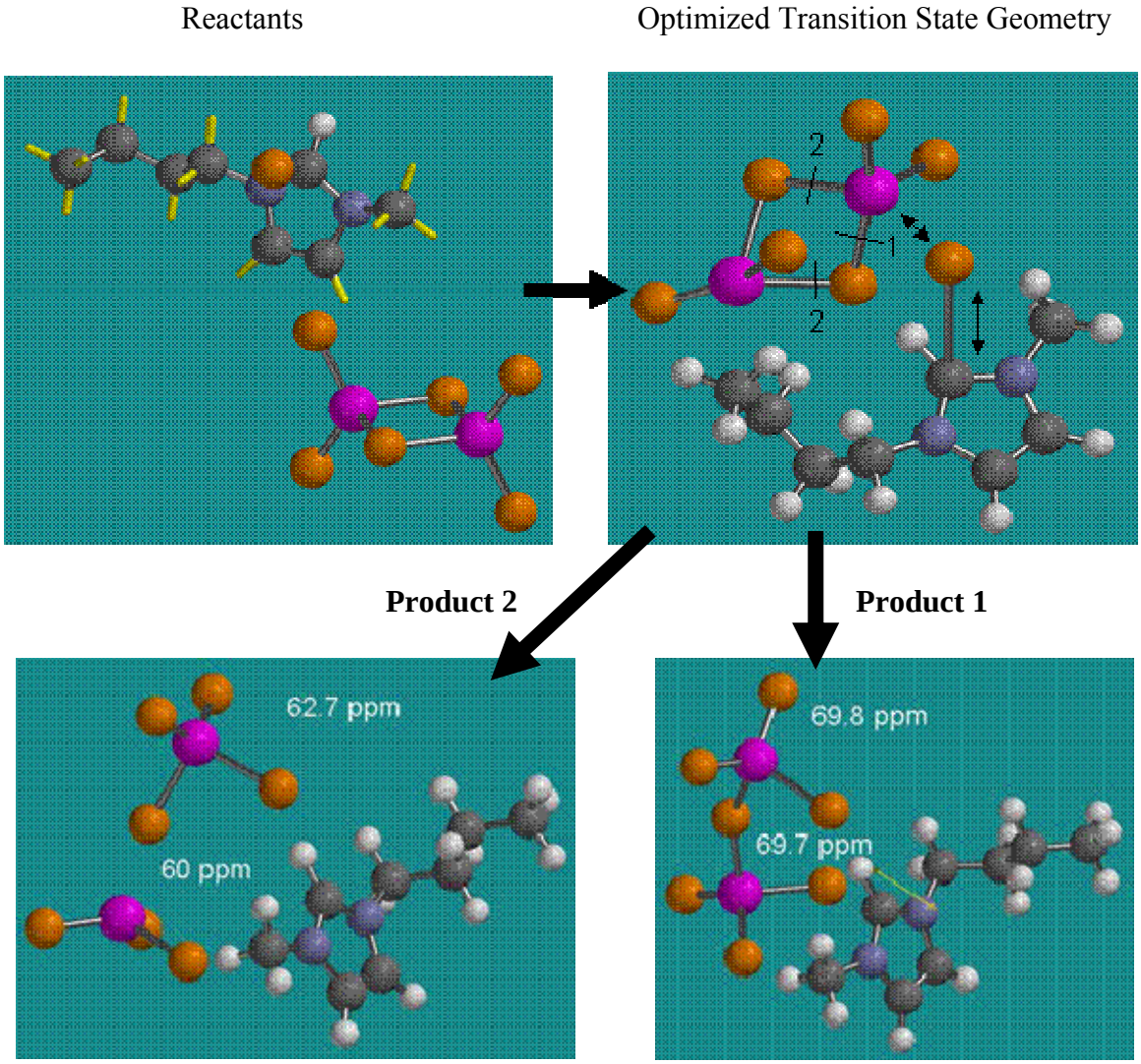

a - Anion Pair: $AlCl_3$ $AlCl_4^-$

$\Delta G^o_{formation}$ = 99.69 kcal/mol

b - Dimeric Anion: $Al_2Cl_7^-$

$\Delta G^o_{formation}$ = 99.68 kcal/mol

Figure 3.16. Ionic liquid formation using Transition State Geometry Optimization.

Given these predictions for the ^{27}Al-NMR for the different structures of aluminum species, it should be possible to predict the spectrum of IL's for a given value of n. Consider the cases when n = 3/2 and 2. Predictions [2] from equilibrium

thermodynamics suggest that monomeric and dimeric aluminum compounds should be present when n = 3/2 and that only dimeric aluminum species should be present when n = 2. Consider our attempt to predict these spectra (Figure 3.17) using the chemical shifts for the three different aluminum species ($AlCl_4^-$; $AlCl_3AlCl_4^-$; and $Al_2Cl_7^-$). The observed data in Figure 3.17 will be described in detail in Chapter V. The adjustable parameters for the predictions were the 1) peak height (*i. e.*, composition) and 2) peak width at the ½ height. Notice that satisfactory predictions of the observed spectra could be achieved by adjusting only these two parameters. One interesting result of this fit is the fraction of the dimer is very large for the $BMIM^+$ cation when n = 2 whereas this fraction of the dimeric aluminum species is much smaller when n = 3/2. It appears that this fitting routine might be appropriate to determine if changing R has an effect upon the Al speciation in the IL's.

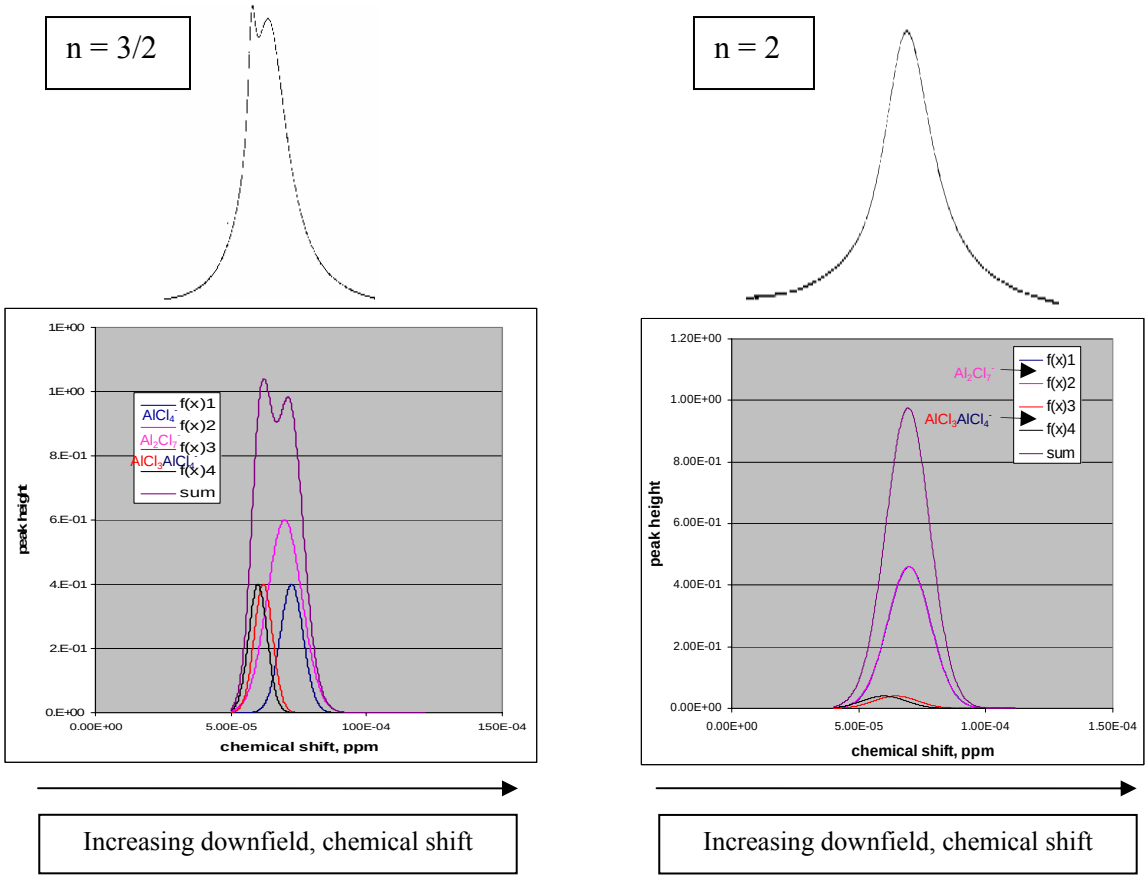

Figure 3.17. Predicted (bottom) and Observed (top) ^{27}Al-NMR Spectra for BMIM-Al_nCl_{3n+1}.

3.5 Discussion

Simple equilibrium thermodynamic calculations were used to predict the composition of chloroaluminate IL's derived from EMIM-Cl and $AlCl_3$ in contact with HCl gas at room temperature. Equilibrium constants developed by Chandler and Johnson [2] were used in these simulations. Our calculations showed $ClHAl_2Cl_7^-$ was the major Brønsted acidic species while $ClHAlCl_4^-$ and $HAlCl_4$ appeared in very small

concentrations. The mole fraction of $ClHAl_2Cl_7^-$ approaches unity for the IL having $[AlCl_3/O^+]^o = 2$ and when the HCl partial pressure approached 500 psia (3.45 MPa). The equilibrium to form $ClHAl_2Cl_7^-$ is favorable as its mole fraction is predicted to be 0.663 when the HCl partial pressure was 19.7 psia (135 kPa) and our calculations suggest that most of the benefit for adding HCl to produce super acidity is realized for HCl partial pressures less than 100 psia (0.69 MPa). Others [2] speculate that $ClHAl_2Cl_7^-$ is a Brønsted super acid and the results shown here for toluene carbonylation are consistent with this speculation. Additionally, the predicted response of the Lewis acidic chloroaluminate species, $Al_2Cl_7^-$, for increasing HCl partial pressure showed that the mole fraction of the Lewis acid decreased as the mole fraction of the Brønsted super acid increased.

When changing the $[AlCl_3/O^+]^o$ from 2 to 3 mol/mol it has been observed that not all of the Al_2Cl_6 dissolved into the liquid and our calculations suggest that applying HCl gas above the two-phase mixture does not change the solubility of the Al_2Cl_6. The predicted amount of super acidic Brønsted species, $ClHAl_2Cl_7^-$, apparently is not different when P_{HCl} = 500 psia (3.45 MPa) as we increase the $[AlCl_3/O^+]^o$ from 2 to 3 mol/mol: 0.96 vs. 0.92 mol, although the *mole fraction* of $ClHAl_2Cl_7^-$ does decrease from ½ to 1/3. If these predictions can be verified by spectroscopic means, the implication is that the super acidic mixture with the largest number of moles of $ClHAl_2Cl_7^-$ that can be developed results from an IL showing $[AlCl_3/O^+]^o = 2$.

With this simple model we were able to predict the data of ultimate toluene conversion when changing the $[AlCl_3/O^+]^o$ ratio at a constant P_{HCl} = 44.7 psia (0.31 MPa) thus confirming that this reaction is not catalytic but rather it is a stoichiometric reaction.

This prediction assumed that the product aldehyde was sequestered by both ($ClHAl_2Cl_7^-$) and ($Al_2Cl_7^-$) with a stoichiometry of one mole of aldehyde per mole of chloroaluminate species. A simple titration with *p*-tolualdehyde in acidic IL without HCl in the gas phase confirmed this assumption for the ($Al_2Cl_7^-$) species.

The data of initial reaction rate of toluene conversion were correlated with the molar amounts of super acidic Brønsted species, $ClHAl_2Cl_7^-$, by assuming that CO solubility into the IL could be simulated by a simple Henry's law model where the Henry's law constant, H, increased with increasing amounts of super acidic Brønsted species, $ClHAl_2Cl_7^-$, in the IL. This favorable CO solubility with increasing acid strength has been observed in other super acidic systems [12].

The small, positive value observed for $k[CO][ClHAl_2Cl_7^-]$ at zero HCl partial pressure in gas phase may be a result of water contaminating the IL before the reaction was initiated. This water could have reacted with the IL to form HCl *in situ* and thus produce the acidity required to initiate the reaction. The magnitude of the reactivity can be estimated by ratioing values of the ordinate of the integrated rate plot (table 3.1, $k[CO][ClHAl_2Cl_7^-]$) for the runs with and without HCl added. The reactivity of the samples for which HCl was added was 15-40 times that of the sample for which no HCl was added. Thus, we speculate that the effect of adventitious water was small (~2-7%) upon the observed reaction rates in those runs for which HCl was added. While the effect of this adventitious water was small, it does not alter the essential conclusions that arise from this modeling study: dimeric Al species are largely responsible for the reactivity observed in these IL's.

These calculations predict that the $AlCl_4^-$ mole fraction depends only upon the ratio of $AlCl_3/O^+$ in the starting mixture and it is also unaffected by the HCl partial pressure. This prediction is contrary to the interpretation of ^{27}Al NMR data reported by Nara [6], *et al.* who showed two peaks in the ^{27}Al NMR spectra of an acidic chloroaluminate/EMIM-Cl melt ($AlCl_3/O^+ = 2$) whose intensities changed with increasing partial pressure of HCl above the melt. The peak at 73.9 ppm decreased steadily with increasing P_{HCl} while the peak at 79.3 ppm increased. The peak at 73.9 ppm was attributed to $Al_2Cl_7^-$ while the peak at 79.3 ppm was assigned to $AlCl_4^-$. These species were reported to be influenced by HCl according the equilibrium described in equation (3.6) earlier. This equilibrium would explain the decrease in the NMR signal attributed to the Lewis acid, $Al_2Cl_7^-$, but it would not explain the existence of the super acidic activity documented by the toluene carbonylation reaction since $H^+AlCl_4^-$ is said to exhibit acidity similar to HF [2]. The acidity of HF alone is not sufficient to catalyze the arene carbonylation reaction. The predictions shown here and the results of the carbonylation reaction suggest that a re-examination is necessary of the NMR assignments reported by Nara, *et al* [6].

Several reports [21, 22] have appeared in the open literature in which the authors described their attempts to model the molecular properties of chloroaluminate ionic liquids described here. They used MNDO and AM-1 to simulate the IR vibrational spectra of O^+Cl^- and $O^+AlCl_4^-$. For the basic and neutral melts, they showed monomeric aluminum chloride species ($AlCl_4^-$) assembling around the organic cation ($EMIM^+$) to form a "sandwich compound". When excess chloride was present (as in the basic melts), it was found between the organic cations. The modeling of the present work focused on

acidic melts for which excess $AlCl_3$ is present, and we revisit the question of aluminum speciation to determine if monomeric or dimeric aluminum chlorides are favored by the thermodynamics.

The modeling of the acidic chloroaluminates starting with monomeric aluminum chloride and chloroaluminate anion with HCl and the $EMIM^+$ cation shows that the aluminum species assemble into a group (Figure 3.11) where the HCl is shared between the two aluminum species (structure 3.11-a), between the anion and the cation (structure 3.11-b), or on the cation (structure 3.11-c). The same result was observed when using any of the semi-empirical programs (AM-1, PM3, and MNDO). It is clear from this modeling that monomeric aluminum species forming a sandwich structure was not favored in the acidic melts as was observed in the neutral and basic melts. Moreover, it was clear that the monomeric aluminum species assembled into a pair in this acidic melt with HCl present. When the dimeric aluminum species ($Al_2Cl_7^-$) were employed to model the acidic melt along with HCl and the $EMIM^+$ cation, the free energies of formation for the structures that were formed (Figure 3.12) were similar to the corresponding structures observed in Figure 3.11. In addition, the HCl molecules sited at positions to form structures with the dimeric aluminum species that were similar to those observed in Figure 3.11. Structure 3.12-a (Figure 3.12) showed the HCl forming a compound with the $AlCl_3$ and $AlCl_4^-$ for which the H was sited between two $\{AlCl_4\}^{1-}$ species; however, the H-Cl bond distances were different when predicted by AM-1 and MNDO: 1.52 and 1.64 Å. The shorter H-Cl bond was found in that part of the structure arising from the anionic chloroaluminate that was closest to the C-2 proton of the cation. The PM3 model showed a nearly symmetrical Al_2Cl_8H anion. For structure 3.12-b, the

HCl was sited between the anion and the cation with an average H-Cl bond distance of 1.34 Å. Structure 3.12-c showed that the HCl was sited on the cation with a bond distance similar to that predicted for an isolated HCl. Apparently, the environment for the HCl plays a role in determining the bond length, and it may play a role in determining the reactivity of these species towards the toluene carbonylation reaction. These structures showed different free energies of formation with the 3.12-c structure showing the highest free energy of formation (-427.26 kcal/mol); whereas, the 3.12-a and 3.12-b structures showed lower free energies of formation (-428.9 and -430.6 kcal/mol, respectively).

After HCl was added to an intrinsic acidic ionic liquid, the chemical shift was strongly dependent of where the HCl was placed. The introduction of HCl into the different structures caused the C-2 to experience a chemical shift and in two of the three structures became very acidic as a result of the addition of HCl to the aluminum anion. For the HCl placed on the cation, the proton resonance was 2.6 ppm, which is only 0.8 ppm downfield from the resonance in isolated, gaseous HCl. These predictions must be confirmed by direct observations.

Using Transition State Geometry Optimization it was observed that the symmetry of Al species has been lowered and that the distance of the C-Cl bond was lengthened and two possible products were obtained. Product 1 is the dimeric anion $Al_2Cl_7^-$ the two aluminums are in similar chemical environment and product 2, the anion pair, $AlCl_3$ $AlCl_4^-$ with the two aluminums in different chemical environment, and based on thermodynamics calculation, these two products have equal opportunity to be formed. It must be added that the forgoing discussions of equilibrium thermodynamics could not distinguish between the anionic dimer and the anion pair since their free energies of

formation were the same. Thus, one must rely upon direct observation of the Al species structure, such as ^{27}Al-NMR, to confirm the existence of these two dinuclear Al species that were predicted from quantum mechanics theory. Based upon these predictions, we were able to predict the observed ^{27}Al-NMR spectra for IL's having n = 3/2 and 2.

It is appropriate that we comment on the success of the model predictions of the properties of the IL's. These predictions are for isolated molecules in an ideal gas where intermolecular attractions are not modeled. We seek to model a fluid that must surely be considered non ideal, since the Hammett acidity function must be used to properly specify the thermodynamic activity of protons in the IL. Thus, one could only be surprised that our simple-minded approach to modeling appeared to predict well the observations.

3.6 Summary

Simple equilibrium thermodynamics can be used to identify the species in the IL, super acidic Brønsted ($ClHAl_2Cl_7^-$) and Lewis acidic ($Al_2Cl_7^-$) chloroaluminate anions that are responsible for the observed ultimate conversion of toluene to tolualdehyde. These calculations predict the systematic increase in the *ultimate* toluene conversion as the ratio $[AlCl_3/O^+]^o$ was varied from 1 to 2. The initial rates of the carbonylation reaction in the IL were correlated with the predicted molar amounts of the super acidic Brønsted chloroaluminate anions assuming that the CO solubility also depended upon the molar amounts of an acidic species having the stoichiometry: $HAl_2Cl_8^-$. Our predictions suggest that the solubility of Al_2Cl_6 in the IL cannot be changed by increasing the HCl

partial pressure above it. While these predictions were not contradicted by visual observations, more accurate direct measurements of the species must be completed to confirm our predictions.

Modeling of the IL by semi-empirical methods showed that HCl could be placed in 3 different places in the IL and that the free energies of formation for these three structures were different. These different energies of formation may suggest that the mole fractions of the HCl residing in these different sites will be different. The H-Cl bond lengths were predicted to be different for the HCl in the different structures and we expect that the acidity of the HCl proton to depend upon the bond length with the most acidic proton residing in the HCl with the longest bond length.

^{1}H NMR predictions demonstrated that the addition of HCl increased the acidity of the system, but more important these predictions suggested that HCl may reside in more than one place in the ionic liquid structure. That is to say, the predictions of ^{1}H-NMR appeared to confirm the earlier predictions that the acidity of the HCl proton depended upon its location in the IL structure. ^{27}Al NMR predictions helped us to have a better idea of the aluminum speciation in the ionic liquids and possible chemical environment. More specifically, the modeling studies suggested the existence of the anion pair, $AlCl_3AlCl_4^-$, which appears to show ^{27}Al-NMR chemical shifts that are different from the dimer or the monomer. It remains to be clarified if this new aluminum species plays any role in the catalysis. Experimental work will be required to confirm the three sites for the HCl, the indicated aluminum speciation and the site dependent acidity of the HCl in the IL.

3.7 References

1. Wasserchеid, P., Welton , T., "Ionic Liquids in Synthesis" Weinheim: Wiley-VCH, 2003.

2. Chandler, W. D., and Johnson, K. E., "Thermodynamic Calculations for Reactions Involving Hydrogen Halide Polymers, Ions, and Lewis Acid Adducts. 3. Systems Constituted from Al^{3+}, H^{+} and Cl^{-}", Inorg. Chem. (1999), **38**, 2050-6.

3. Olah, G. A., Ohannesian, L., and Arvanaghi, M., "Formylating agents", Chem. Rev. **87**, 671 (1980); Olah, G. A., Laali, K., and Farooq, O., "Aromatic substitution. 52. Superacid-catalyzed carbonylation of aromatics with carbon monoxide", J. Org. Chem. **50**, 1483-6 (1985).

4. Toniolo, M., Graziani, J., Organometallic Chemistry, **194**, 221-228 (**1980**)., & Smith, B. M., Integrated Laboratory Systems, Aluminum Compounds, Review of Toxicological Literature, Abridged Final Report, October **2000**.

5. Wasserscheid, P., and Keim, W., "Ionic Liquids—New Solutions for Transition Metal Catalysis", Angew. Chem. Int. Ed. **39**, 3772-89, (2000).

6. Nara, S.J, Harjani, J.R. Salunkhe, M.M., "Friedel-Crafts Sulfonylation in 1-Butyl-3-methylimidazolium Chloroaluminate Ionic Liquids", J. Org. Chem., **66**, 8616-8620 (2001).

7. Angueira, E. J., and White, M.G., A. I. Ch. E. Annual Meeting, San Francisco, CA, November, 2003, paper 511a.

8. Angueira, E. J., and White, M.G., "Arene Carbonylation in Acidic, Chloroaluminate Ionic Liquids", *J. Mol. Catal. A: Chemical,* 227, 51-58 (2005).

9. Doug Gordon, private communication, Hoechst Celanese Corporation, Technical Center, Corpus Christi, Texas, May 30, 1995.

10. Sood, D.S., Sherman, S.C., Iretskii, A.V., Kenvin, J.C., Schiraldi, D.A. and White, M.G., "Formylation of Toluene in Triflic Acid", J. Catalysis **199**, 149 (2001).

11. DeLaplane, R.G., and Lundgren, J.O., Olovson, I., Acta Crystallogr. Sect. B. **31**, 2202 (1975).

12. Booth, B.L., and El-Fekky, T.A., "A comparison of the effectiveness of sulfuric acid and trifluoromethanesulfonic acid in Koch carboxylation reactions ", J. C. S. Perkin I, p. 2441-6 (1979).

13. Zawodzinski, T.A., Carlin, R.T., Osteryoung, R.A., "Removal of Protons from Ambient – Temperature Chloroaluminate Ionic Liquids", *Anal. Chem*. **1987**, *59*, 2639.

14. Brown, H. C., and Pearsall, H., "The Catalytic Halides. I. A Study of the Catalyst Couple, Aluminum Chloride – Hydrogen Chloride, and the Question of the Existence of $HAlCl_4$", *J. Am. Chem. Soc*. **1951**, *73*, 4681.

15. MOPAC 2002 Manual: http://www.cachesoftware.com/mopac/Mopac2002manual/node650.html

16. Haw, J.F., Richardson, B.R., Oshiro, I.S., Lazo, N.D., and Speed, J.A., "Reactions of Propene on Zeolite HY Catalyst Studied by in Situ Variable-Temperature Solid-state Nuclear MagneticResonance Spectroscopy", *J. Am. Chem. Soc*. **1989**, *111*, 2052-2058.

17. Haw, J.F., "Zeolite acid strength and reaction mechanisms in catalysis", Phys. Chem. Chem. Phys., 2002, 4, 5431–5441

18. W.J. Hehre, L. Radom, P.v.R. Schleyer and J.A. Pople, "Ab Initio Molecular Orbital Theory", Wiley, New York, 1986.

19. Kubicki, J.D., Sykes, D., Apitz, S.E., "Ab Initio Calculation of Aqueous Aluminum and Aluminum-Carboxylate Complex Energetics and ^{27}Al NMR Chemical Shifts", J. Phys. Chem. A (1999), 103 (7), 903-915. Kerven, G.L, Larsen, P.L., Bell, L.C., Edwards, D.G., "Quantitative ^{27}Al NMR spectroscopic studies of Al(III) complexes with organic acid ligands and their

comparison with GEOCHEM predicted values", Plant and soil (1995), 171(1), 35-39.

20. Fannin, A.A. Jr., King, L. A., Levisky, J.A., and Wilkes, J.S., "Properties of 1,3,-Dialkylimidazolium Chloride-Aluminum Chloride Ionic Liquids. 1. Ion interactions by NMR", *J. Phys. Chem.* **1984**, 88, 2609-14.

21. Dieter, K.M., Dymek, C.J., Heimer, N.E., Rovang, J.W., and Wilkes, J.S.. "Ionic structure and interactions in 1-methyl-3-ethylimidazolium chlroide-$AlCl_3$ molten salts", *J. Am. Chem. Soc*. **1988**, *110*, 2722-6.
22. Davis, L.P., Dymek, C.J., Stewart, J.P., "MNDO calculations of ions in chloroaluminate molten salts", *J. Am.Chem. Soc.,* **v. 107** (Sept. 4 '85) p. 5041-6.

CHAPTER IV

IONIC LIQUID STRUCTURE EFFECT UPON REACTIVITY OF TOLUENE CARBONYLATION: ORGANIC CATION AND INORGANIC ANION STRUCTURE[1]

Acidic, chloroaluminate ionic liquids (IL's) formed from combining two moles of $AlCl_3$ with 1 mole of 1-R-3-methyl-imidazolium-chloride (RMIM-Cl, R = ethyl, *n*-butyl, *n*-hexyl, *n*-octyl, *n*-dodecyl, or benzyl) were examined as conversion agents for toluene carbonylation at room temperature when HCl and CO were present in the gas phase at partial pressures of 3.04 and 8.16 atm, respectively. The structure of the anion was also varied to study the effect on the system reactivity. The solubilities of HCl and CO into the ionic liquids were measured at room temperature in separate experiments to determine the effect, if any, of the cation structure upon gas solubility. Molecular modeling by semi-empirical methods (AM-1; PM3, and MNDO) was used to simulate the absorption of HCl into the IL's when R was changed.

4.1 Structure-Properties Relationships Revealed in the Literature of Similar IL's

It had been established that the structure of these ionic liquids may influence the transport processes [1] and the physical properties of the ionic liquid [2, 3] as a result of the intimate association between the organic cation and the anion(s). It has been shown

[1] Material in this chapter has been previously published in the following article: Angueira, E.J., and White, M.G., "Ionic liquid structure effect upon reactivity of toluene carbonylation: 1. Organic cation structure" *J. Mol. Catal. A: Chemical*, 238 (2005) 163-174.

that the cation, the R-groups on the cation, and the anion can be chosen to enhance or suppress the solubility of other compounds in the ionic liquid [3]. For example, Waffenschmidt [4], showed how the solubility of octene increased in tosylate IL's prepared from tri-*n*-R-methyl ammonium cations where R was *n*-butyl, *n*-pentyl, and *n*-hexyl. The olefin was miscible in the IL prepared from the tosylate where R = *n*-octyl. They explained the increasing olefin solubility in the IL as a result of the decreasing dipole moment when R was replaced with alkyl groups of increasing chain length.

Ohlin, *et al.*, reported the solubility of CO in several ionic liquids derived from 1-R-3-methyl-1*H*-imidazolium chloride (RMIM-Cl) at room temperature for which the R-group was changed from methyl to octyl when the anion was either *bis*(trifluoromethylsulfonyl)imide or BF_4^- [5]. They showed that the CO Henry's law constant, $K_H = P_{CO}/x_{CO}$, decreased from a value of 1.34 kbar with R = methyl to a value of 0.67 kbar for R = octyl. When R was benzyl, the Henry's law constant was 1.41 kbar suggesting that the π-electron system of the benzyl group leads to decreased CO solubility in the IL. The CO solubility in these IL's was similar to that observed for CO in toluene at room temperature (K_H = 1.29 kbar) which results in very small mole fractions of CO in the toluene under a CO partial pressure of 1 atm ($x_{CO} \sim 0.001$).

For the toluene carbonylation reaction in IL's for which a gaseous Brønsted acid (HCl) was added, the solubilities of toluene, CO, and HCl were important to the reactivity in the IL. Thus, one might imagine that an optimum "design" for the IL could exist which considers the solubility of gaseous species, such as CO and HCl, as well as the solubility of liquid species, such as toluene, in the ionic liquid. Apart from reactant

solubility, one must also consider other factors that influence the formation of reactive species in the IL, such as strongly acidic species.

Carey and Sundberg [6] reported in their book that the strength of association between species depended upon LUMO and HOMO energies and the symmetries of the orbitals. Researchers studied the effect of changing structure and its effect on the MOs using the approach of the perturbation molecular orbital theory [7], and the interactions of orbitals in reacting molecules by incorporating the concept of frontier orbital control, which proposes that the most important interactions will be between a particular pair of orbitals [8]. These considerations have led investigators to examine the molecular environment of ionic liquids so as to understand better the experimental characterizations of these systems. Dieter, *et al.* showed that the imidazolium cations and the chloroaluminate anions with the chlorides are closely associated to form layers in the neutral and basic IL's [9]. Moreover, Chandler and Johnson [10], showed how the formation of certain reactive chloroaluminate species, such as the Brønsted super acid ($HAl_2Cl_8^-$) and the Lewis super acid ($Al_2Cl_7^-$) depended upon the free energy of formation of the species in the melt [10] and Angueira [11] showed how the partial pressure of HCl above the melt determined the relative mole fractions of the Brønsted to Lewis super acid species. Several structures (monomeric [12] and dimeric [10, 11] Al species) have been proposed for the Brønsted super acid species; therefore, it is appropriate to model these and other structures that might be present in the IL to determine how the solubility of HCl may be influenced by the structure of cation present in the IL.

4.2 Cation Structure-Properties Hypothesis

We hypothesize that the structure of IL can 1) control the solubility of the gaseous reactants, 2) promote the formation of reactive species and 3) therefore influence the reactivity of system towards a substrate. This hypothesis will be tested by experimental and by molecular modeling efforts in which the IL's would be formed from $AlCl_3$ (2 moles) and members of a family of 1-R-3-methyl-imidazolium-chloride (RMIM-Cl, 1 mole), where R = ethyl, *n*-butyl, *n*-hexyl, *n*-octyl, *n*-dodecyl, or benzyl. The modelling of HCl solubility in these IL's will describe the free energy for the formation of HCl-adducts with the IL's when R is changed. Where appropriate, the molecular modelling may indicate when more than one HCl-adduct can be formed. These model predictions will be compared to experimentally-determined, room-temperature, absorption equilibrium constants for HCl in the ionic liquids as a function of R for gas pressures up to 3.04 atm. Additionally, we will determine by experiment the effect of R upon the reactivity of a toluene carbonylation probe reaction completed at room temperature in the presence of HCl (3.04 atm) with CO added to a total pressure of 11.2 atm.

4.3 Experimental

4.3.1 Chemicals

The imidazolium compounds 1-ethyl-3-methyl-imidazolium-chloride (EMIM-Cl), 1-butyl-3-methyl-imidazolium-chloride (BMIM-Cl), and 1-hexyl-3-methyl-imidazolium-chloride (HMIM-Cl), and the anions $SbCl_3$, $SbCl_5$ and PCl_3 were obtained from Sigma Aldrich; whereas, 1-octyl-3-methyl-imidazolium-chloride (OMIM-Cl), 1-Dodecyl-3-methyl-imidazolium-chloride (DoMIM-Cl), and 1-benzyl-3-methyl-imidazolium-chloride (BeMIM-Cl), were obtained from Merck Chemicals and used without further purification. Aluminum chloride (99.99%), obtained from Sigma Aldrich, was sublimed under vacuum before use. Toluene (anhydrous, 99.8%) was obtained from Sigma Aldrich and used without further purification. Carbon monoxide, CP grade, and HCl (anhydrous, 99+%) were obtained from Airgas and Sigma Aldrich, respectively.

4.3.2 Preparation of IL's

The weighing instrument and chemicals were placed in an AtmosBag filled with dry Ar. MCl_3 (M = Al, Ga, In, P, Sb) or $SbCl_5$ was weighed, and $RMIM^+$-Cl^- was added so as to obtain the desired metal chloride/$RMIM^+$-Cl^- molar ratio.

4.3.3 Absorption of HCl gas in IL's

1. The amounts of HCl gas absorbed by the IL's were determined using a volumetric apparatus from a measurement of the system volumes, gas pressures and temperatures (Figure 4.1). The moles absorbed were computed using the ideal gas law.
2. A calibrated stainless steel vessel (150 cm^3) was filled initially with HCl at room temperature and the pressure was measured to the nearest 0.1 psia (0.0068 atm) using a 750B Baratron Pressure Transducers with a type LDM-B display module. This level of uncertainty in measuring the gas pressure leads to a minimum detection limit of 0.003 in the mole fraction of the absorbate in the IL.
3. The gas in this vessel was expanded into the Fisher-Porter reaction tube which contained a known amount of the IL at room temperature.
4. All IL's were stirred at 1000 RPM during the absorption experiment except for the one IL derived from 1-dodecyl-3-methyl-imidazolium-chloride which could only be stirred at 300 RPM, and the one derived from 1-benzyl-3-methyl-imidazolium-chloride which could only be stirred at 475 RPM due to their high viscosity.

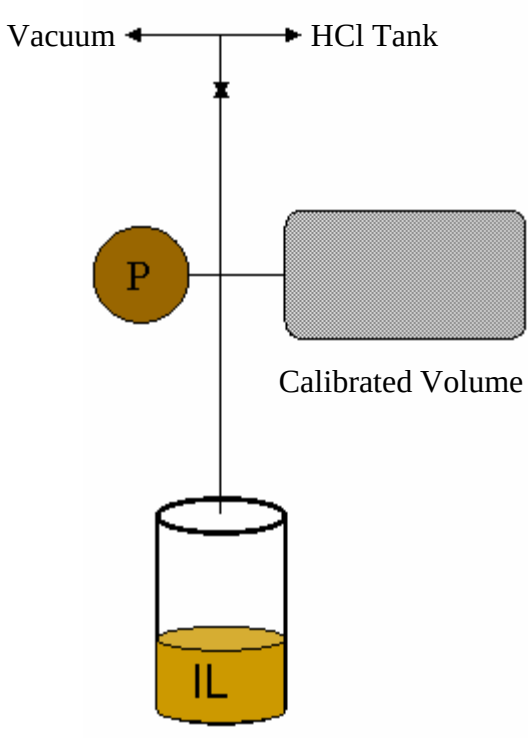

Figure 4.1. Volumetric apparatus for HCl and CO absorption experiments.

5. From these data, the amount of gas remaining in the gas phase could be calculated before and after the expansion.
6. The system was evacuated and the absorption repeated to determine if the process was reversible. That is, the amount of HCl absorbed was the same in subsequent runs for which the system was evacuated at room temperature between absorption runs.
7. Care was taken to remove the gas dissolved in the IL sample initially, but this is easily accomplished because no volatization of the IL occurs during the evacuation process.
8. The dead volume of the apparatus was determined using Ar for each

partial pressure of gas studied at room temperature.

9. The partial pressures of HCl were varied from 0 to 3.04 atm.
10. A control was completed for the absorption of HCl gas into toluene at room temperature for HCl partial pressures between 0 and 3.04 atm.
11. Subsequently, the HCl absorption was determined at room temperature above the neat, acidic IL's derived from $AlCl_3$ and RMIM-Cl in the ratio of 2 mol/1 mol (R = ethyl, *n*-butyl, *n*-hexyl, *n*-octyl, *n*-dodecyl, and benzyl).
12. One more test was completed for the acidic IL developed from $AlCl_3$/BMIM-Cl (2 mol/1 mol) and toluene (1 mol toluene/mol $AlCl_3$) over the range of HCl partial pressures of 0 to 3.04 atm.

4.3.4 Absorption of CO gas in IL's

1. The amounts of CO gas absorbed by the IL's [$AlCl_3$/RMIM-Cl = 2 mol/mol; R = ethyl, *n*-butyl, *n*-hexyl, *n*-octyl, *n*-dodecyl, and benzyl] were determined using the same volumetric apparatus and procedure as described above (Figure 4.1).
2. The partial pressures of CO were varied from 0 to 6.80 atm. The minimum detection limit for CO mole fraction in the IL's was 0.003 in the mole fraction (*vide supra*).

4.3.5 Absorption of HCl + Ar and HCl + CO mixtures in IL's

1. Experiments using acidic IL and gas mixtures of either HCl + Ar or HCl + CO were conducted to determine if HCl enhanced the CO solubility in the IL.
2. The lower detection limit for CO may prevent us from actually observing any enhanced CO solubility.
3. In the volumetric apparatus 2.02 atm HCl and Ar were mixed for a total pressure of 7.22 atm.
4. The gas mixture was expanded into the acidic IL.
5. The same procedure was repeated for HCl and CO mixture. It was expected here, that Ar would be a non-absorbing gas.

4.3.6 Reaction studies—Low pressure

1. Low pressure reactions were completed in a Fisher Porter glass tube affixed with a stirring magnet that was placed in an AtmosBag.
2. The desired metal chloride/$RMIM^{+}$-Cl^{-} IL was weighed into the Fisher Porter tube (~ 8 g) and dry toluene (3.5 cm^3) was added to obtain the desired M^{3+} /toluene ratio: 1 mol/1 mol (M = Al, Ga, In, P, Sb) or Sb^{5+}/toluene ratio: 1 mol/1 mol.
3. The reactor was sealed, removed from the AtmosBag and purged with

HCl gas before HCl gas was added to the desired partial pressure and then this mixture was stirred for ½ h at room temperature.

4. Carbon monoxide was then added to give a total pressure of 11.2 atm. The reaction temperature was room temperature and the CO pressure was monitored at the beginning of the experiment to verify CO consumption.
5. After the reaction was completed, the reactor was slowly vented and purged with Ar.
6. The mixture was poured into a separatory funnel filled with an ice/distilled water mixture so as to dilute the acidic components.
7. The organic layer was collected after it was neutralized with a saturated sodium bicarbonate solution.
8. Previous experiments [13] with trifluoromethane sulfonic acid (HOTf) showed that a stirring rate of 800 rpm was sufficient to overcome mass transfer resistance.
9. Since the conversion rate in the IL [14, 15] is similar to that for HOTF (*vide infra*) when the acid/substrate = 10 mol/mol, we will use a similar stirring rate of 1000 RPM.
10. A control experiment was completed for which no IL was added to the reaction mixture described above but the reaction was continued for 18 h. The product mixture when worked up and analyzed by GC/MS showed no aldehyde, which confirmed the inactivity of the system without the IL.

4.3.7 Analytical

1. Organic products were analyzed in a HP-5890 Series II Plus GC equipped with a HP-5972 mass spectrometer. High purity helium (99.995 %, Airgas) was the carrier gas and the column was 15 m long, 0.25mm i.d., and 0.25 μm film thickness obtained from Supelco (SPB-5 24032).
2. An analytical method was developed to separate all the liquid-phase products using the following GC oven protocol: initial temperature = 35ºC, hold for 5 minutes, then increase temperature 10ºC per minute, and finally hold temperature at 180ºC for the final 5.50 minutes.

4.4 Results

4.4.1 Modeling of IL's for HCl Absorption in Acidic IL's

It was discussed in Chapter III that modeling of the IL by semi-empirical methods revealed three possible optimized structures, (Figure 3.12 from Chapter III) that developed upon absorption of HCl gas in the IL's at room temperature. The three structures are: HCl inserted into the $Al_2Cl_7^-$ anion to form a bridging species (Figure 3.12-a). In the second structure, HCl was associated with the $Al_2Cl_7^-$ anion through a terminal Cl and also associated with the imidazolium cation through the C-2 proton

(Figure 3.12-b). The third structure shows the HCl species involved with the cation only (Figure 3.12-c).

It was hypothesized that changes in either the cation or the anion would affect the amount of HCl absorption into the IL and thus could have a direct influence of the reactivity of the IL for Brønsted-demanding reactions. One can interrogate the degree of influence these structural changes in the cation might have on the HCl absorption. Tables 3.2-3.4 in Chapter III showed the free energies of formation for the three structures of the absorbed species as R was changed using three semi-empirical quantum mechanical programs: AM-1, PM3, and MNDO.

4.4.2 Predictions—effect of changing R upon $\Delta G_{absorption}$ of HCl in Acidic IL's

Now consider the trends in the predicted amounts of HCl absorption for changing R when HCl was absorbed in structure 3.12-a, 3.12-b, and 3.12-c and how this change affects the free energy of HCl absorption as predicted from the AM-1, PM3, and MNDO models (Tables 3.2-3.4 Chapter III). The predicted free energy of HCl absorption into a particular structure (say 3.12-a) is the same for all R groups if one considers the error of these calculations to be ± 4.0 – 5.0 kcal/mol regardless of the model used [16]. These free energies of absorption can be used to predict the absorption amounts by recalling the relationship between the free energy of absorption and the equilibrium absorption constant, K:

$$\ln K = -\Delta G_{absorption}/RT \qquad (4.1)$$

From a consideration of the free energies of absorption, (Table 4.1), it is clear that very little HCl will be absorbed as structure 3.12-a and that the likelyhood of HCl absorbing in structure 3.12-b or 3.12-c are the same when using the results of the AM-1, MNDO models. The PM3 predictions suggest that all structures are equally likely. Molar-weighted averages (column 5, Table 4.1) show that the predicted free energy for HCl absorption is 1-4 kcal/mol, which is within the error of the calculations when compared to the observed free energy of HCl absorption, ~2 kcal/mol.

Table 4.1. Summary of Predictions for all R Groups.

$\Delta G_{absorption}$ (kcal/mol)				
Model	3.12-a	3.12-b	3.12-c	ΔG, average
AM-1	13.3	4.00	6.10	4.06
PM3	2.30	0.90	4.30	1.03
MNDO	16.9	2.60	2.50	2.55

4.4.3 Predictions—effect of changing inorganic anion

To formulate another hypothesis, we studied the thermodynamics of different sets of cation/anion pairs to form the IL's after a consideration of the anions' hard-soft acids properties as defined by Pearson [17] who introduced the concept of hard and soft acid and bases (HSAB) in order to explain affinities between acids and bases that do not depend on electronegativity or other related macroscopic properties [17, 18]. This theory may be attractive in modeling IL's formed from the interaction of one cation with a

family of anions, such as MCl_3. The proposed hypothesis is that the hard/soft acidity of the Lewis acids determines the strong Brønsted acidity resulting from contacting the IL with HCl gas. First we review the hard/soft acid theory.

Pearson formulated one thermodynamic rule saying that hard acids prefer to associate with hard bases, and soft acids prefer to associate with soft bases, and a kinetic rule from which hard acids react readily with hard bases and soft acids react readily with soft bases. Hard acids are defined as small-sized, highly positively charged, and not easily polarizable electron acceptors, while in soft ones the acceptor atom is large, possesses a small positive charge, and has some valence electrons which can be easily removed [17, 19, 20]. Although the HSAB theory is qualitative, there have been proposals to define a hardness-softness quantitative scale associated with physical properties. In this way, Fukui's function is related, by density functional theory, [21] to Fukui's frontier density [22] and can be interpreted as a local softness [23]. Two other approaches have been based on quantum mechanical principles using perturbation molecular orbital theory [24] and density functional theory [21]. This approach discusses the softness-hardness as defined from the charge and frontier orbital control. The larger the difference between the energy of the highest occupied molecular orbital (HOMO) of the donor atom and the lowest unoccupied molecular orbital (LUMO) of the acceptor atom, the larger the charge control is and hard-hard interactions are favored. On the other hand, when the above energy difference is small, soft-soft interactions become preferred and the interaction is frontier orbital controlled.

The hypothesis to be tested assumes that a dimer of the Lewis acid (M_2Cl_6) exists and it engages the Lewis base (*e. g.*, $BMIM^+Cl^-$) into a transition state such as that

described earlier for M = Al, chapter 3, page 92, scheme I. The existence of the dimer M_2Cl_6 in significant amounts is a necessary assumption in this hypothesis, since it was shown earlier (Chapter 3, page 68, Figure 3.8) that the conversion scaled with amounts of dimeric aluminum chloride anion ($Al_2Cl_7^-$). The predicted (HF for geometry optimization followed by PM3 for SPE calculation) free energies of formation for the dimer M_2Cl_6 and the monomeric MCl_3 are shown in Table 4.2 along with thermodynamic data from the literature (in parentheses) so that we may estimate the amount of M_2Cl_6 that appears at room temperature.

Table 4.2. Predicted Free Energies for Gas Phase Dissociation of M_2Cl_6.

M_nCl_{3n}	ΔG^o_f, kcal/mol	ΔG_{disscn} kcal/mol	K_{disscn}	x_{dimer}
$AlCl_3$	-1.46E+02	54.4 (18.0)	1.17E-40	1
Al_2Cl_6	-3.47E+02			
$GaCl_3$	-1.04E+02	82.2	5.18E-61	1
Ga_2Cl_6	-2.91E+02			
$InCl_3$	-9.88E+01	53.6 (21.0)	4.96E-40	1
In_2Cl_6	-2.51E+02			

The free energy of dissociation is for the following reaction:

$$M_2Cl_6 \Leftrightarrow 2\ MCl_3 \qquad (4.2)$$

So that a positive value for the free energy of dissociation suggests that the dimer, M_2Cl_6, is not inclined to dissociate, and therefore would be favored at equilibrium. From the gas phase calculations, we then infer the speciation of the solid phase before mixing with the

dialkylimidazolium chloride. The equilibrium constant for dissociation is related to the free energy for dissociation by the following:

$$K_{disscn} = \exp(-\Delta G_{disscn}/R/T) \quad (4.3)$$

$$x_{dimer} = 1 - K_{disscn}/(1+K_{disscn}) \quad (4.4)$$

The mole fraction of the species that is dimeric is 1 – fraction of the species that has dissociated.

The results of Table 4.2 suggest that very little of the dimer is expected to dissociate in the gas phase at room temperature. Data for Al_2Cl_6 dimerization shows $\Delta H^o_{(298)}$ = -121 +/- 4 kJ/mol [25] and the $\Delta S^o_{(298)}$ = -154 +/- 7 J/mol-K [26] for a free energy of dimerization equaling -17.95 kcal/mol. The corresponding free energy of dissociation is just the negative of this number of 17.95 kcal/mol. The thermochemical values for dissociation of In_2Cl_6 at 298 K has been reported as $\Delta H°_{(298)}$ = 31.7 kcal/mole and $\Delta S°_{(298)}$ = 36.6 eu for a free energy of dissociation of 20.97 kcal/mol [27]. While our estimates overpredicted the measured values for the free energy of dissociation (*i. e.*, our numbers show free energies that are more positive), it is clear that the assumption is fulfilled that dimers do exist for all three metal chlorides in group III-A.

The next calculation is to predict the speciation of the anion species in the IL assuming that when the IL is intrinsically acidic (*i. e.*, moles MCl_3/moles of cation = 2), the anion species exist as the anionic dimer ($M_2Cl_7^-$) or the anion pair (MCl_3 MCl_4^-). Table 4.3 shows the predictions for the free energies of these anionic species in equilibrium with $BMIM^+$.

Table 4.3. Predictions for the free energies of anionic species in equilibrium with $BMIM^+$.

	ΔH^o(kcal/mol)	ΔS^o(kcal/mol*K)	ΔG^o(kcal/mol)	K, dimer	x, dimer
$BMIM^+In_2Cl_7^-$	-237.93	0.2197	-303.43	1.000	0.500
$BMIM^+InCl_3InCl_4^-$	-237.94	0.2193	-303.34		
$BMIM^+Ga_2Cl_7^-$	-364.10	0.1925	-421.48	0.998	0.499
$BMIM^+GaCl_3GaCl_4^-$	-365.81	0.1911	-422.80		
$BMIM^+Al_2Cl_7^-$	-349.66	0.2041	-410.50	1.000	0.500
$BMIM^+AlCl_3AlCl_4^-$	-349.70	0.2038	-410.47		

The predicted free energies are the same for the anionic dimer and its anion pair for each M = Al, Ga, or In. Accordingly, the equilibrium constant for the reaction between the anionic dimer and is anion pair is nearly unity suggesting that these two species are present in the IL in equal amounts. Thus, the predictions suggest that the identity of the group III-A metal has no effect upon the speciation in the melt. This finding must be compared to experimental data obtained from NMR of the metal forming the anion chloride.

Given that the hardness/softness of the anion has no predicted effect upon the speciation, we turn to the effect of the anion on the strength of the Brønsted acid formed upon introduction of HCl gas to the melt. ^{1}H-NMR predictions were completed for the $BMIM^+MCl_3$ melt under the conditions of intrinsic acidity and for which the HCl was sited either totally on the anion between the metal (III) species [structures 3.11(a) and 3.12(a)], between the anion and the cation [structures 3.11(b) and 3.12(b)], or totally on the cation [structures 3.11(c) and 3.12(c)]. These predictions (Table 4.4) suggest that the chemical shift of the HCl proton is the nearly same for Al and Ga when it is sited in the anion pair in the 3.12(b) position or on the anionic dimer in the 3.12(a) position (*i. e.*,

between the MIII ions in the anion). However, the predicted chemical shift of the proton resonance is 3-5 ppm upfield in the IL created from indium chloride in either the 3.11(a), 3.11(b), 3.12(a), or 3.12(b) positions. The proton chemical shift is very far upfield for all anions when the HCl resides on the cation (c) positions.

If we can assume that increased proton acidity is correlated with increased chemical shift *downfield* from TMS, then, these predictions suggest that the HCl protons in IL formed from indium chloride are much less acidic than the corresponding protons formed from either Al or Ga chloride regardless of the absorption site. Moreover, the chemical shifts predicted in the IL on the cation sites are very similar to those predicted for gas phase HCl (~3 ppm) and thus we expect this site will have no reactivity towards an acid catalyzed reaction required high Bronsted acidity.

Table 4.4. Predictions of the chemical shift of the HCl proton in MCl_3 (M= Al, Ga, In).

	ppm downfield from TMS		
Position of HCl in IL	Al	Ga	In
3.11 (a) pair	15.3	17.4	12.4
3.11 (b) pair	14.3	14.2	12.4
3.11 (c) pair	2.50	2.50	1.40
3.12 (a) dimer	15.4	15.1	10.7
3.12 (b) dimer	14.4	5.70	9.80
3.12 (c) dimer	2.60	2.40	1.10

The highest chemical shifts are predicted for HCl residing in the (a) positions either on the anion pair [MCl_3 MCl_4^-] or the anionic dimer [$M_2Cl_7^-$]. These predictions suggest that the IL derived from the Ga anion pair should have the highest proton chemical shift (17.4 ppm) with the next highest chemical shift predicted for and IL derived from Al

anionic pair or dimer (15.3, 15.4 ppm). Results from the ^{27}Al-NMR before HCl was added to the IL showed that most of the anion species were the anionic dimers (Chapter V), thus if one assumes that the principal activity for toluene carbonylation arises from HCl in the 3.12(a) dimer structure, then these predicted results suggest that the kinetic rate constants should be ordered as follows: k(Al) > k(Ga) >> k(In). If, the principal activity arose from the 3.11(a) pair structures, then one would predict rate constants as follows: k(Ga) > k(Al) > k(In). These predictions will be compared with observations for reactivity and ^{13}C-NMR of a probe molecule sensitive to Brønsted acidity: 2-^{13}C-acetone (Chapter V).

4.4.4 HCl absorption Observed in Acidic IL's

The HCl absorption at room temperature in $AlCl_3$/$RMIM^+$-Cl^- intrinsically acidic IL's was studied at different partial pressures of HCl. The amounts of HCl absorbed as a function of time were recorded for all RMIM-Cl IL's first at two different partial pressures (1.34 and 3.04 atm) to determine the minimum time required to confirm that equilibrium had been established. In Figure 4.2 we show the data of HCl pressure above the IL as a function of time for the BMIM-Cl and DoMIM-Cl as these represent the two extremes in viscosity with the IL derived DoMIM-Cl showing the highest viscosity. Most of the HCl was absorbed within the first 10-15 minutes; however, the HCl absorption rate into the DoMIM-Cl IL was consistently less than that observed into the BMIM-Cl at each sampling time. The stirring rate for the *n*-dodecyl tests was 300 RPM, for the benzyl tests it was 475 RPM, and it was 1000 RPM for all other IL's. But, the

total amount HCl absorbed at ½ h was nearly the same for both systems thus validating the protocol used here to pretreat the IL with HCl for ½ h before starting the toluene carbonylation reaction.

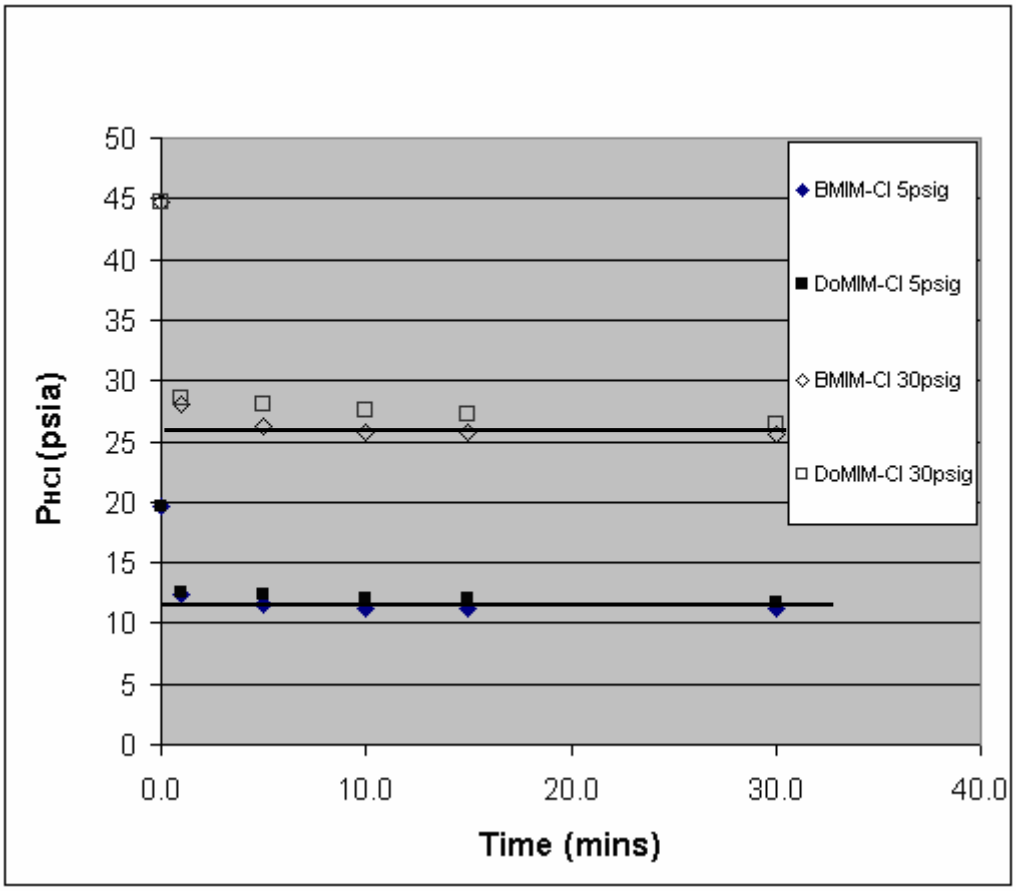

Figure 4.2. Rate of HCl Absorption in intrinsically acidic Ionic Liquids.

We hypothesized that the HCl solubility in the IL's might be influenced by the size of the alkyl group in the organic cation. Figure 4.3 shows the data of HCl absorption, mole fraction HCl in IL *versus* equilibrium HCl pressure above the IL at room temperature that were developed from IL's containing RMIM-$Al_2Cl_7^-$ for R = ethyl, *n*-butyl, *n*-hexyl, *n*-octyl, *n*-dodecyl, and benzyl. We also show the error bars for three

series of measurements: the *n*-butyl cation, *n*-dodecyl cation, and the benzyl cation. Most of the data were observed to be described by a single line when one considers the magnitude of the measuring errors, indicated here by the error bars in Figure 4.3, which represents an uncertainty of ± 0.1 psia (0.0068 atm) in measuring the pressures.

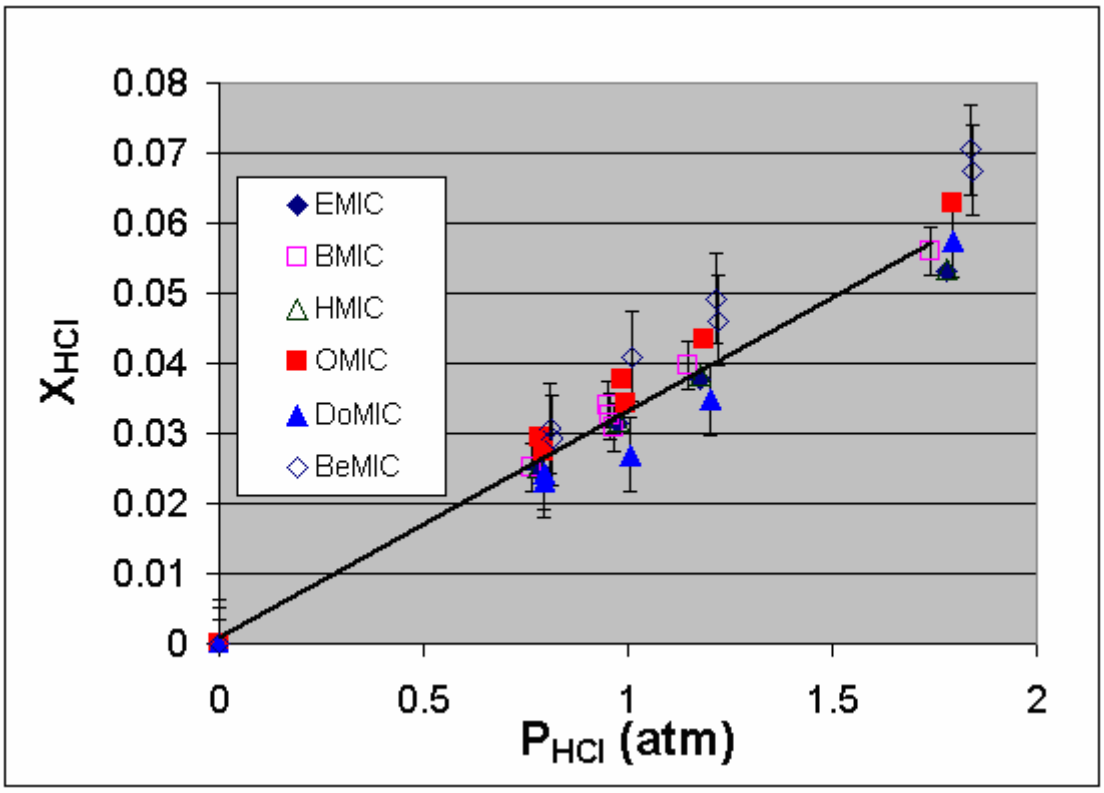

Figure 4.3. HCl absorption as a function of HCl partial pressures at 298 K.

For each data set from an IL, values were determined for the experimental equilibrium absorption constant and the free energy of absorption were calculated (Table 4.5). The average value of K for all of the data was 0.0327 ± 0.002 atm^{-1} and the corresponding free energy of absorption was 2.03 ± 0.04 kcal/mol. The observed $\Delta G_{absorption}$ for HCl (~2 kcal/mol) is remarkably similar to the molar, weighted average of

the $\Delta G_{absorption}$ predicted (Table 4.1) from AM-1 (3 to 4.8 kcal/mol), PM3 (-0.7 to 1.8 kcal/mol), and MNDO (1.4 to 3.8 kcal/mol). From these observations, it is clear that the total amount of HCl absorption does not depend upon the cation structure (R-group).

Table 4.5. Summary of Total HCl Absorption Data Observed in Acidic IL's.

Cations	K_i, atm^{-1}	ΔG (kcal/mol)
EMIM-Cl	0.0296	2.08
BMIM-Cl	0.0323	2.03
BeMIM-Cl	0.0389	1.92
HMIM-Cl	0.0297	2.08
OMIM-Cl	0.0353	1.99
DoMIM-Cl	0.0312	2.05
All Data	0.0327 ± 0.002	2.03± 0.04

Table 4.6. Summary of Total HCl Absorption into R-methylimidazolium Cl *n*$AlCl_3$.

IL's	K_i, atm^{-1}	ΔG (kcal/mol)
EMIM-Cl -neutral	0.0531	1.738
BMIM-Cl -basic	0.7012	0.210
BMIM-Cl -neutral	0.0610	1.656
BMIM-Cl -acidic	0.0323	2.033

Table 4.7. Summary of Total HCl Absorption into BMIM-Cl:MCl_3.

IL's	K_i, atm^{-1}	ΔG (kcal/mol)
BMIM-Cl - $AlCl_3$	0.0323	2.03
BMIM-Cl - $GaCl_3$	0.0284	2.11
BMIM-Cl - $InCl_3$	0.0422	1.87

The solubility of HCl was also studied in basic and neutral chloroaluminates IL's containing the *n*-butyl-methyl imidazolium cation (Figure 4.4) (Table 4.6). It was shown that the HCl absorption was linear with respect to the HCl pressure for the neutral and acidic IL's, but not for the basic IL. Moreover, the amount of HCl absorption was most for the intrinsically basic IL (K_{HCl} = 0.7 atm^{-1} when n = ½), least for the intrinsically acidic IL (K_{HCl} = 0.0321 atm^{-1} when n = 2) and the HCl absorption was intermediate to these two for the neutral IL (K_{HCl} = 0.061 atm^{-1} when n = 1) where n is the $AlCl_3$/$RMIM^+Cl^-$ ratio. The equilibrium constant for HCl uptake in a neutral $AlCl_3$/EMIM-Cl was 0.053 atm^{-1} also measured at room temperature. Neutral EMIM-Cl and BMIM-Cl ionic liquids showed very similar free energies of absorption for HCl (1.6-1.7 kcal/mol). This trend that was observed for the BMIM-Cl chloroaluminates was similar to that described by Campbell and Johnson for the ionic liquid derived from the EMIM-Cl chloroaluminate they studied [28].

The solubility of HCl was also studied in ionic liquids composed of BMIM-Cl:MCl_3 (M= Al, Ga, In) (Table 4.7). In Figure 4.5 it is shown that the HCl absorption was linear with respect to the HCl pressure for all the different anions, where the mole fraction of HCl in the IL decreased as the anion was changed from In, Al to Ga. The

equilibrium absorption constants were not statistically different for the Al and Ga IL's (0.0323 ± 0.003 *versus* 0.0284 ± 0.004). The In system absorbed more HCl than Ga and Al, and this can be explained as follows. The intrinsically neutral IL BMIM-Cl:$InCl_3$ formed a clear liquid, but a precipitate formed upon addition of InCl3 in excess of the neutral IL, 1:1 ratio. Thus, we conjecture that the In system could not form an intrinsically acidic IL and therefore, the neutral IL, absorbed more HCl than intrinsic acidic IL (Table 4.6 and Figure 4.4) as was observed for the Al IL's. This unusual physical property of the In IL system may also show unexpected results in its chemical properties.

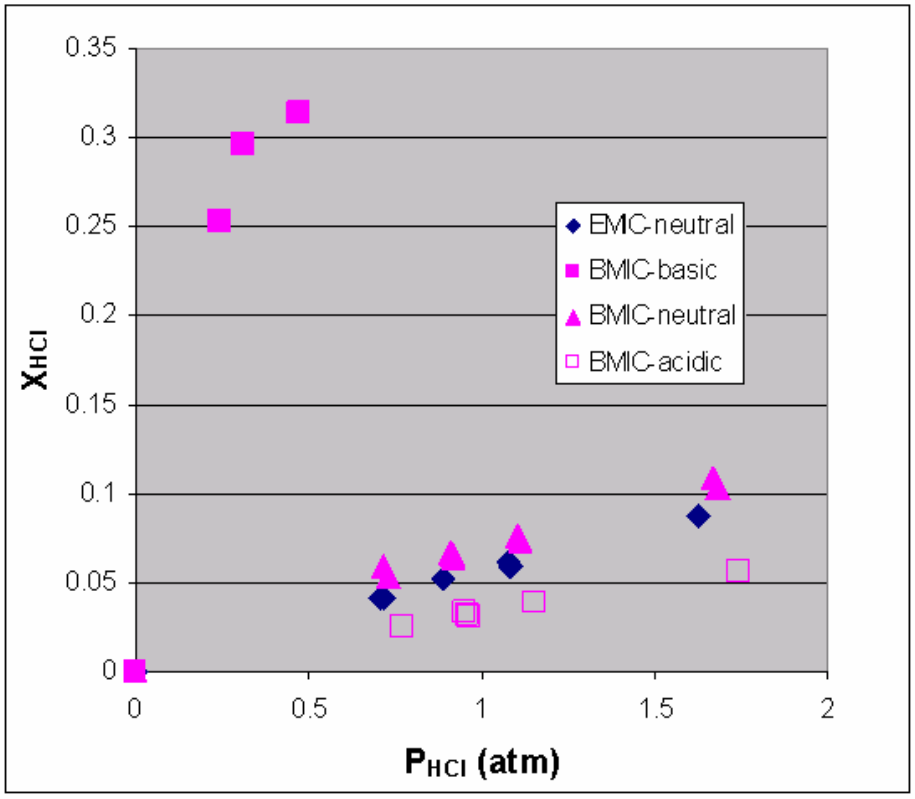

Figure 4.4. HCl absorption in *n*-butyl-methyl imidazolium n-$AlCl_3$.

The response of the intrinsically acidic Al and Ga IL's to HCl absorption met our expectation that the Al IL would not absorb more HCl than the Ga IL after one considers the errors in the measurements. Thus, we do not expect that differences in the reactivity of arene carbonylation can be ascribed to any differences in total HCl absorption, but rather, we expect that variations in the reactivity with changes in the Lewis acid may be due to differences in the strong Brønsted acidity generated upon HCl absorption.

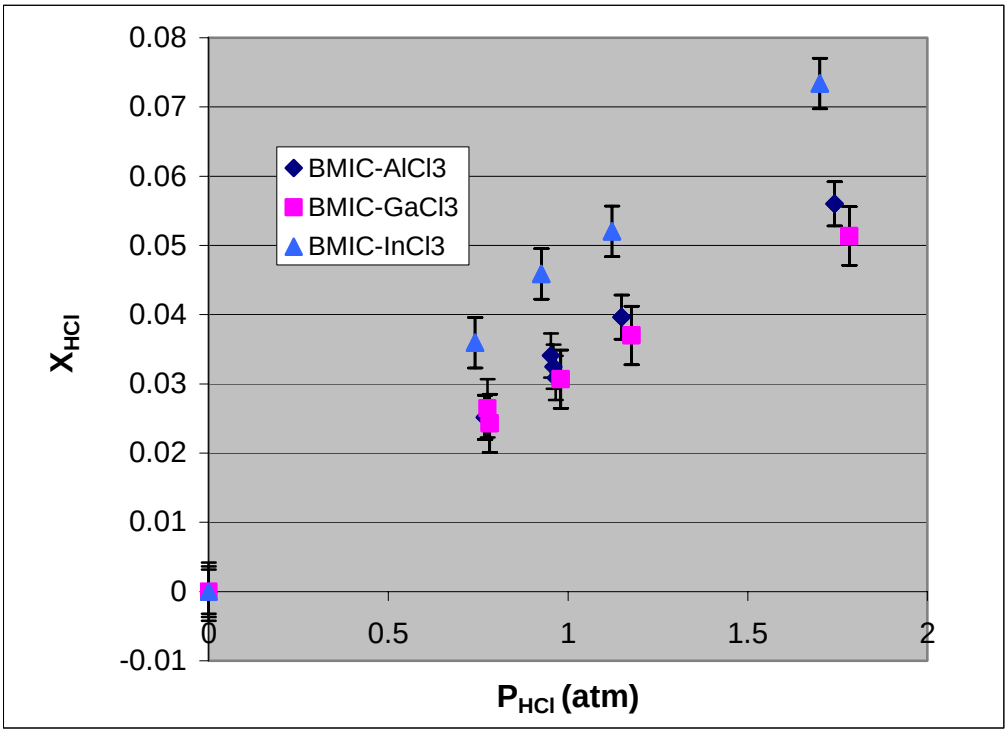

Figure 4.5. HCl absorption in BMIM-Cl:MCl_3.

4.4.5 HCl Absorption in dry Toluene

Additional HCl absorption studies were completed in dry toluene as a control for these studies. Toluene picked up 0.0479 moles HCl per mole of toluene at room

temperature and at an equilibrium pressure of 16.3 psia (1.11 atm). These data suggest an equilibrium absorption coefficient at room temperature of 0.0457 atm^{-1}. An IL derived from $AlCl_3$/BMIM-Cl (2 mol/mol) and mixed with an amount of toluene equal to the moles of $AlCl_3$ showed HCl absorption of 0.1011 moles HCl per mole of toluene in the mixture at room temperature. The equilibrium absorption coefficient for this liquid was 0.0408 atm^{-1}. The difference in the HCl absorption between these two liquids was 0.1011-0.0479 = 0.0532 mole HCl/mol toluene. This absorption amount will be compared to that of the neat IL (*i. e.*, no toluene added) at the same conditions which shows 0.0571 mole HCl per mol $AlCl_3$ and since the moles of $AlCl_3$ equals the moles of substrate, it appears that the incremental absorption of HCl in the IL with toluene added to the IL equals that absorption in the toluene alone at the same conditions.

4.4.6 CO absorption in Acidic IL's

The CO absorption was studied for the acidic IL's described above at a partial pressure of CO between 0 and 6.8 atm. While Anthony, *et al.*, were not able to detect CO solubility [29] in the IL's they studied, Ohlin, *et al.*, reported the solubility of CO increased with increasing size of the R-group chain from methyl, ethyl, *n*-butyl, *n*-hexyl, and *n*-octyl in two ionic liquids derived from RMIM-Cl with either the *bis*(trifluoromethylsulfonyl)imide or the tetrafluoroborate anions [5]. Using the same volumetric apparatus and the same procedure as in the HCl absorption, we were not able to detect any CO absorption. It may be speculated that the detection limit of our apparatus (x_{CO} ~ 0.003) was greater than the amount of CO that could be absorbed into

these IL's. We find support for this speculation in the data reported by Ohlin, *et al.* who showed that the CO mole fraction was ~ 0.001 at CO partial pressures near 1 bar for non-acidic IL's derived from the combination of the same cations but having either *bis*(trifluoromethylsulfonyl)imide or tetrafluoroborate anions [5].

4.4.7 Mixed gas absorption in Acidic IL's

In the gas mixtures experiments we did not observe an increase in the total moles absorbed by the HCl + CO mixture when compared to the HCl + Ar mixture.

4.4.8 Reactivity of Acidic IL's having different R-groups

The reactivity of the toluene carbonylation reaction at room temperature (HCl partial pressure = 3.04 atm, CO partial pressure = 8.16 atm) was determined for a series of intrinsically acidic IL's ($AlCl_3$/RMIM-Cl^+ = 2) for which the R-group was varied: ethyl, *n*-butyl, *n*-hexyl, *n*-octyl, *n*-dodecyl, benzyl (Figure 4.6).

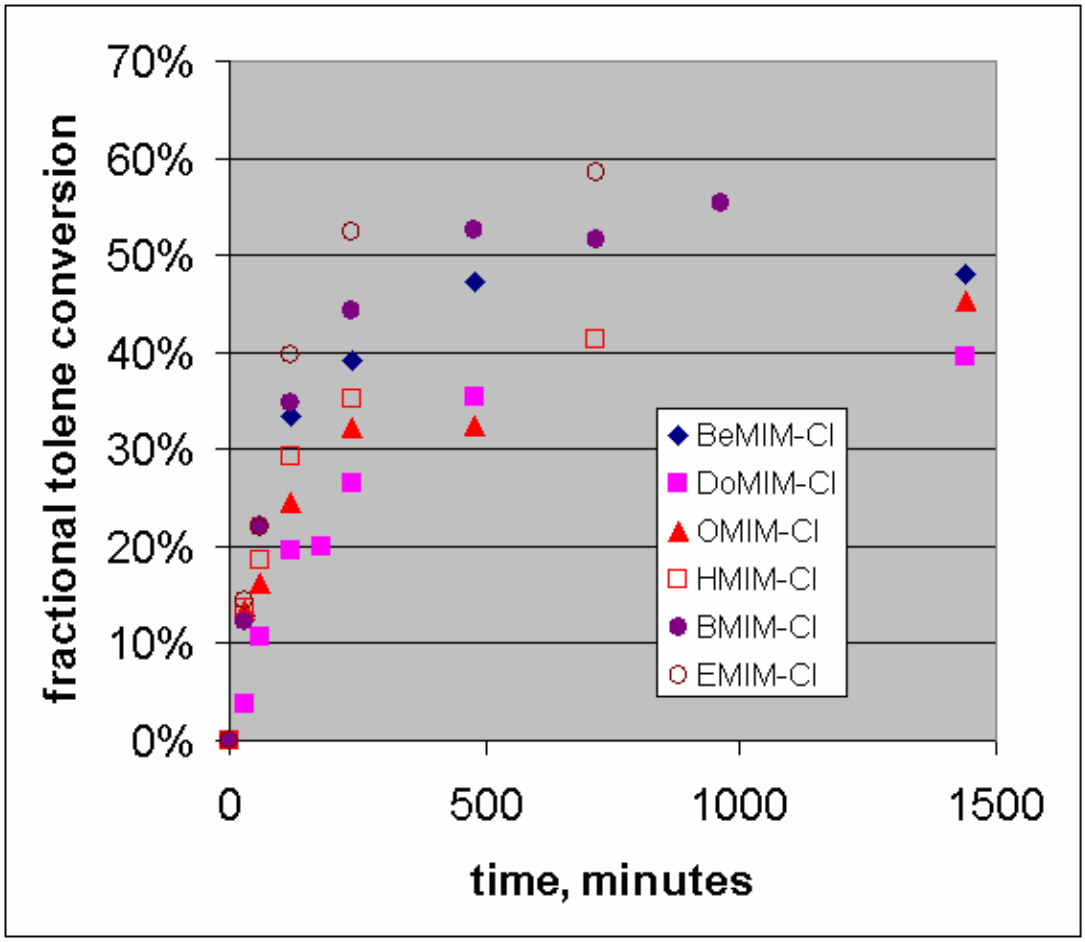

Figure 4.6. Fractional toluene conversions versus time for Me-imidazolium-R cations.

The reactivity's of the IL's prepared from $RMIM^+$ cation having either ethyl or *n*-butyl were very similar but the cation having the *n*-butyl group appeared to be slightly lower in reactivity than the cation showing the ethyl group. However, the reactivity was systematically lower for the IL's prepared from the cations having the benzyl, *n*-hexyl, n-octyl, and *n*-dodecyl groups on the imidazolium ring, especially evident in the data for conversions greater than 10%. These data for reaction times less than 2 h could also be correlated by the integrated rate equation that we described earlier [14, 15] as shown in Figure 4.7. Data obtained at short reaction times were chosen for correlation so as to

minimize the effect of the product aldehyde for inhibiting the reaction rate as was observed in reaction catalyzed by triflic acid [13]. The slope of this integrated plot is the product of the rate constant, the dissolved CO concentration, the initial concentration of Al^{3+}, and the Brønsted acid concentration in the IL: $k[CO][H^+][Al^{3+}]_o$. These slopes vary as shown below:

Ethyl>*n*-Butyl >Benzyl > *n*-Hexyl > *n*-Octyl > *n*-Dodecyl=4.68 > 3.92 > 3.65 > 2.98 > 2.34 > 1.35 $kmin^{-1}$.

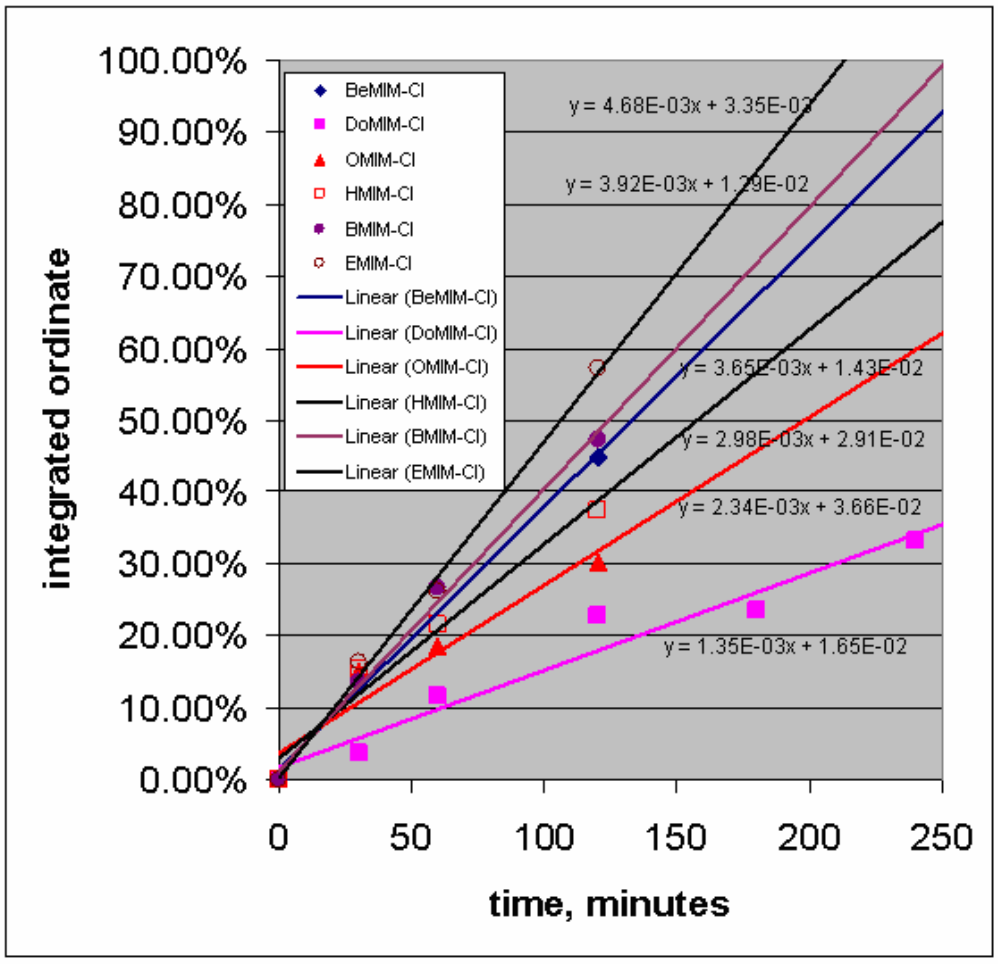

Figure 4.7. Integrated Rate Plot: Effect for Changing the Size of the Alkyl Group.

4.4.9 Reactivity of IL's derived from $BMIM^{\pm}$ and having different inorganic anion

As mentioned above, aluminum chloride is often reported as the Lewis acid partner to the organic cation. However, one report shows the use of In^{3+} to form IL which is active for the reaction between toluene and benzoic anhydride at 100 ºC and this report is significant in that the authors claim tha the IL can be reused [30]. The use of $InCl_3$ has also been observed to form RTIL's with $EMIM^+Cl^-$ only when the mole fraction of In^{3+} was 0.4 to 0.75 [31]. This same group reported RAMAN spectroscopy results which were consistent with the model that $In_2Cl_7^-$ was not observed in IL's comprised of excess $InCl_3$. Others report the use of IL's derived from dialkyl imidazolium halides with $GaBr_3$, $GaCl_3$, PF_5, and $SbCl_5$ [32]. One group reported the activity of an IL derived from N-(1-butyl)pyridinium chloride mixed with the anions $AlCl_3$ and $SbCl_3$ [33]. Therefore, it seems appropriate and fruitful to examine the properties of IL's that can be formed by mixing $BMIM^+Cl^-$ with M^nCl_n where M is Ga^{3+}, In^{3+}, Sb^{3+}, Sb^{5+} and P^{3+}. The purpose of this study was to examine tendency of these anions to form IL's at room temperature and when an IL is formed, to determine the effect of anion properties (*i. e.*, "hard" or "soft" acids) upon the activity of the IL towards a Brønsted demanding reaction when HCl was added to the system.

4.4.10 Formation and characterization of IL's from $BMIM^{\pm}Cl^-$ and M^nCl_n

Gallium chloride, $GaCl_3$, was found to be a good partner to the organic cation in that it readily formed an ionic liquid at room temperature, but it was less reactive than

$AlCl_3$ towards the toluene carbonylation reaction (Figure 4.8). A very viscous liquid was obtained when combining BMIM-Cl/$InCl_3$ in a mole ratio of 1:1. If the IL consisted of BMIM-Cl/$InCl_3$ (1:2 ratio) a slurry was formed, which is the one that Seddon used in their work [30]. We were able to reproduce the toluene and benzoic anhydride reaction in the IL composed of BMIM-Cl/$InCl_3$ (1:2 ratio), which demonstrated that we could reproduce the literature preparation for this IL; however, BMIM-Cl/$InCl_3$ (1 mol/2 moles) was not active for the toluene carbonylation reaction (Figure 4.8).

An ionic liquid could be formed from BMIM-Cl/$SbCl_3$ (1:2) that was very viscous at room temperature and it formed two liquid phases. When the IL was heated to 50ºC one phase was obtained but this one-phase system was not active to carbonylate toluene under the standard conditions after 4 hrs of reaction. Repeating the reaction at 50ºC, where only one liquid phase was observed, did not change the outcome of the carbonylation reaction.

We attempted to form an ionic liquid from BMIM-Cl/PCl_3 (1:2) by mixing one equivalent of the solid BMIM-Cl with two equivalents of the clear liquid, PCl_3. The BMIM-Cl and the PCl_3 were not completely miscible in that not all of the solid BMIM-Cl would dissolve into the PCl_3. The mixture was heated in an unsuccessful attempt to form one form phase, since after the heating and cooling process two liquid phases were observed. Once toluene was added to this system, three phases were observed. It is believed that the top phase was toluene, BMIM-Cl was the middle phase and PCl_3 was in the bottom phase. After shaking the FP tube, two phases were observed and it is believed that PCl_3 phase combined with the toluene phase. After 4 hrs of reaction no activity was obtained.

An ionic liquid could be formed of BMIM-Cl/$SbCl_5$ (1:2) and this mixture was used to carbonylate toluene at standard conditions. The $SbCl_5$ is a liquid with a light yellow color. Once the BMIM-Cl was contacted with the $SbCl_5$, the BMIC turned dark. and a slurry was obtained (not completely liquid.). After 4 hrs of reaction no aldehyde was observed, but some chlorinated products were observed in good yields. It appears that Sb^{5+} is active for a chlorination reaction; whereas Sb^{3+} is in active.

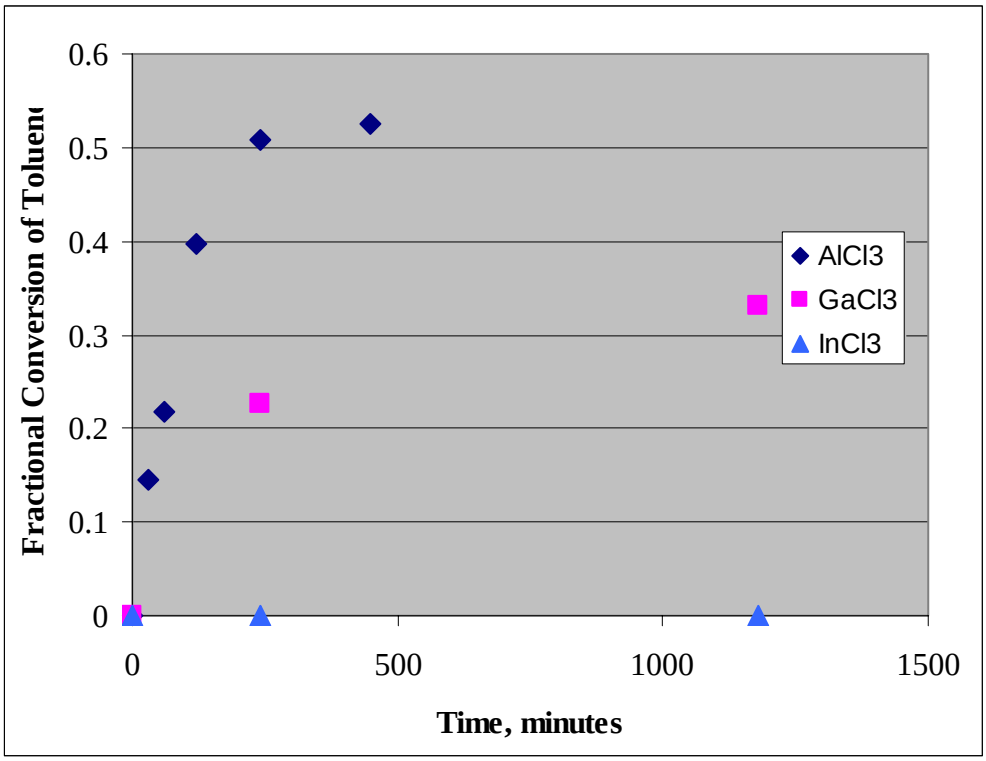

Figure 4.8. Fractional toluene conversions versus time for different inorganic anions.

The initial reaction rates shown in Figure 4.8 were 0.127, 0.0565, and 0 h^{-1} for $BMIM^{+}Cl^{-}/MCl_3$, with M = Al, Ga, and In, respectively.

4.5 Discussion

Several reports [9, 34] have appeared in the open literature in which the authors described their attempts to model the molecular properties of chloroaluminate ionic liquids described here. The modeling of the present work focused on acidic melts for which excess $AlCl_3$ is present.

As discussed in Chapter III, the HCl molecules were predicted to be sited at different positions. Similar structures were observed, when this modeling was repeated for the IL's derived from the other cations ($RMIM^+$, R = *n*-butyl, benzyl, *n*-hexyl, *n*-octyl, *n*-dodecyl). The free energy predicted by a particular model for absorption for HCl into the structures 3.12-a, 3.12-b, and 3.12-c, while different from one structure to another, did not change much for a particular structure as the R-group was changed using a particular model. Thus, it would appear that the affinity of HCl into these IL's is not influenced much by the type of R-group. In addition, the free energy for absorption predicted by AM-1 and MNDO was highest for siting the HCl on the anion between the two $\{AlCl_4\}^{1-}$ species, the (a) structures, and it was lower for siting the HCl between the anion/cation and on the cation for IL's derived from all R-groups, (b) and (c)-type structures.

The data for HCl absorption into the IL's were collected after a sufficient time to allow for the effects of mass transfer to be absent from the data set, even for the IL's derived from *n*-dodecyl and benzyl. The data in table 4.5 for K_{HCl}, show no systematic change in the values as the chain length (hence viscosity) increases. Thus, we believe that the data reported here had sufficient time to become equilibrated. These results for HCl

absorption into the acidic IL's derived from different R-groups appear to show a single value for the equilibrium absorption coefficient, $K_{absorption}$, equal to 0.0327 ± 0.002 atm^{-1}. Campbell and Johnson [28] reported HCl solubility data as an equation (#5, p 7793) for the neutral and acidic IL's. They showed a slightly higher value than our reported value for the absorption coefficient into acidic chloroaluminates derived from the EMIM-Cl IL (x_{AlCl3} = 2/3, K = 0.0337 ± 0.004 atm^{-1}). The values of the absorption coefficients (K) reported by us and others [28] are within experimental error and thus can be considered the same. K-values were also determined for the neutral IL derived from BMIM-Cl (0.061 atm^{-1}), from EMIM-Cl (0.051 atm^{-1}) and a basic IL (n=1/2) also derived from BMIM-Cl (0.70 atm^{-1}). The K-value reported here for the neutral IL derived from EMIM-Cl was slightly lower than that reported by Campbell and Johnson (0.051 *vs* 0.062 atm^{-1}) [28]. The K-value that we report for the basic melt (n = 1/2) cannot be compared to the correlated data reported by Campbell and Johnson. However, our data for n = 1/2 fall between curves (a) and (b), Figure 2-A, p 7794 in reference [28]. These two curves reflect the ternary HCl solubility into imidazolium chloride – HCl (curve a) and $AlCl_3$/ImCl = 0.451 mol / 0.549 mol (curve b).

The reported value of the average equilibrium absorption coefficient (0.0327 ± 0.002 atm^{-1}) corresponds to a free energy of absorption equal to 2 kcal/mol. The AM-1 model predicts a similar value for the free energy of absorption (4.0 kcal/mol) when one considers siting most of the HCl between the cation/anion (structure 3.12-b). This model predicts that very little of the HCl would be sited totally on the anion since its free energy of absorption (13 kcal/mol) is so much larger that the free energies for the other two structures. The AM-1 model for structure 3.12-c shows HCl having a bond distance

similar to that predicted for isolated HCl. These results are consistent with the reports that molecular HCl has been observed in the NMR spectrum of HCl gas in acidic chloroaluminates derived from the $EMIM^+$ cation [35]. In addition, another type of HCl species (structure 3.12-b) was predicted by this model, which shows an HCl species with a bond length of 1.32-1.36 Å. The $\Delta G_{absorption}$ into the IL predicted by the PM3 model was 0.9 – 4.3 kcal/mol for all three sites. These predicted $\Delta G_{absorption}$ are similar to the measured value of 2 kcal/mol. The MNDO model also predicted $\Delta G_{absorption}$ that were close to the observed value (2.5 – 2.6 kcal/mol) when it is considered that few HCl molecules will be sorbed into the higher energy sites (16.9 kcal/mol). Thus, all three, semi-empirical methods predicted $\Delta G_{absorption}$ for HCl into the IL's that were remarkably similar to the observed value of 2.0 kcal/mol.

The gas mixtures experiment showed that CO absorption was not enhanced by the presence of HCl, within the detection limits of the apparatus. We speculate that either we were not able to detect any CO solubility even after the HCl addition, or that the CO was displacing the HCl absorbed while reaching equilibrium, and in this case we were not able to detect any pressure difference. A more powerful tool such as NMR could be used to measure the solubility of ^{13}CO in the IL [5] and this approach is discussed in Chapter V).

We can only speculate on the reactivity of species in the IL towards the toluene carbonylation reaction, but it has been shown that 1) HCl does absorb into toluene in significant amounts (~0.05 mol/mol toluene @ 1.2 atm) at room temperature, 2) molecular modeling shows that HCl associates with the substrate, but that the H-Cl bond distance is only slightly longer than isolated HCl in the gas phase, and 3) that toluene,

HCl, and CO in the absence of IL does not react at room temperature. Moreover, when the IL's were made more basic by decreasing the $AlCl_3$/RMIM-Cl ratio from 2 to ½, it was observed that the total HCl absorption increased. However, the neutral and basic IL's were unreactive [14, 15] towards the toluene carbonylation reaction; thus the increased amount of HCl absorption in these neutral and basic IL's did not contribute to their reactivity. Accordingly, we suggest that more than one type of HCl species is present in the IL's and some of these HCl species may be unreactive towards the toluene carbonylation reaction. We conjecture that structures predicted to have the longer H-Cl bond lengths in IL's (3.12-a: 1.53 Å and 3.12-b: 1.32-1.35 Å) may be the reactive species having some activity for toluene carbonylation but additional experimentation will be necessary to confirm this speculation.

The data of toluene carbonylation show reaction rate constants that decrease from 4.7 to 1.4 x 10^{-3} min^{-1} with increasing length of the R-group in the imidazolium cation, and these data, free from mass transport effects, do not appear to correlate with the total HCl absorption into the same IL's. A significant amount of the total HCl absorption into the IL with toluene present (~0.05 moles HCl/mol toluene) appears in the toluene itself, while an equal amount appears in the IL. In addition, the CO absorption was apparently below the detection limit for our volumetric apparatus. Indeed, the detection limit of the instrument used here corresponds to a CO absorption that was greater than what was observed by Ohlin *et al.* [5] for CO absorption into a non-acidic IL having the same cations as was examined here. Toluene was miscible in the IL's when HCl was added to the gas phase, which suggests that toluene solubility in the IL is not a limiting factor. These results indicate that the variation in the reactivity with increasing chain length of

the R-group cannot be correlated to the total amount of HCl absorption or toluene solubility. The apparatus here was not sufficiently sensitive to detect CO absorption.

The batch reaction studies with BMIM-Cl/MCl_3 showed that the reactivity of the system decreased as the anion was changed from Al^{3+}, Ga^{3+} to In^{3+}. No reaction observed for anions: Sb^{3+}, Sb^{5+}, and P^{3+}. Reactivity pattern of group III-A appears to mimic the strength of the Lewis acidity in these metal ions. Highest activity correlated with highest acidity of Lewis acid partner: Al > Ga >> In. Members Group V metal chlorides, Sb and P, are inactive for the toluene carbonylation reaction. Total HCl absorption was greatest for the In IL; whereas, the HCl absorption was within experimental error for IL's prepared from Al and Ga. Modeling of the proton NMR resonances in some of these systems (Al, Ga, and In) shed light upon these chemical reactivity data in that the chemical shift of the proton changed with the identity of the Group III anion for one absorption structure in which the HCl was sited on the anion between the Cl_3MCl-H-$ClMCl_3^-$, M = Al, Ga, and In. The anion shown to produce the most active IL, Al, also was predicted to have the highest chemical shift of the proton downfield from TMS. The IL derived from Ga showed a predicted chemical shift that was ~ 0.3 ppm upfield for this same absorption structure, and the observed reactivity of the Ga system was about ½ that of the IL derived from Al. The In IL was not active for toluene carbonylation and it showed a predicted chemical shift that was 4 ppm upfield of either Al or Ga. Thus, the observed results for toluene activity were consistent with the trends in hard/soft acidity demonstrated by these cations and also consistent with the predicted ^{1}H-NMR chemical shifts.

Modeling of the same liquids for HCl absorption suggests that more than one type of HCl absorbed species is present, and the reactive species, a Brønsted acid derived from absorbed HCl, could be present in amounts much different that what observed for the total HCl pickup. Therefore, additional experiments will be needed 1) to determine if multiple HCl species are present in the acidic melts and characterize them for acidity, and 2) to quantitate the CO uptake as was done by Ohlin, *et al.* [5]. This will be discussed in Chapter V.

4.6 Summary

The length of the R-group in a family of organic cations apparently plays an important role in the chemistry of toluene carbonylation reaction. The activity for the toluene carbonylation reaction demonstrated a systematic decrease as the chain length in the cation was increased. Modeling of the IL by semi-empirical methods showed that 3 types of structures were predicted for the HCl/IL and that the free energies of formation for these three structures were different. The predicted free energy of HCl absorption into the IL's was remarkably close to the observed free energy of absorption when one considers the absorption of HCl as structures 3.12-b and 3.12-c. Moreover, the H-Cl bond lengths were predicted to be different for the HCl in the different structures. In this work we showed that the variation in the reactivity as R was changed could not be correlated to the amount of HCl absorbed in the ionic liquid since all of the IL's showed similar absorption amounts for HCl. The amount of CO dissolved in the IL's was apparently below the detection limit of the apparatus used here.

Highest activity correlated with highest acidity of Lewis acid partner: Al > Ga >> In. Group V metal chlorides are inactive.

4.7 References

1. Hussey, C.L., Oye, H.A., "Transport Numbers in Molten Acidic Aluminum Chloride – 1-Methyl-3-ethyl imidazolium chloride. Theirs Relationship to emf measurements in chloroaluminate melts", *J. Electrochem. Soc.* **131**, 1621 (1984).

2. Fannin, A.A., Jr., Floreani, D.A., King, L.A., Landers, J.S., Piersma, B.J., Stech, D.J., Vaughn, R.L., Wilkes, J.S., and Williams J.L., "Properties of 1,3-Dialkylimldazollum Chloride-Aluminum Chloride Ionic Liquids. 2. Phase Transitions, Densities, Electrical Conductivities, and Viscosities" *J. Phys. Chem.* **88**, 2614-21 (1984).

3. Wasserscheid, P. and W. Keim, "Ionic Liquids—New Solutions for Transition Metal Catalysis" *Angew. Chemie (Int. Ed.),* **2000** *39,* 3772-89.

4. Waffenschmidt, H., Ph. D. thesis, RWTH, Aachen, GERMANY (2000).

5. Ohlin, C. A., Dyson, P.J., and Laurenczy, G., "Carbon monoxide solubility in ionic liquids: determination, prediction and relevance to hydroformylation", *ChemComm*., **2004**, 1070-1.

6. Carey, F.A., Sundberg, R.J., "*Advanced Organic Chemistry Part A: Structure and Mechanisms*", Kluwer Academic/Plenum Publishers, 4th edition, 46-64, 2000).

7. Coulson, C.A., and Longuet-Higgins, H.C., "The electronic structure of conjugated systems. II. Unsaturated hydrocarbons and their hetero-derivatives", *Proc. R. Soc. London, Ser. A*, **192**, 16-32 (1947); Salem, L., "Intermolecular orbital theory of the interaction between conjugated systems. I. General theory", *J. Am. Chem. Soc.*, **90**, 543-552 (1968); Dewar, M.J.S., and Doughherty, R.C., "The PMO Theory of Organic Chemistry", Plenum Press, N.Y., (1975); Klopman, G., "Chemical Reactivity and Reaction Path", Wiley-Interscience, N.Y., Chapter 4, (1974).

8. Fukui, K., “Recognition of stereochemical paths by orbital interaction”, *Acc. Chem. Res.*, **4**, 57-64, (1971); Fleming, I., “Frontier Orbitals and Organic Chemical Reactions”, John Wiley & Sons, N.Y., (1976); Salem, L., “Electrons in Chemical Reactions: First Principles” John Wiley & Sons, N.Y., Chapter 6, (1982).

9. Dieter, K. M., C. J. Dymek, N. E. Heimer, J. W. Rovang, and J. S. Wilkes, “Ionic structure and interactions in 1-methyl-3-ethylimidazolium chlroide-$AlCl_3$ molten salts”, *J. Am. Chem. Soc*. **1988**, *110*, 2722-6.

10. Chandler, W. D. and K. E. Johnson, “Thermodynamic Calculations for Reactions Involving Hydrogen Halide Polymers, Ions, and Lewis Acid Adducts. 3. Systems Constituted from Al^{3+}, H^{+} and Cl^{-}“, Inorg. Chem. (1999), **38**, 2050-6.

11. Smith, P., Dworkin, A. S., Pagni, R. M. and Zingg, S. P., “Brønsted Super acidity of HCl in Liquid Chloroaluminate. $AlCl_3$-1-Ethyl-3-methyl-1*H*-imidazolium Chloride”, *J. Am. Chem. Soc.*, 1989, **111**, 525.

12. Angueira, E. J. and M. G. White, “Predicting the Composition of Acidic, Ionic Liquids in Contact with HCl Gas”, in press, *A. I. Ch. E. Journal*.

13. Angueira, E.J., and White, M.G., A.I.Ch.E. Annual meeting, San Francisco, CA November, 2003., “Arene Carbonylation in Acidic, Chloroaluminate Ionic Liquids”, paper 511a.

14. Angueira, E.J., and White, M.G., “Arene Carbonylation in Acidic, Chloroaluminate Ionic Liquids”, *J. Mol. Catal, A,* Vol 227/1-2 pp 51-58 (2005).

15. Sood, D. S., S. C. Sherman, A. V. Iretskii, J. C. Kenvin, D. A. Schiraldi, M. G. White, "Formylation of Toluene in Triflic Acid", *J. Catalysis* **199**, 149 (2001).

16. MOPAC 2002 Manual: http://www.cachesoftware.com/mopac/Mopac2002manual/node650.html

17. Pearson, R. G., "Hard and Soft Acids and Bases", *J. Am. Chem. Soc.* **(1963)**, **85**(22), 3533.

18. Pearson, R. G., "The Principle of Maximum Hardness", *Acc. Chem. Res.* **1993**, *26*, 250.

19. Pearson, R. G. *Chem. Eng. News* **1965**, *43* (May 31), 90.

20. Pearson, R. G. *Chem. Br.* **1967**, *3*, 103.

21. Parr, R. G.; Donelly, R. A.; Levy, M.; Palke, W. E. *J. Chem. Phys.***1978**, *68*, 3801.

22. Parr, R. G.; Yang, W., "Density Functional Approach to the Frontier-Electron Theory of Chemical Reactivity", *J. Am. Chem. Soc.* **(1984)**, *106*, 4049.

23. Lee, C.; Yang, W.; Parr, R. G. *J. Mol. Struct.* **1988**, *163*, 205.

24. Klopman, G.; Hudson, R. F. *Tetrahedron Lett.* **1967**, *12*, 1103.

25. Borodkin, G.I., Gaitlov, Y.Y., Nagy, S.M., and Shubin, V. G.J., *Struct. Chem*. 1996, 37, 464.

26. Chase, M.W., Davies, C.A., Downey, J.R., Frurip, D.J., McDonald, R. A., and Syverud, A.N., JANAF Thermochemical Tables, 3^{RD} ed. *J. Phys Chem. Ref. Data* **1985**, *14*, Suppl. 1.

27. Komshilova, O.N., Novikov, G.I., Polyachenok, O.G., " Thermodynamic study of the dimerization of gaseous indium trichloride", USSR. Zhurnal Fizicheskoi Khimii (1969), 43(11), 2979-80.

28. Campbell J.L., and Johnson, K.E., "The chemistry of protons in ambient-temperature ionic liquids: solubility and electrochemical profiles of HCl in HCl;ImCl:$AlCl_3$ ionic liquids as a function of pressure (295K)", *J. Am. Chem. Soc.* **1995,** 117, 7791-7800.

29. Anthony, J.L., Maginn, E.J., Brennecke, J.F, "Solubilities and Thermodynamic Properties of Gases in the Ionic Liquid 1-*n*-Butyl-3-methylimidazolium Hexafluorophosphate", *J. Phys. Chem. B* **2002,** *106,* 7315-7320.

30. Seddon, K. R., Hardacre, C., and Mcauley, B. J., WO 03/028883 A1.

31. Yang, J.Z., Tian, P., He, L., and Xu, W.G., "Studies on room temperature ionic liquid $InCl_3$-EMIC", *Fluid Phase Equilibria,* **204** (2003), 295-302.

32. Saleh, R.Y, US Patent 6,320,083, September 10, 1999.

33. Zing, S.P., Dworkin, A.S., Sorlie, M., Chapman, D.M., Buchanan, A.C., and Smith, G.P., "Reactivity of anthracene in liquid $SbCl_3$-$AlCl_3$-N-(1-butyl)pyridinium chloride mixtures", *J. Electrochem. Soc.*, **13**, 1602-8.

34. Davis, Larry P.; Dymek, Chester J.; Stewart, James J. P., "MNDO calculations of ions in chloroaluminate molten salts", *J. Am.Chem. Soc.,* **v. 107** (Sept. 4 '85) p. 5041-6.

35. Zawodzinski, T. A., R. T. Carlin, R. A. Osteryoung, "Removal of Protons from Ambient – Temperature Chloroaluminate Ionic Liquids", *Anal. Chem*. **1987**, *59*, 2639.

CHAPTER V

THE MOLECULAR ENVIRONMENT IN ACIDIC CHLOROALUMINATE IONIC LIQUIDS

Several groups have examined the molecular environment of acidic chloroaluminate IL's using ^{1}H-, ^{13}C-, and ^{27}Al-NMR spectroscopies [1-5]. In Chapter III, molecular modeling tools were used to predict the structures of several different molecular species in acidic chloroaluminate ionic liquids, and in this Chapter, we discuss the use of NMR spectroscopy to gain insight into the nature of these species present in the ionic liquids. The ^{27}Al-NMR spectra were also examined of the dialkyl imidazolium chloroaluminates (ethyl, methyl) with and without HCl added to show that the spectrum depends upon the ratio of Al/cation and upon the presence of HCl in the system. The effect upon the spectrum for changing the Al/cation ratio was attributed to either one or more equilibria involving anionic aluminum species [6].

$$O^{+}[Al_2Cl_7]^{-} + O^{+}Cl^{-} \Leftrightarrow 2\ O^{+}[AlCl_4]^{-} \qquad (5.1)$$

The effect of adding HCl to the IL was thought to alter the Al-speciation by the following equilibrium:

$$O^{+}[Al_2Cl_7]^{-} + HCl \Leftrightarrow O^{+}[AlCl_4]^{-} + H^{+}[AlCl_4]^{-} \qquad (5.2)$$

In Chapter III, we discussed modeling efforts, after the manner of Chandler and Johnson [7], to show the effect of adding HCl upon the Al-speciation as determined by purely

equilibrium thermochemical considerations. In addition, these results suggested two structures for the anion $[Al_2Cl_7]^-$: symmetric dimer $[(Cl_3Al\text{-}Cl\text{-}AlCl_3]^-$ or the unsymmetrical, anion pair ($Cl_3Al\ AlCl_4^-$). Subsequent molecular modeling suggested that the HCl molecule could reside in three different environments and these sites showed different free energies of formation [8]. The decreasing reactivity of these IL's as the structure of the cation was changed to show increasing chain length of R $[R\text{-}Me\text{-}Im]^+$, R = Et, Bu, Bz, Hex, Oct, and Dodec, could not be simply related to the amount of HCl adsorbed into the IL's. In fact, all of these IL's showed equilibrium adsorption coefficients that were indistinguishable within the error of the measurements. It became apparent that the molecular environment of these IL's was more complicated than what has been reported in the literature, and this is discussed in detail in this chapter.

The aim of this chapter is to examine the molecular structure of the IL as the ratio of Al/O^+ is changed with and without HCl added. Nuclear magnetic resonance spectra will be recorded with and without HCl present so as to determine the environments of the nuclei and thereby infer the structure of the species present. The working hypothesis is that the aluminum speciation determines the reactivity of the IL and this speciation depends upon the structure of the cation.

Also in this chapter, the acidity of the IL's was characterized using ^{13}C-NMR chemical shifts in the probe molecule 2-^{13}C-acetone, which was enriched in isotopic carbon. Others showed how the ^{13}C-NMR chemical shifts of the #2 carbon of this probe molecule were very sensitive to the acidity of solid and liquid acids when the probe molecule combined with the target acid. We measured the chemical shifts of this probe molecule in sulfuric acid and triflic acid so as to develop a scale of acid strengths based

upon these chemical shifts. By this method, then we could interrogate the number and strength of acid sites in the ionic liquids so as to confirm the predictions, which suggested that three types of Bronsted sites were present in the IL's having different strengths. The goal of this acidity strength scale is ultimately to find a correlation between the catalytic activities measured in various acidic reactions.

5.1 Experimental

5.1.1 Calculations

The Spartan '02 and Spartan '04 molecular modeling software packages were used to predict the geometry upon optimization and the NMR spectra.

5.1.2 Chemicals

The dialkylimidazolium compounds were obtained from Sigma Aldrich and used without further purification. Aluminum chloride (99.99%), obtained from Sigma Aldrich, was sublimed under a vacuum before use. Toluene (anhydrous, 99.8%) was obtained from Sigma Aldrich and used without further purification. Carbon monoxide, CP grade, and HCl (anhydrous, 99+ %) were obtained from Airgas and Sigma Aldrich, respectively. ^{13}C-labeled CO (99.9% ^{13}C) and Acetone, enriched in ^{13}C in the 2 position were obtained from Sigma Aldrich and used without further purification.

5.1.3 ^{1}H, ^{13}C, and ^{27}Al-NMR

The external standard for ^{1}H, and ^{13}C was a capillary filled with dimethyl sulfoxide (99%, DMSO). The aluminum external reference was a capillary tube filled with aqueous, aluminum nitrate (Fisher) at a concentration of 1 M. The capillary tube was approximately 76.2 - 88.9 mm long 1.5 mm diameter and was filled to approximately 50.8 - 63.5 mm of the tube's length with the standard. All data were recorded on a Bruker 300X, with a 5 mm multinuclear probe. Typically, 256, 64, and 16 numbers of scans were obtained for ^{13}C, ^{27}Al, and ^{1}H, respectively. The spectrometer settings for these analyses were standard settings already established by the scientists at the Georgia Tech NMR Center.

5.1.4 Preparation of IL's

The weighing instrument, chemicals, and material transfers for MCl_3 (M=Al, Ga, In), and RMIM-Cl were placed in an AtmosBag filled with dry Ar. $AlCl_3$ was weighed; and RMIM-Cl was added to it so as to obtain the desired $AlCl_3/O^+$ molar ratio.

Three samples were prepared having R = butyl, but the Al/cation ratio was 1/1, 3/2 and 2 mol/mol. One sample each was prepared having R = ethyl, hexyl, octyl, and dodecyl for which the Al/cation = 2 mol/mol.

5.1.5 HCl and CO absorption - NMR studies

1. The pressure valve sample NMR tube (obtained from NEW ERA Enterprises, Inc; size = 5 mm O.D. x 130 mm long; model number NE-PCAV-5-130) was placed in the Atmosbag with the different ILs.
2. The capillary tube containing the standard was placed inside the NMR tube and the IL or acid (sulfuric or triflic acid) was added (Figure 5.1).
3. NMR tube was sealed, evacuated and filled up with the desired gas to the desired pressure, and contacted with this gas for 30 minutes.
4. During the gas addition, sample was shaken to promote mixing of the gas with the liquid, and bubbling of the liquid was observed to indicate that good mixing had been achieved.
5. Sample was analyzed for ^{1}H, ^{13}C, and ^{27}Al NMR on a Bruker 300X.

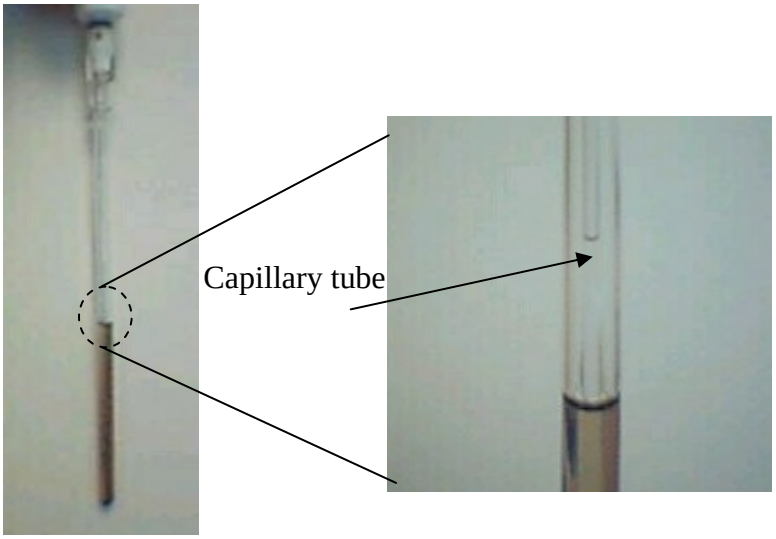

Figure 5.1. Pressure valve sample NMR tube with capillary tube inside.

5.1.6 Acid strength

1. The pressure valve sample NMR tube was placed in the Atmosbag with the different IL's or acids and the Acetone-^{13}C.
2. The capillary tube containing the standard was placed inside the NMR tube. Acid (1.0 – 1.3 g) and a drop of the acetone were added.
3. NMR tube was sealed and sample was analyzed for ^{1}H and ^{13}C NMR on a Bruker 300X.

5.2 Results

5.2.1 Transition state calculations—formation of the IL

The transition state geometry was predicted using the semi-empirical PM3 method and these predictions were described in Chapter III. The initial system was one Al_2Cl_6 molecule and one n-butyl-methyl imidazolium chloride molecule (Figure 3.16 in Chapter III). The optimized transition state geometry showed a very long distance between the N-Cl on the imidazolium chloride (2.6 Å); whereas the Cl appears to associated with one Al atom in the aluminum chloride dimer. It is obvious that the symmetry of the aluminum dimer has been lowered causing significant distortion of the molecule. Depending upon which bonds were broken to exit the transition state, we observed that two possible products could be obtained. The free energies of these products were 99.7 kcal/mol for their formation suggesting that either structure was

equally likely to be formed at room temperature. The existence of these two species may be interrogated by ^{27}Al-NMR.

5.2.2 ^{27}Al NMR spectrum

5.2.2.1 Aluminum speciation - Effect of changing BMIM-Cl/$AlCl_3$ mol ratio – No HCl

The ^{27}Al-NMR spectra of the $AlCl_4^-$ and the dimer species (Figure 3.16 on Chapter III) were predicted using the Spartan '04 package at the *ab initio* level (Hartree-Fock, 3-21G* basis set). For the neutral IL (n = 1), the predicted resonance was shifted 72.4 ppm downfield from the external reference [$Al(OH_2)(NO_3)_3$]. For the aluminum anion pair $(AlCl_3)(AlCl_4)^-$, a pair of resonances were predicted at 60 and 62.7 ppm downfield from the standard. The symmetrical $Al_2Cl_7^-$ anion showed predicted resonances at 69.7 and 69.8 ppm downfield.

Consider how Gaussian peaks located at these predicted resonances may be added (Figure 5.2) so as to simulate the observed ^{27}Al-NMR spectra for n = 3/2 and n = 2 mol/mol. In Figure 5.2, increasing values of the chemical shift downfield were represented by increasing positive numbers to the right. For n = 3/2, the basis set of NMR peaks contained $AlCl_4^-$, $(AlCl_3)(AlCl_4)^-$, and $Al_2Cl_7^-$; whereas, for n = 2, the basis set contained only $(AlCl_3)(AlCl_4)^-$, and $Al_2Cl_7^-$. For n = 3/2, there are 5 peaks: 1 peak for $AlCl_4^-$, 2 peaks for $(AlCl_3)(AlCl_4)^-$(1 for each Al, and based on NMR prediction Chapter III, these two peaks are separated by 0.1 ppm), and 2 peaks for $Al_2Cl_7^-$, but the two Al are in a similar environment producing one big peak (Figure 5.2). We observed that for n =

3/2 the peak to the left (upfield) resulted from of the anion pair $(AlCl_3)(AlCl_4)^-$. The identification of this anion pair helps to explain our data and data of others [6]; the spectra are complicated and the upfield peak is not isolated $AlCl_4^-$ monomer as claimed by others. Our new contribution is the use of an internal standard and molecular modeling to guide us during the identification of the different species in the ionic liquid.

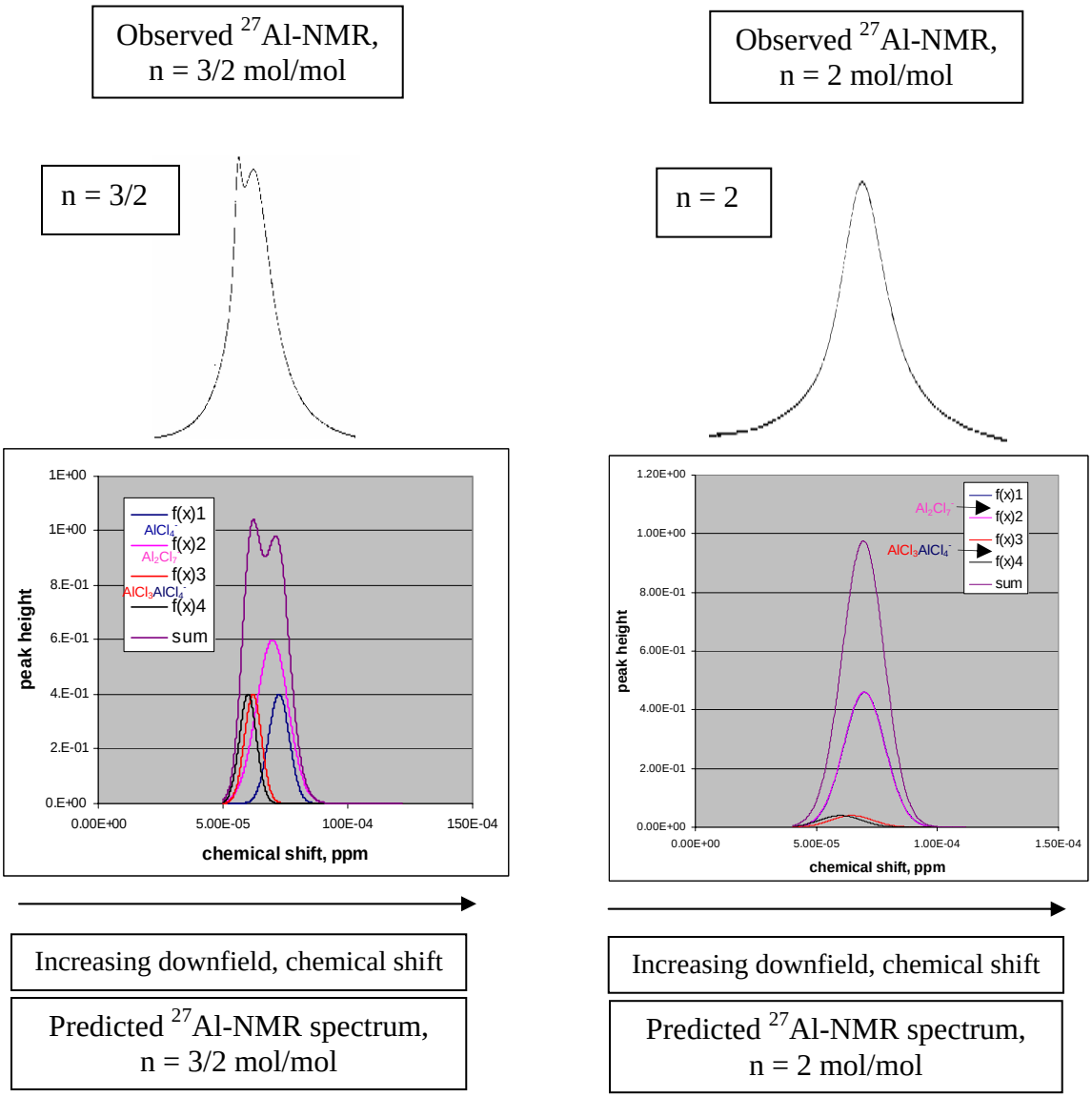

Figure 5.2. Predicted (bottom) and Observed (top) ^{27}Al-NMR Spectra for BMIM-Cl/Al_nCl_{3n+1} (n = $AlCl_3$/BMIM-Cl).

Good agreements between predicted and observed shapes of the spectra were possible by altering only the peak heights and peak widths; however, the absolute values of the observed resonances were shifted further downfield by 30-35 ppm from the predicted values.

Consider the effect of changing the ratio of moles aluminum to mole of diaklylimidazolium cation, Figure 5.3, for the ^{27}Al-NMR spectra of Al/RMIM^{+} = 1/1, 3/2, and 2 mol/mol when R = butyl. For the neutral IL (n = 1), the resonance is sharp ($\Delta\nu_{1/2}$ = 3 ppm) and located at 103.4 ppm downfield from the standard. The acidic IL's (n = 3/2 and 2 mol/mol) show wider peaks ($\Delta\nu_{1/2}$ = 35 and 125 ppm, respectively) that are fused (*e. g.*, n = 3/2). When n = 3/2 two peaks were observed having maxima at 98.2 and 102.2 ppm downfield; however, only a single, asymmetric peak was observed at 102.2 ppm when n = 2. These observations are similar to those reported earlier by Gray and Maciel [6] and by Wilkes, *et al*. [3]. Neither of these earlier studies used an internal standard as we have shown here, nor did they employ quantum mechanical methods to assist in the peak assignment.

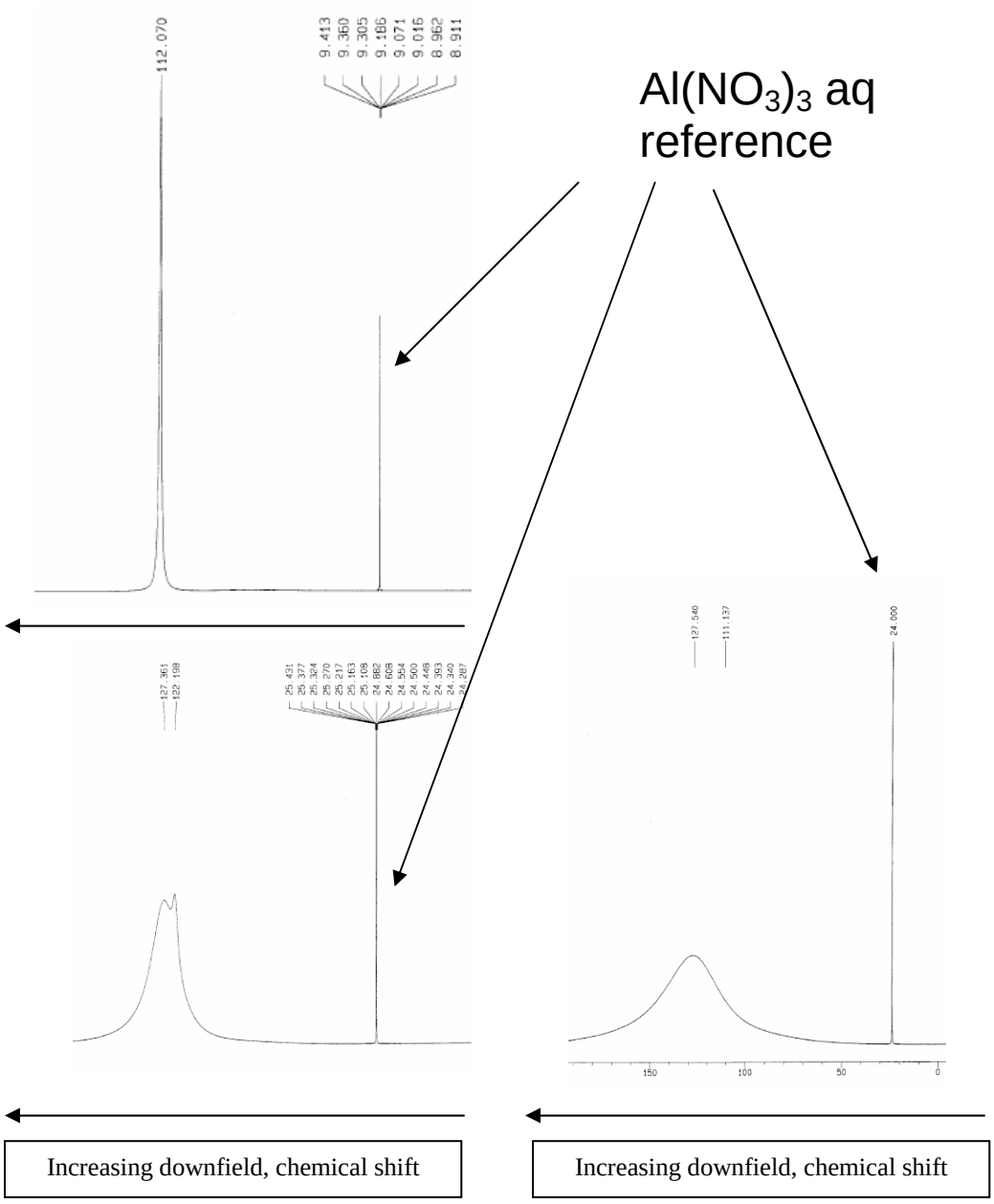

Figure 5.3. ^{27}Al-NMR of IL's with R = butyl and n = 1; 3/2; and 2 mol/mol.

5.2.2.2 Aluminum speciation - Effect of changing R when n= 2 – No HCl

^{27}Al-NMR spectra were recorded for the chloroaluminate IL's prepared with Al/RMIM^{+} = 1/1, 3/2, and 2 mol/mol when R = ethyl, butyl, hexyl, octyl, and dodecyl. The ^{27}Al-NMR spectra recorded at room temperature are different for n = 2 when R is changed (Figure 5.4). For increasing chain length of R, the peak at 98.2 ppm grew at the expense of the peak at 102.2 ppm. Additional systems were examined for changes in the ^{27}Al-NMR chemical shift when the R-group of the acidic chloroaluminate cation was n-butyl, n-hexyl, and n-octyl (Figure 5.5). If we use the peak assignments developed by us (98.2 ppm = anion pair; 102.2 ppm = dimer), then these results suggest that the relative amounts of the anion pair to dimer changes as the ligand in the cation grows from ethyl to dodecyl (Figure 5.5).

These spectra were deconvoluted to determine that the fractional area of the peaks at 102.2 ppm decreased monotonically from a high value of 0.812 for the IL derived from EMIM^{+} cation to the lowest value of 0.377 for the IL derived from DoMIM^{+} (Table 5.1). In the same table, we show how the observed rate constant ($k[Al]_o[CO][H^+]$) decreased monotonically from a high value of 4.67 $kmin^{-1}$ obtained from the IL derived from EMIM^{+} cation to the lowest value of 1.35 $kmin^{-1}$ obtained from the IL derived from DoMIM^{+} for the toluene carbonylation reaction at room temperature for which the CO partial pressure was 150 psig and the HCl partial pressure was 30 psig. These data are plotted in Figure 5.6 to show that a linear relationship exists between the observed rate constants and the fractional peak area assigned to the 102.2 ppm peak, which we interpret here as the dimer: $Al_2Cl_7^-$. In Figure 5.6 we show the relationship between the observed rate constant and the fraction of all of the Al species that are protonated dimers. The

abscissa on this plot is calculated from the fraction of Al species that is dimmers multiplied times the fraction of dimers that were protonated at a HCl pressure of 44.7 psia (Figure 3.2, page 59).

The observed reaction rate constant is function of the intrinsic rate constant, the amount of Al placed into the reactor, $[H^+]$ and [CO] absorbed in the IL. For all studies, the amount of Al put in the reactor was the same in each run as was the CO and HCl partial pressures. These experiments were completed at the same temperature. These results suggest that the reactivity depends upon the amount of the dimer in the IL before HCl gas was added: $Al_2Cl_7^-$. From the modeling of the macroscopic thermodynamics, we showed that the Brønsted acid was derived directly from the Lewis acid, $Al_2Cl_7^-$. Thus, if we assume that all of the "reactive" Bronsted acid is derived from only the dimer, then a linear relationship might be expected between the observed rate constant after HCl was added and the amount of dimer before HCl was added.

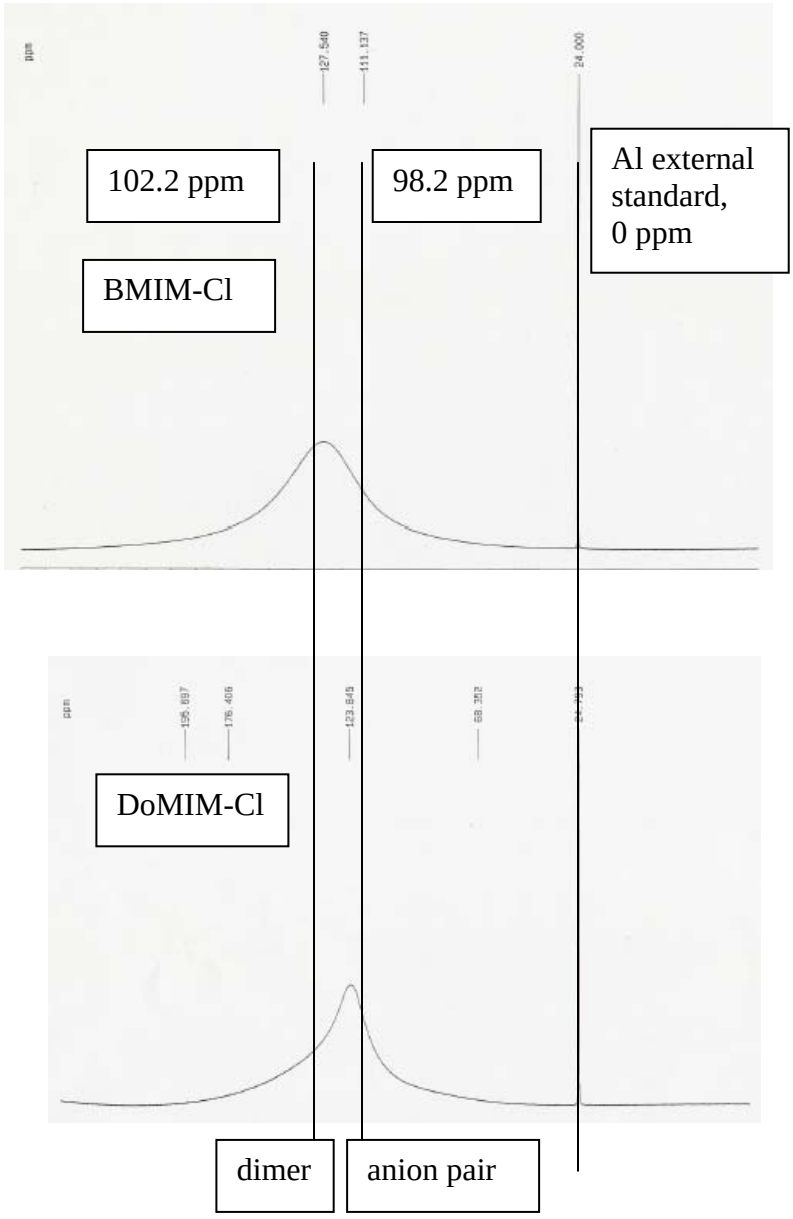

Figure 5.4. Effect of Changing R upon the ^{27}Al-NMR Spectra – dimer and anion pair.

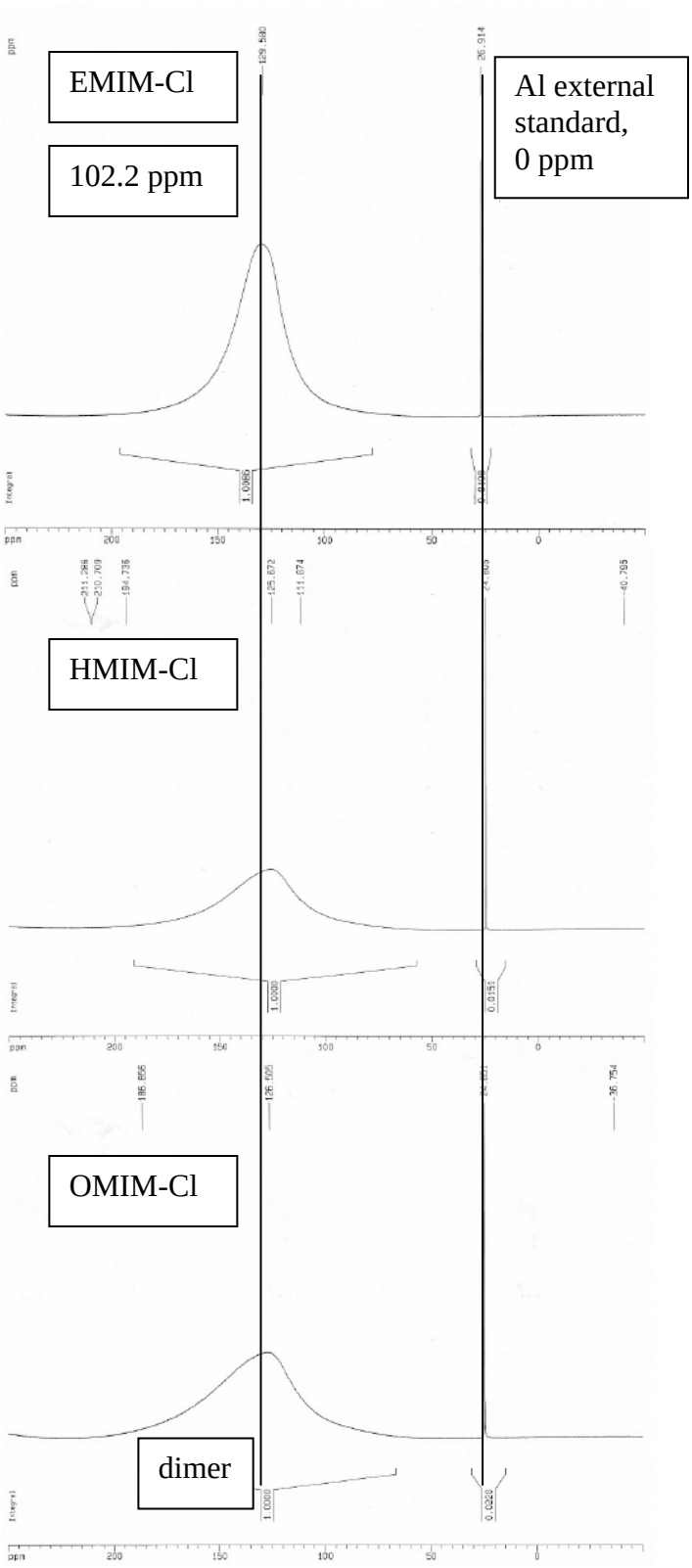

Figure 5.5. Effect of Changing R upon the ^{27}Al-NMR Spectra – 102 ppm peak.

Table 5.1. Effect of Cation Structure upon Al-Speciation, x_{102}, and the Observed Toluene Carbonylation Rate Constant.

Cation	x_{total}, 102 peak	$x_{reactive}$, 102 peak	k, $kmin^{-1}$
EMIM-Cl	0.812	0.663	4.67
BMIM-Cl	0.702	0.574	3.92
HMIM-Cl	0.599	0.490	2.98
OMIM-Cl	0.512	0.418	2.34
DoMIM-Cl	0.377	0.308	1.35

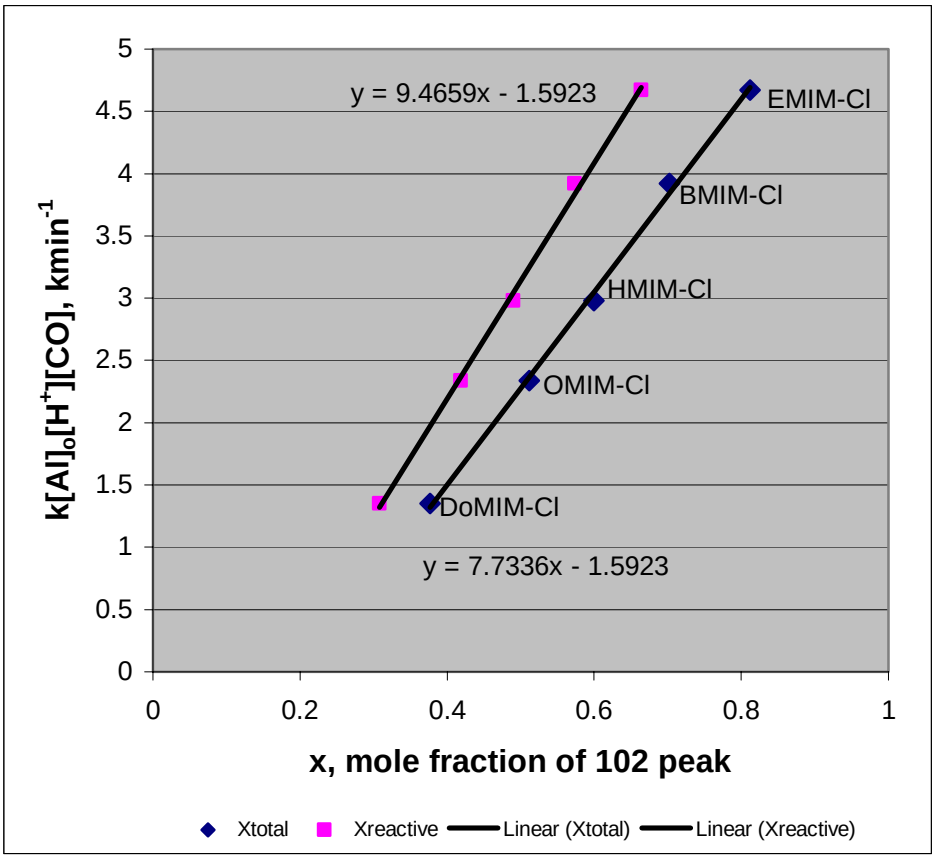

Figure 5.6. Correlation of Toluene Rate Constant with Al-Speciation.

5.2.2.3 Aluminum speciation - Effect of HCl partial pressure

Figure 5.7, shows the effect of adding HCl in an intrinsic acidic IL. After HCl was added a chemical shift downfield of approximately 2 ppm was observed, which confirmed that HCl interacts with the aluminum species. Moreover, the asymmetry of the peak in the downfield direction appears to be increased with the addition of HCl to the system. The next step is the interpretation of this observation, which is usually done by comparing the observed spectrum with the spectra of standards where for which the structures are known. In this case, we do not have these standards; therefore we resort to comparing the observed spectra with simulated ^{27}Al NMR spectra before and after HCl addition as a guide to how we might interpret the observed spectra. These predictions will help us to assign the peaks that result from adding HCl gas to the IL.

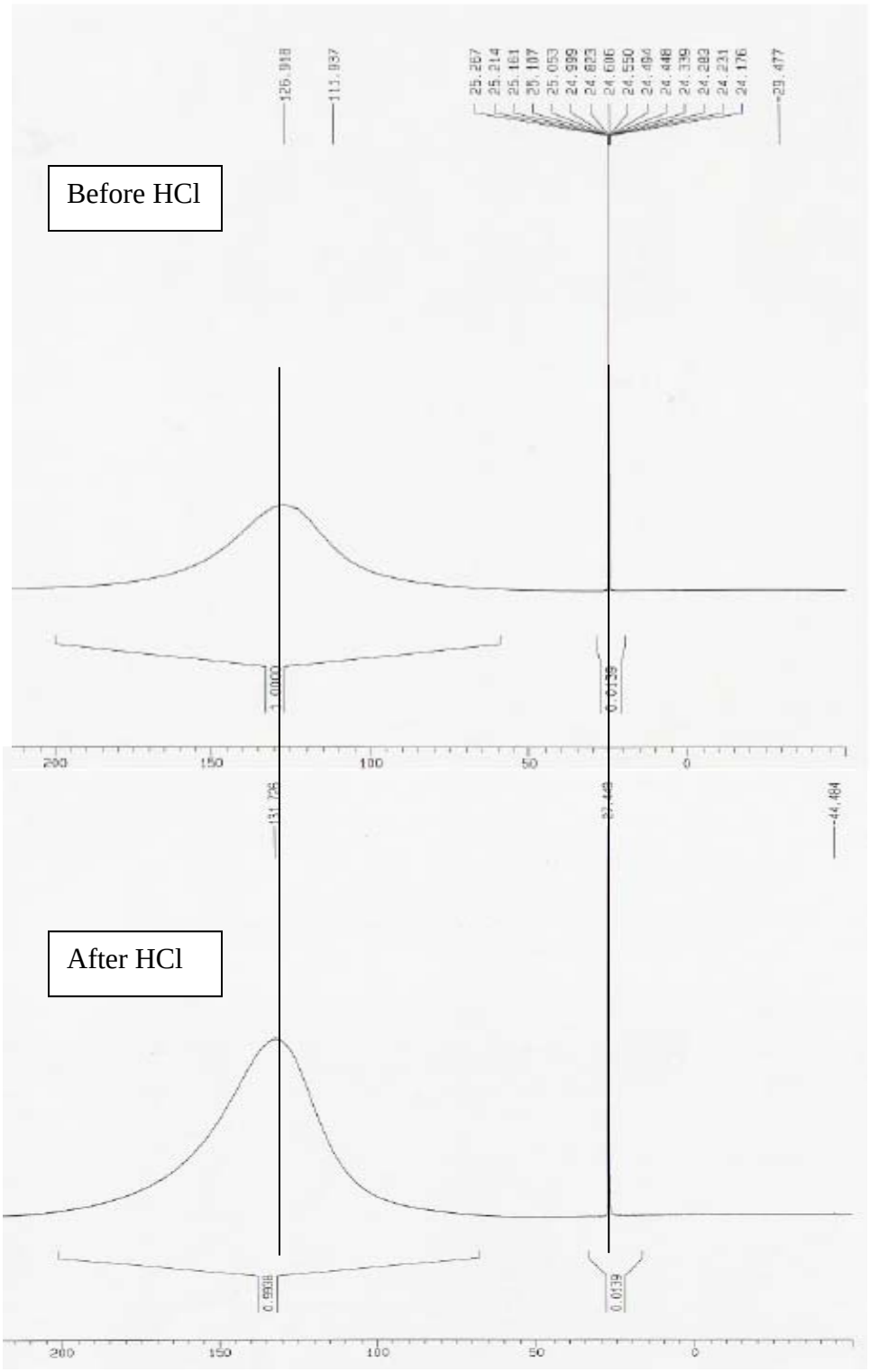

Figure 5.7. ^{27}Al NMR for BMIM-Cl/AlC_3 (1/2) IL, before and after HCl addition.

The Spartan '04 software was used to predict the ^{27}Al-NMR of the butyl-methyl imidazolium chloride/$AlCl_3$ IL (n = 2) beginning with Al in the anion pair (structure 3.11-a, -b, or -c) or the dimer structure (structure 3.12-a, -b, or –c) before and after HCl was added to the IL. For each structure containing two aluminum atoms, two chemical shifts are predicted (Table 5.2). The predictions show that ^{27}Al resonance depends upon placing HCl in the IL at each of the 3 sites for the two structures (Table 5.2) (Figure 5.8).

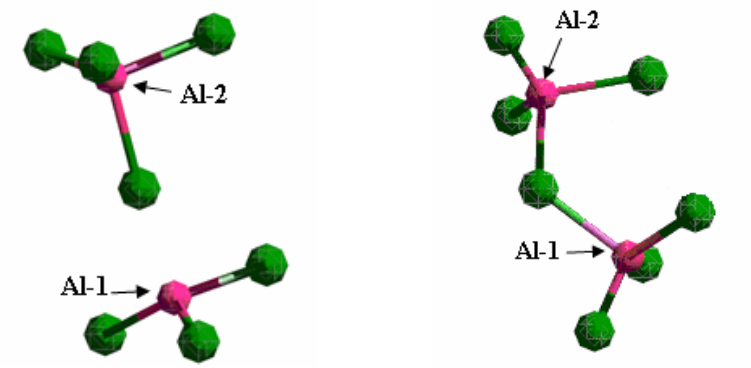

Figure 5.8. Aluminum identification for $(AlCl_3)(AlCl_4)^-$, and $Al_2Cl_7^-$.

The predictions show that large chemical shifts downfield result from adding HCl in the 3.11-a site of the anion pair (7.5 and 9.0 ppm); whereas only very small shifts upfield were predicted for adding HCl to the 3.11-c site of the anion pair (0.3 and 0.5 ppm). When HCl was placed in the 3.11-b site of the anion pair, chemical shifts upfield of 0.7 and 2.9 ppm were predicted. Quite different results were predicted when HCl was added to the dimer in the 3.12-a site (~ 3 ppm upfield and 1 ppm downfield); in the 3.12-b site (8 and 12 ppm upfield); and in the 3.12-c site (6 and 8 ppm upfield).

Table 5.2. Predictions of ^{27}Al resonance upon placing HCl in the IL.

Structure (from fig 3.11 and 3.12 – Chapter III)	Before HCl		After HCl		Difference, ppm	
	Al_1	Al_2	Al_1	Al_2	Al_1	Al_2
(11-a)	62.0	64.7	71.0	72.2	9.0	7.5
(11-b)			59.2	64.0	-2.9	-0.7
(11-c)			61.7	64.2	-0.3	-0.5
(12-a)	69.8	69.9	67.2	70.9	-2.7	1.0
(12-b)			58.2	62.3	-11.6	-7.6
(12-c)			61.7	63.9	-8.1	-6.0

The difference in chemical shifts, reported in ppm, Table 5.2, indicates the chemical shifts either upfield (negative number) or downfield (positive number). The observed data (Figure 5.7) showed that new species are created after HCl was added with chemical shifts that are downfield; therefore based on the predictions the HCl may be interacting with the anion pair (peaks at 71 and 72.2 ppm) or the Al dimer, peaks at 67 and 71 ppm (Figure 5.8).

To have a better understanding of the observed ^{27}Al NMR we decided to use the following approach: 1) Using same Al dimer/anion pair composition before and after HCl addition; examine predicted NMR before and after HCl addition (Figure 5.9 - top). In Figure 5.7, it is observed that after HCl was added a chemical shift downfield of approximately 2 ppm was observed. In the prediction the chemical shift is upfield after HCl was added, which is just the opposite direction of the observation. Using this approach, where the Al dimer/ anion pair composition remains unchanged, we can conclude this prediction does not agree with the observation and therefore suggest that addition of HCl to the IL may actually change the relative concentration of Al dimer/anion pair in the IL.

The other approach, 2) is having a different Al dimer/anion pair composition after HCl was added. If we consider the extreme case (Figure 5.9 – bottom), where the IL contains only the anion pair and no dimer after HCl was added, and compare the predicted *versus* the observed; the two spectra were found to have similar shapes, and chemicals shifts downfield, indicating that perhaps dimer/anion pair composition does change with HCl addition to the IL.

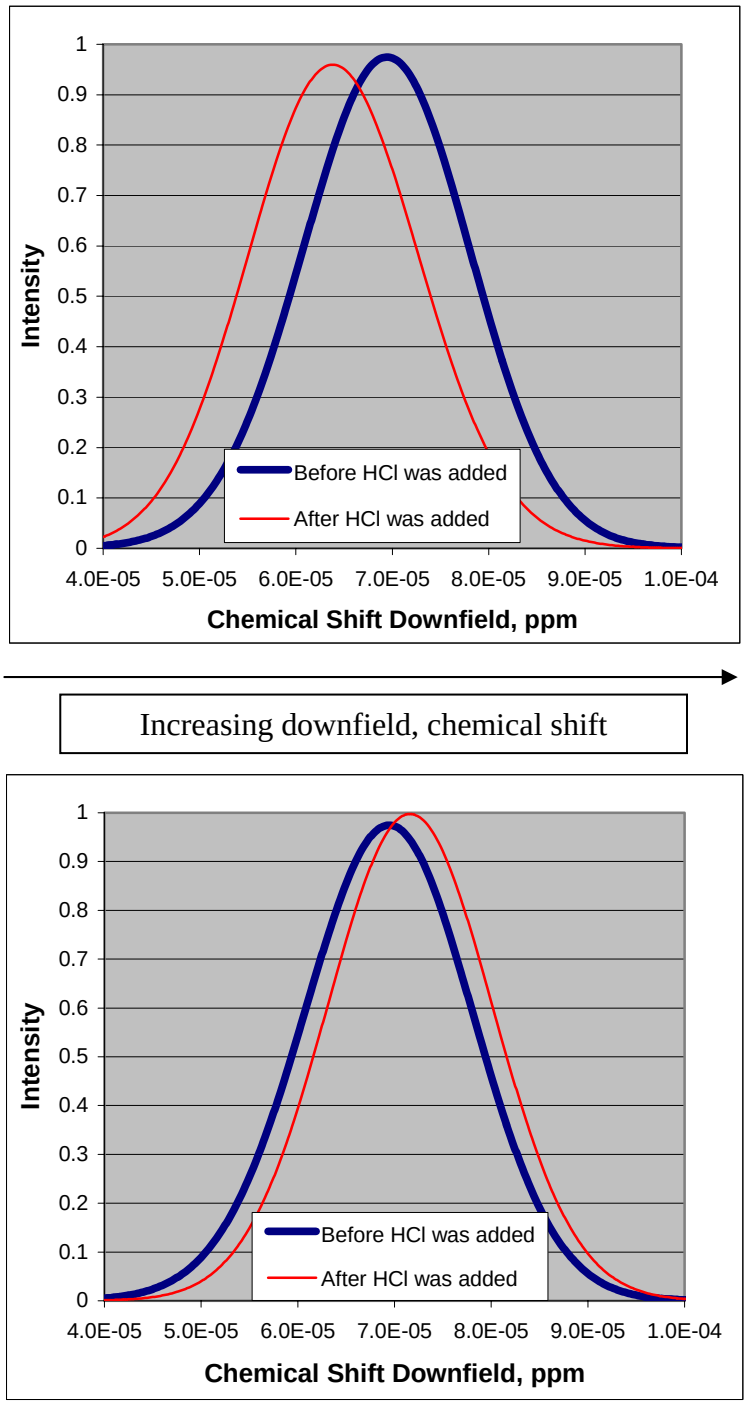

Figure 5.9. Predicted ^{27}Al-NMR Spectra Before and After HCl addition to the 3.11-a and 3.12-a sites. Same (top) and different (bottom) Al dimer/anion pair composition. Abscissa values are ppm/10^6; thus 100 ppm is 1 x 10^{-4} on this reported scale.

5.2.3 Effect of HCl on ^{1}H and ^{13}C NMR

One could examine the ^{1}H and ^{13}C NMR of the IL's directly before and after addition of HCl to determine how the HCl interacts with the IL and to compare these observations with our predictions Table 3.6, Chapter (III). After HCl addition, the prediction chemical shifts for proton NMR on the C-2 carbon showed a resonance approximately 15 ppm downfield from TMS. We repeated these calculations for the IL at the PM-3 level for the geometry optimization followed by a single point energy calculation at the *ab initio* level so as to predict the ^{13}C-NMR spectrum. The predicted chemical shifts in the ^{13}C-NMR spectra of the C-2, C-4 and C-5 carbons in the acidic $EMIM^{+}Al_2Cl_7^{-}$ IL without added HCl were 159.8, 124.2 and 123.7 ppm downfield from TMS. The predicted ^{13}C-NMR after adding HCl to the three positions in either the dimer or the anion pair are shown in Table 5.3.

Table 5.3. Predicted ^{13}C-NMR Spectra Before and After Adding HCl to IL.

	No HCl		HCl added (to structure a)		HCl added (to structure b)		HCl added (to structure c)	
C-position	anion pair	dimer	anion pair	dimer	anion pair	dimer	anion pair	dimer
C-2	159.8	160.4	159.7	159.1	158.6	158.8		160.3
C-4	123.7	121.4	123.5	121.5	122.1	123.8		121.5
C-5	124.2	124.2	123.9	127.7	125.1	124.0		124.7

The predicted changes in the chemical shifts were 1-3 ppm for adding HCl to the IL, which is considered to be indistinguishable. Thus, we do not expect to see significant changes in the ^{13}C-NMR that could be indirectly attributed to adding HCl to the IL.

5.2.4 ^{1}H and ^{13}C-NMR of IL's Before HCl was added

Figure 5.10 shows the proton NMR spectrum of $RMIM^{+}/Al_2Cl_7^{-}$ (R = butyl) before HCl was added. The identification of the carbons is shown in the Figure 5.11. The assignment of the proton resonances was confirmed upon comparison with data from the literature [1]. We observed proton chemical shifts at 7.43, 6.50, 6.48 ppm downfield from DMSO which compare well with those in the literature at 6, 5.05, and 5.05 ppm that have been assigned to protons residing on the C-2, C-4, and C-5 carbons for intrinsically acidic IL's. We could not detect any change in the proton NMR spectrum upon adding HCl gas to this IL at a pressure of 30 psig. This result is unexpected from a consideration of the modeling here and Chapter 3 which suggested that new peaks in the ^{1}H-NMR spectrum were expected to appear downfield (~ 14-17 ppm) upon HCl exposure to the IL.

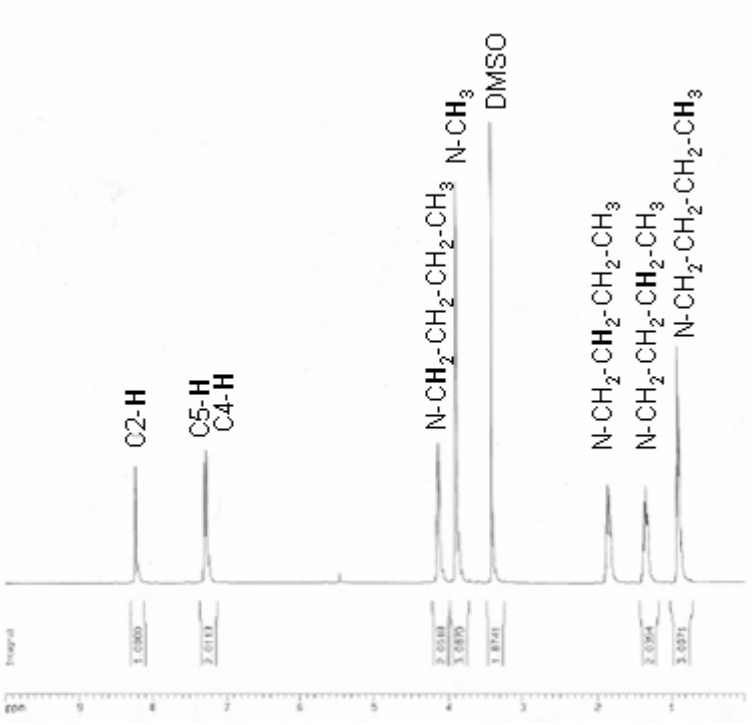

Figure 5.10. ^{1}H NMR spectrum of $BMIM^{+}/Al_2Cl_7^{-}$ before HCl was added.

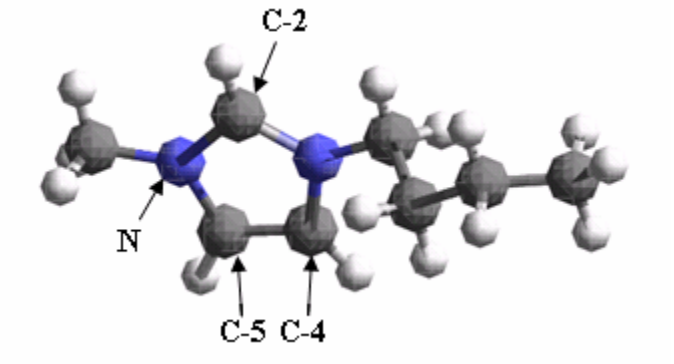

Figure 5.11. Identification of carbons in the $BMIM^{+}$.

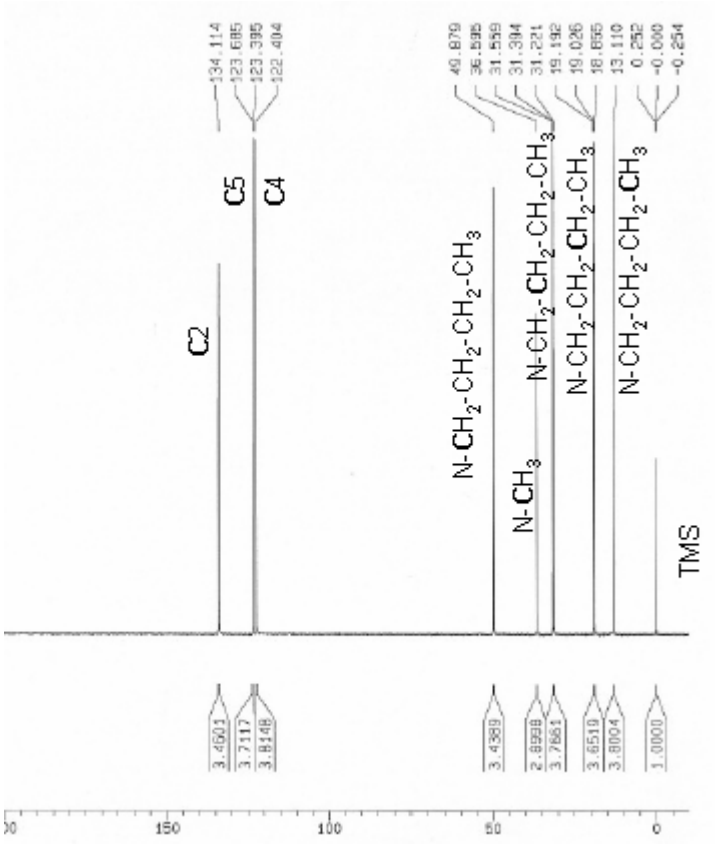

Figure 5.12. ^{13}C NMR spectrum of $BMIM^+/Al_2Cl_7^-$ before HCl was added.

The ^{13}C-NMR (Figure 5.12) shows the chemical shifts of the intrinsically acidic $RMIM^+/Al_2Cl_7^-$ IL before HCl was added. Resonances were observed at 133.67, 123.26 and 121.98 ppm downfield from DMSO, which has been assigned to the C-2, C-5, and C-4 carbons. Wilkes, *et al*. [3], reports a chemical shift of 146.0 ppm downfield from TMS (trimethylsilane) for an IL derived from ethyl-methyl imidazolium chloride/$AlCl_3$ (n = 2). They observed a chemical shift of 146.7 ppm for the neutral IL derived from the same cation which suggests that the intrinsic acidity has almost no effect upon the chemical shift of the C-2 carbon. Wilkes, *et al*. [4], reported a ^{13}C chemical shift of 134.5 ppm downfield of DMSO for a neutral IL derived from ethyl-methyl imidazolium

chloride/$AlCl_3$ which is similar to our value of 133.67 ppm for the acidic IL (n = 2) derived from the butyl/methyl imidazolium chloride/$AlCl_3$. Because of the discrepancies reported using the TMS standard and DMSO, we examined again the intrinsic acidic $BMIM^+/AlCl_3$ ionic liquid with a different internal standard: TMS instead of DMSO. We observed similar chemical shifts of 134.11, 123.685, and 122.404 ppm for the C-2, C-5, and C-4 carbons, respectively. We believe that the chemical shift of 146.0 ppm downfield from TMS reported by Wilkes, *et al*. may include some experimental errors due to the fact that they used TMS as an external standard. In our studies, we analyzed the sample with the standard inside the NMR sample tube with the IL.

We were not able to see any resonance in the proton NMR that could be directly attributed to HCl dissolved in the IL nor were we able to observe the indirect effects in the ^{13}C-NMR of adding HCl to the IL after repeated attempts to do so. While the results for the ^{13}C-NMR were expected and seems to be supported by the modeling, it is surprising that we were not able to observe directly the effect of adding HCl to the IL and therefore we were not able to understand the effect of HCl in the IL on the ^{1}H and ^{13}C NMR. Since this approach failed to characterize the acidity in these IL's, it was necessary to appeal to an indirect method to characterize the acidity. One such indirect method involves the use of a probe molecule that is a weak Lewis base: acetone.

5.2.5 ^{13}CO absorption NMR studies

We studied the ^{13}CO absorption by NMR following Ohlin *et. al.* [9] method, but we were not able to detect any CO in the vicinity.

5.2.6 Probe of superacidity

Since the direct approach to visualize the proton acidity developed upon adding HCl gas to IL's did not work, we decided to use a probe molecule, such as acetone-2-^{13}C. Wang, *et al* [10], showed that the ^{13}C-NMR chemical shifts of labeled acetone could be used to characterize the acidities in different liquid acids, solid acids such as zeolites, and $AlCl_3$. The goal of characterizing the IL's using labeled acetone is to reveal the presence and acid strength of protons (*via* the chemical shifts), while the area under the curve indicates the amount of acid sites having the indicated acid strength. Previous workers [10, 11] showed that the ^{13}C-resonace of the carbonyl carbon was a sensitive indicator of superacidity (Table 5.4) by the following equilibrium:

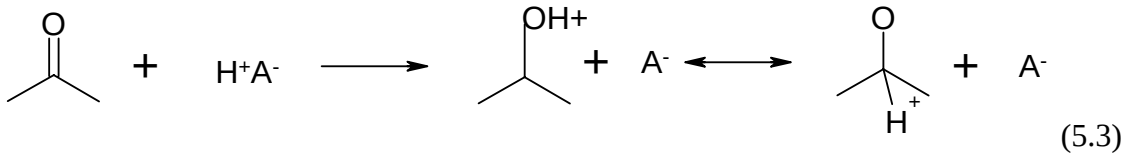

(5.3)

It is clear from this equation, that the chemical shift observed in the NMR (*i. e.*, amount of deshielding from the carbonyl carbon) will be directly influenced by the acid strength of the proton.

We repeated the calibration standards reported by Wang, *et al* [10], using concentrated sulfuric acid and triflic acid as the Brønsted acids and DMSO was the external standard (Table 5.4, see Figure 5.11 for peak identifications). The goal was to calibrate the Bruker NMR spectrometer for the effects of acid strength, reported as Hammett acidity function, upon the chemical shift of the labeled carbon in the acetone

probe. Notice how, the reported chemical shifts by Wang, *et al* [10]. increase from a value of 205 ppm for acetone in the non-acidic solvent CD_3Cl to higher values for the acetone in contact with the solid acids: zeolite HX (215 ppm); zeolite HY (220 ppm), zeolite HZSM-5 (223 ppm); and $AlCl_3$ (245 ppm). Consider further the data for the strongly acidic liquids: H_2SO_4, 80 wt% (235 ppm); H_2SO_4, 100 wt% (244 ppm); SO_3/H_2SO_4 (246 ppm); FSO_3H/SbF_5 (249 ppm) and SbF_5 (250 ppm). It is clear from the literature, that the ^{13}C-NMR spectrum of labeled acetone can be used to characterize the acidity of liquid and solid acids. Using the data for triflic and sulfuric acid, we developed the following equation relating the chemical shift of the labeled acetone with the Hammett acidity function:

$$-H_o = a + b[ppm] \qquad (5.4)$$

where a = -0.3298 and b = 67.36 from a fit of chemical shift, reported in ppm, to Hammett acidity functions of these standards, as reported in the literature.

The peaks at 240, 243, and 246 ppm observed for the acetone in contact with the IL's indicates values of the Hammett acidity function of -12, -13, and –14 corresponding to these three resonances using equation 4.4 to relate the chemical shifts to the values of H_o. Only the resonance at 246 ppm is suggested to be superacidic and thus can be attributed to the fast toluene carbonylation reaction in these samples.

In the same table (Table 5.4) we report the resonances of the labeled acetone as a probe of the acidity in the IL's. Notice how the IL's not in contact with gaseous HCl show two resonances at 240 and 243 ppm downfield from TMS after correcting with the DMSO standard. When HCl gas was added at 44.7 psia and the samples were agitated, a

third peak was observed at 246 ppm (Table 5.5). This peak at 246 ppm disappeared when the sample was evacuated to a total pressure of 200 mT at 298 K for ½ h.

An estimate of the relative amounts of the species given rise to these three peaks can be had from a consideration of the relative peak areas of these the three peaks. For BMIM the relative fractions are 0.033/0.087/0.878 and for DoMIM the relative fractions are 0.013/0.051/0.936, for 246 ppm/243 ppm/240 ppm peaks.

Table 5.4. ^{13}C Chemical Shift of Acetone-2-^{13}C When Exposed to Different Acid Species.

Acid Media	Chemical Shifts (ppm) [10]
$CDCl_3$	205
Ze-HX	215
Ze-HY	220
HZSM-5	223
H_2SO_4-80%	235
H_2SO_4-100%	244
$AlCl_3$	245
SO_3/H_2SO_4	246
FSO_3H/SbF_5	249
SbF_5	250

Acid Media	Chemical Shifts (ppm)	$-H_o$[1]
CD_2Cl_2	205.89	0.54
80% (wt) H_2SO_4	228.23	7.91
100% H_2SO_4	243.41	12.91
Triflic acid	245.70	13.67
BMIM-Cl:$AlCl_3$ IL 1:2 Before HCl	240.28 243.10	11.88 12.81
BMIM-Cl:$AlCl_3$ IL 1:2 After HCl (30mins)	240.09 243.02 246.65	11.82 12.79 13.99
DoMIM-Cl:$AlCl_3$ IL 1:2 Before HCl	239.91 242.99	11.76 12.78
DoMIM-Cl:$AlCl_3$ IL 1:2 After HCl (30mins)	239.97 242.78 246.47	11.78 12.71 13.92
BMIM-Cl:$GaCl_3$ IL 1:2 Before HCl	236.04 208.33	10.49 1.35
BMIM-Cl:$GaCl_3$ IL 1:2 After HCl	245.85 208.41 204.33	13.72 1.37 0.03
BMIM-Cl:$InCl_3$ 1:1.07 IL Before HCl	211.61	2.43
BMIM-Cl:$InCl_3$ 1:1.07 IL After HCl	218.44	4.68

[1] Estimate of Hammett acidity function using reported value of chemical shift and fitting parameters for equation 4.4. The actual values of $-H_o$ for 100 wt% sulfuric acid and triflic acid should be 12 and 14, respectively.

Table 5.5. ^{13}C Chemical Shift of Acetone-2-^{13}C in BMIM-C:/$AlCl_3$ (1:2) before and after HCl addition.

Chemical Shift of Acetone-2-^{13}C in BMIM-C:/$AlCl_3$ (1:2)		
Peak identification	Before HCl	After HCl
Acetone	No peak	246.65
Acetone	243.10	243.02
Acetone	240.28	240.09
C-2	133.83	133.75
C-5	123.46	123.38
C-4	122.18	122.10
N-**C**H_2-CH_2-CH_2-CH_3	49.66	49.57
DMSO	40.96	40.96
N-**C**H_3	36.36	36.27
N-CH_2-**C**H_2-CH_2-CH_3	31.16	31.07
N-CH_2-CH_2-**C**H_2-CH_3	18.80	18.71
N-CH_2-CH_2-CH_2-**C**H_3	12.87	12.78

We predicted 3-sites for sequestering HCl by the IL, and this prediction was observed for chloroaluminate ionic liquids using the following organic cations BMIM-Cl and DoMIM–Cl (Figure 5.13) after HCl was added (resonances at 240, 243, and 246 ppm downfield). The Hammett acidity functions corresponding to these three resonances were -11.8, -12.8 and nearly -14. Of these three resonances, only the peak at 246 ppm can be considered as arising from a super acidic species since its corresponding Hammett acidity function is nearly –14. The predicted ^{1}H-NMR chemical shifts were 15, 14, and 3 ppm for the HCl sited in the three positions suggesting that one site would show very little acidity (3 ppm) and the other two sites should be much more acidic. The observed ^{13}C-NMR spectra of ^{13}C-enriched acetone suggests that the ^{13}C resonance at 246 ppm would be the most acidic site and might be implicated in the toluene carbonylation which requires super acidity since the literature data suggests that enriched ^{13}C acetone in contact with $AlCl_3$ shows a chemical shift of 246 ppm and it is a known conversion agent

for toluene carbonylation. We know that 100% sulfuric acid is not a conversion agent for arene carbonylation and its chemical shift (244 ppm) would seem to mark a lower limit on the acid strength needed to initiate the arene carbonylation reaction. Therefore, the peaks observed at chemical shifts of 244 ppm and lower may not be sufficiently acidic to cause rapid carbonylation of the arene.

To determine if this site having a resonance at 246 ppm is largely responsible for this catalysis, we estimated the fraction of the 246 ppm peak observed for the two IL's derived from $BMIM^+$ (0.0334) and $DoMIM^+$ (0.0133). The ratio of the 246 ppm peaks in $BMIM^+/DoMIM^+$ = 2.51 and the ratio for the observed reaction rate constants for $BMIM^+/DoMIM^+$ = 3.92 $kmin^{-1}$/1.35 $kmin^{-1}$ = 2.90. The change in the observed reaction rate constant is similar to the change in the fraction of the strong acidity that is probed by the labeled acetone as super acidity.

The IL composed of $BMIM^+/GaCl_3$ was also characterized using labeled acetone and it showed 1 strong peak in the ^{13}C-NMR spectrum of 236.04 ppm before HCl was added and a strong peak having a chemical shift of 245.85 ppm after HCl was added. The chemical shift of 245.85 ppm is higher than that observed for 100 wt% sulfuric acid and this increased acid strength may account for its activity towards the toluene carbonylation reaction (1.22 $kmin^{-1}$) but not as high as the reactivity observed for the IL derived from $AlCl_3$ (3.92 $kmin^{-1}$). The IL derived from $InCl_3$ having n = 1.07 was examined using labeled acetone. We did not attempt to characterize an In IL having n = 2 since it contained undissolved solids even at temperatures approaching the melting point of the cation. This In IL showed a single, strong resonance at 211.61 ppm before the HCl was added and a strong resonance at 218.44 ppm after the addition of HCl gas to

the IL at a pressure of 30 psig. Since no resonances greater than 244 ppm were observed in the In system, we take this result to mean that no super acidity was developed in this system sufficiently strong to initiate arene carbonylation even though the same IL could initiate Friedel-Crafts chemistry. In table 5.4, the reported chemical shifts for zeolites are between 215 – 223 ppm. The In system had a chemical shift of 218 ppm, which is similar to the reported for zeolites, which do initiate Friedel-Crafts reactions, but not carbonylation reactions. Thus, the acid strength indicated by the ^{13}C-NMR of labeled acetone appears to explain the modest acidity of the In IL to initiate Friedel-Crafts chemistry and also explains why this same IL cannot initiate the arene carbonylation reaction.

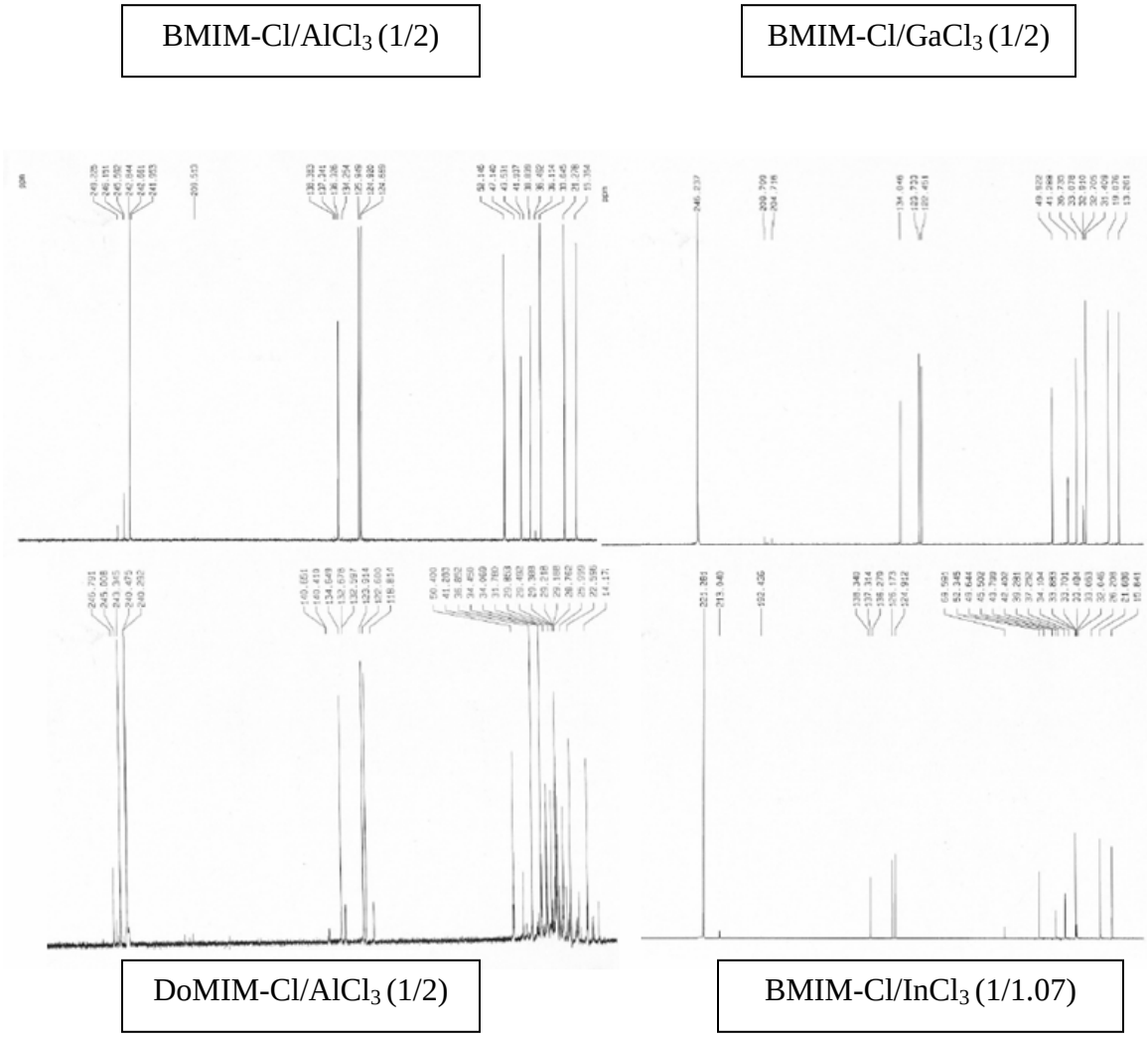

Figure 5.13. ^{13}C NMR to determine acid strength and HCl siting for different IL's (after HCl).

This probe of super acidity provided information about the 3 sites for HCl observed in Al, the different proportions of strong acid sites when R was changed and different acidity strength when the anion was changed Al, Ga and In. Data of rate constants divided by the mole fraction dimer (x_{102}) could be correlated with the Hammett acidity function, $-H_o$, for the $BMIM^+Cl^-$ chloroaluminates at two pressures of HCl (as prepared IL and 30 psig HCl added), the $DoMIM^+Cl^-$ chloroaluminate (30 psig HCl) and

for the $BMIM^+Cl^-$ galloaluminate (Figure 5.14). Data for x_{102} were taken from Table 5.1 for $BMIM^+$ and $DoMIM^+$. It was assumed that the mole fraction dimer for the galloaluminate was the same as that reported for the chloroaluminate.

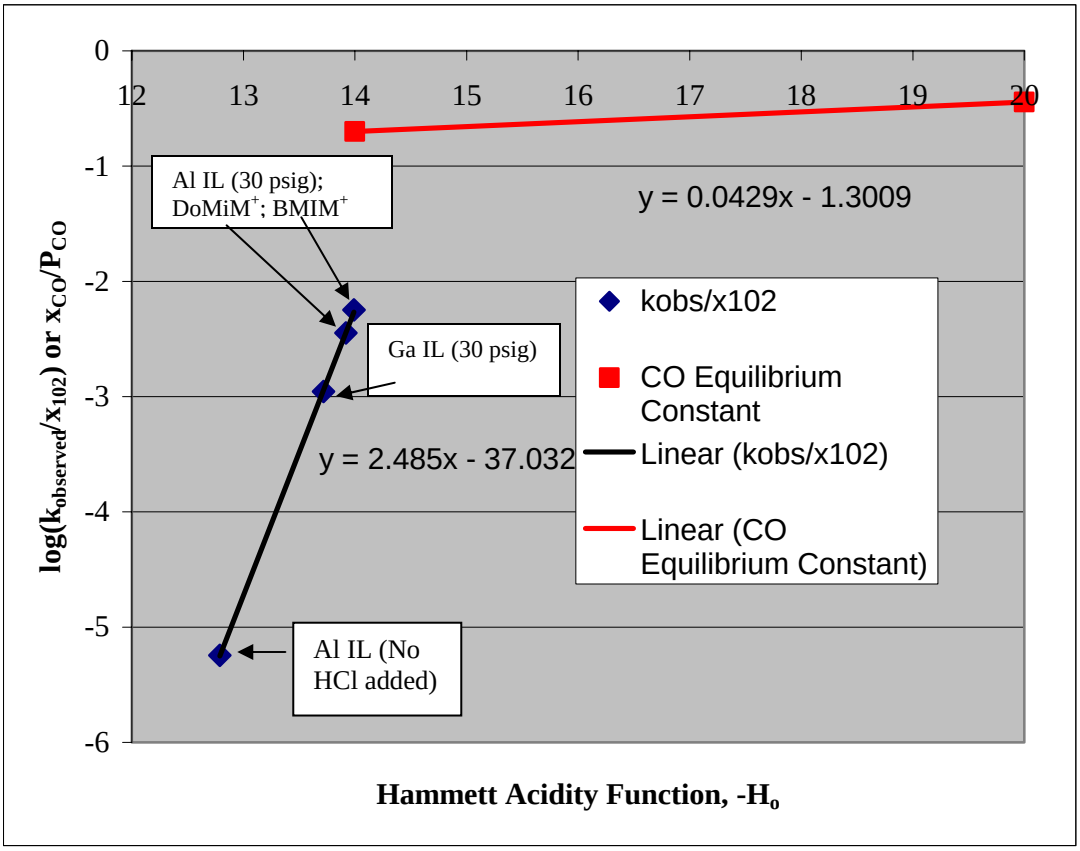

Figure 5.14. Correlation of Observed Rate Constant and Henry's Law Constant for CO Absorption *versus* $-H_o$.

It is remarkable that data from different metal anions could be correlated by a single equation (line) suggesting for these systems, that the strength of the acidic protons determines its reactivity for the arene carbonylation reaction when one accounts for the number of protons *via* the mole fraction of dimer in the IL (x_{102}).

5.3 Discussion

^{27}Al-NMR modeling was used to interpret the observed NMR spectrum of intrinsically neutral and acidic IL's. A successful interpretation of the observed data was possible when we included a new Al species in the acidic IL's: the anion pair, $[Cl_3Al\ AlCl_4]^-$. The existence of this species may have been predicted by Wilkes, *et al.*, as evidenced by the following statements in the discussion of this paper:

> "…If only the high-temperature results had been considered, the data could have been simulated more exactly by using a smaller chemical shift difference. This leads us to propose that a three-site or higher exchange mechanism occurs in the acidic melts at these temperatures…Perhaps a future ultrahigh-field NMR study of these melts will identify additional aluminum-containing species that will allow a more accurate simulation of the temperature dependent resonances."

Thus, we propose that the additional aluminum-containing species mentioned by Wilkes, *et al.*, could be the anion pair that we postulate here.

NMR simulations of the IL for proton and ^{13}C- resonances suggest that the three-site model we proposed to model HCl absorption in the IL (Chapter 3) leads to protons having different acid strengths while not really affecting the ^{13}C spectra. Moreover, the ^{1}H-NMR spectra of HCl protons residing at a particular site were not influenced by the R-group of cation. This prediction was confirmed by comparing the ^{13}C-NMR spectra of labeled acetone in contact with acidic, chloroaluminate melts containing either $BMIM^+$ or $DoMIM^+$ which showed that the chemical shifts of the most acidic sites were 246.65 and

246.47 ppm, respectively. The Hammett acidity functions for this site in each IL was super acidic: $-H_o$ = 13.99 and 13.92, respectively. We consider the difference in chemical shifts reported here to be insignificant thus suggesting that the acidity of the HCl protons in these sites are not different when R = $BMIM^+$ or $DoMIM^+$. Therefore, the variations in the chemical reactivity between these two IL's could not be attributed to differences in the Brønsted acidity, but rather to another factor. Further examination of the ^{27}Al-NMR showed that systematic changes in the aluminum speciation were observed when the R-group was varied on the cation. That is, the relative concentrations of the dimer $(Cl_3Al\text{-}Cl\text{-}AlCl_3)^-$ and the anion pair $(Cl_3Al\ AlCl_4)^-$ changed in a fashion that suggested that the dimer species was largely responsible for developing the strong Brønsted acidity upon admission of HCl to the system. Additional ^{27}Al-NMR spectra were recorded to document the effects upon the aluminum speciation when HCl was admitted and these data suggested that the dimer reacted with the HCl to give the following species: $[Cl_3AlCl\text{-}HCl\ AlCl_3]^-$. We can imagine a mechanism for HCl addition that appears as follows:

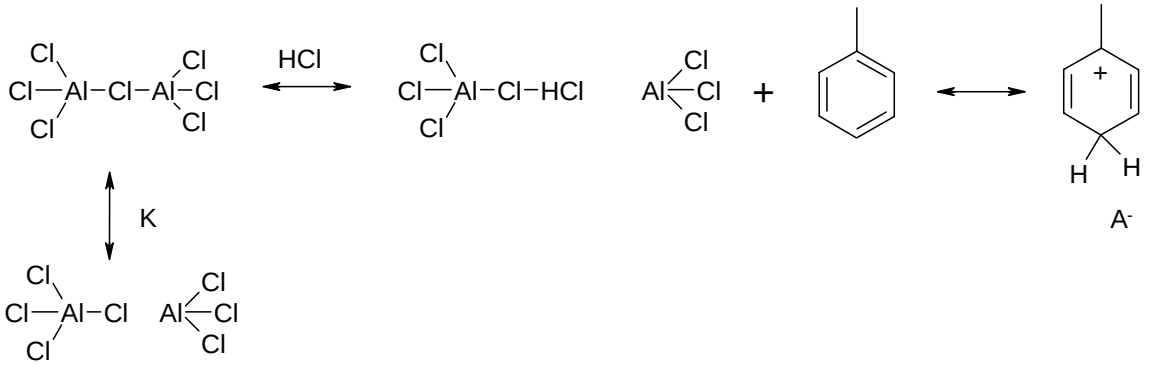

Here we show as A^- the anion after it has combined with the toluene to form the tolyl-carbocation. The stoichiometry of A^- is $O[Al_2Cl_8]^-$ where O is the organic cation, but we

don't know its structure. The equilibrium constant, K, describing the equilibrium between the dimer and anion, is regulated by the structure of the cation (*i. e.,* the R-group). The HCl responsible for the conversion is added to the dimer to form the anion pair HCl adduct. We speculate that it is this species that is responsible for initiating the reaction and for sequestering the aldehyde adduct *via* the $AlCl_3$ species in the anion pair. Without the $AlCl_3$ partner, we believe that 1) HCl cannot be accommodated as a super acidic species on the $AlCl_4^-$ and that 2) the aldehyde partner will not be stabilized as an Ar-CHO—adduct, thus there is no agent to lower the free energy of the final product. We offer as evidence to 1), no conversion is observed for the neutral IL even though it absorbed 50% HCl that the acidic IL, and as evidence to support 2) is the stoichiometric relationship that we observed between the overall conversion of toluene and the Al/substrate ratio, initially. Since the $AlCl_3$ partner to the pair is tied up with the product, the initiation species, $[Cl_3AlCl\text{-}HCl\ AlCl_3]^-$, cannot be regenerated and therefore the reaction stops after all of the dimeric species has been consumed. As the dimer is consumed, additional dimer can be formed from the anion pair, $(Cl_3Al\ AlCl_4)^-$, until it too becomes exhausted. The effect of changing the cation structure is to shift the equilibrium between the anion dimer and the anion pair prior to addition of HCl to the system. Upon adding HCl, we speculate that only the dimer reacts with the HCl to produce the super acidic Brønsted species to initiate the carbonylation reaction. Other acidic species were produced in the IL, but the data from the ^{13}C-NMR of the labeled acetone studies suggests that these species were not sufficiently acidic to initiate the carbonylation reaction.

In the scheme above, we show the super acidic Brønsted acid combining with toluene to form the carbocation, which then reacts with the CO to give the aldehyde. Without any loss of generality, we believe that the super acidic Brønsted acid could also combine with CO to give the formyl cation, which then continues to react by the electrophilic substitution mechanism that is so often connected with this reaction.

Changing the identity of the Lewis acid partner to the organic halide from Al, Ga, to In showed a profound effect upon the activity of the toluene carbonylation reaction that could be easily explained upon a consideration of the ^{13}C-NMR of the labeled acetone studies. Apparently, the strength of the super acidic protons developed upon addition of HCl to the IL was influenced by the strength of the Lewis acid partner. That is, the relative strength of the protons in the IL decreased according to the following: Al > Ga >> In so that the protons developed in the In Il were not sufficiently acidic to initiate the toluene carbonylation reaction.

The ^{1}H-NMR predictions (Table 4.4; structure 3.12-a) suggested that the Brønsted acidity of IL's systematically decreased for HCl that adds to the Lewis acid dimer $(M_2Cl_7)^-$ for the series Al, Ga, and In. These predictions would appear to explain well the trend in Hammett acidity that was revealed in the $BMIM^+/M_2Cl_7^-$ IL's:

$$-H_o \text{ of Al/Ga/In} = 13.99/13.72/4.68$$

The usefulness of the Hammett acidity function to correlate reactivity data was illustrated well by the results shown in Figure 5.14. Here, the observed rate constants ($k[Al_o][H^+][CO]$) divided by the mole fraction of the dimer (x_{102}) appears to increase

with increasing values of the Hammett acidity function for systems having different cation structures (R = n-butyl and n-dodecyl); different anions (M = Al or Ga); and for different partial pressures of HCl (200 mTorr and 30 psig). The modeling work suggested that HCl adds stoichiometrically to the Lewis acid dimer to form the Brønsted acid; therefore, the increasing values of the ordinate with increasing Hammett acidity function, suggests that $\ln\{k_{observed}/x_{102}\}$ is proportional to the Hammett acidity function:

$$\ln\{k[CO]\} = \alpha(-H_o) + \ln[\beta] \qquad (5.4)$$

but the Hammett acidity function is defined for the equilibrium $H^+ + B \Leftrightarrow HB^+$

$$H_0 = -\log_{10}\left[a_{H+}\left(\frac{\gamma_B}{\gamma_{BH+}}\right)\right] = -(2.303)\ln[a_{H^+}\gamma_B/\gamma_{BH^+}] \qquad (5.5)$$

We now interpret this correlated result with what is known about the solubility of CO in strong acids such as triflic acid and “Magic acid”. CO gas shows increasing solubility in strong acids with increasing values of the Hammett acidity function. Consider the data [12] of CO solubility in super acids (Table 5.6) where we have converted the original data to equilibrium absorption constants.

Table 5.6. Effect of Hammett Acidity Function on CO Solubility.

Acid	T, ^{o}C	P, CO atm	solubililty[2]	-H_o	$H = x_{CO}/P_{CO}$	log(H)
FSO_3H-SbF_5	20	1.23	90	20	0.360027	-0.44366
CF_3SO_3H	27	2.05	155	14	0.199141	-0.70008

These data were plotted on the same figure (Figure 5.14) as the reactivity of the arene carbonylation as a function of $-H_o$. Notice that the equilibrium absorption constant for CO in the strong acids increases with increasing acid strength but with a slope of 0.04 whereas the ratio of $k_{observed}/x_{102}$ increases with a much greater slope of ~2.49. If we assume that the CO solubility in the IL's responds with Hammett acidity function in a manner similar to the CO solubility in these super acids, then the trends in the reactivity data [$k_{observed}/x_{102}$] cannot be attributed solely to CO solubility effects. The observed rate constants reported here are the product of the aluminum concentration originally placed in the IL, [Al_o], the intrinsic rate constant, k, the super acidic proton concentration in the IL, [H^+], and the dissolved CO concentration in the IL, [CO]. Previous modeling efforts shown here suggest that the super acidic protons arise from the reaction of HCl with the anionic dimer so that an estimate of the [H^+] is the mole fraction of anionic dimer in the IL. We showed here that the mole fraction of dimer is a function of the cation structure by changes in the R-group. Thus, the ratio of the observed rate constant to the mole fraction of anionic dimer accounts for the effect of the R-group in the cation for the number of super acidic HCl protons that have been activated by the effect of the anionic dimer, [H^+] in the observed rate constant. Moreover, the moles of Lewis acid added to the original is the same in each IL as is the partial pressure of CO above the IL (150

[2] Solubility expressed in STP cm^3 CO absorbed in one liter of acid.

psig). Thus, the remaining factors that have not been accounted are the intrinsic rate constant, $k_{intrinsic}$, for protonation of the nucleophile (*i. e.*, CO) and the solubility of CO in the IL, HP_{CO}. For all tests, the partial pressure of CO remains the same, thus, the [CO] in the IL is proportional to the value of K_{CO}.

The slope of the reactivity data ($k_{observed}/x_{102}$) *versus* $-H_o$ (2.49) should be the sum of the slope in the order with respect to hydrogen ion activity added to the slope of the CO equilibrium constant as it varies with $-H_o$ (0.04). Thus, the order with respect to proton activity is ~2.45. This intrinsic rate constant represents the kinetic process for the protonation of the nucleophile (CO) to form the electrophile that then engages the arene in an electrophillic substitution reaction.

We expected that the physical property of CO solubility and the order of reaction for the proton activity should depend upon the Hammett acidity function, alone, when all other factors have been properly accounted for, such as cation structure and anion type, plus HCl partial pressure. This last result suggests that we have properly accounted for the structural and process parameters of the IL system used for arene formylation.

5.4 Summary

The results of quantum mechanical modeling methods suggested the existence of an aluminum-containing species having an unique structure not previously reported in the literature; however, the existence of an aluminum-containing species had been speculated by others [6]. The ^{27}Al-NMR data of the IL before and after addition of HCl could be explained by a scheme that included this extra aluminum-containing species which

apparently participates in an equilibrium with the anionic dimer $(Al_2Cl_7)^{-1}$ that has been reported in the literature. Only the anionic dimer was used in the reaction mechanism to initiate the carbonylation of toluene and to form an adduct with the product aldehyde thus lowering the free energy of the reaction so that high conversions can be realized. This equilibrium between the two dinuclear, aluminum-containing species was controlled by the structure of the organic cation as influenced by the length of the R-group ligand. The kinetically-controlled reactivity of this reaction apparently was related directly to the amount of the Brønsted super acid that was formed when HCl combines with the dimeric anion. The super acidity of the Brønsted species is the same when the Lewis acid is aluminum and for varying the R-group; however, IL's formed from $BMIM^+$ and MCl_3 show decreasing acid strengths as M is changed from Al to Ga to In, with the In IL being unreactive to arene carbonylation even though it shows activity towards some Friedel-Crafts alkylation reactions.

5.5 References

1. Fannin, A.A. Jr., King, L. A., Levisky, J.A., and Wilkes, J.S., Properties of 1,3,-Dialkylimidazolium Chloride-Aluminum Chloride Ionic Liquids. 1. Ion interactions by NMR", *J. Phys. Chem*. **1984**, 88, 2609-14.

2. Nara, S.J, Harjani, J.R. Salunkhe, M.M., "Friedel-Crafts Sulfonylation in 1-Butyl-3-methylimidazolium Chloroaluminate Ionic Liquids", *J. Org. Chem.*, **66**, 8616-8620 (2001).

3. Wilkes, J.S., Frye, J.S., and Reynolds, G.F., "^{27}Al and ^{13}C NMR Studies of Aluminum Chloride-Dialkylimidazolium Chloride Melts Salts", *Inorg. Chem*. (1983) 22, 3870-3872.

4. Wilkes, J.S., Hussey, C.L., and Sanders, J.R., "NMR Chemical Shift Studies of Ion Association in Aluminum Halide-Organic Halide Melts", *Polyhedron* Vol. 5, No. 10, pp. 1567-1571 (1986).

5. Carper, W.R., Pflug, J.L., Elias, A.M., Wilkes, J.S., "^{13}C NMR and Viscosity Studies of Ionic Structure in 1-Methyl-3-Ethylsimidazolium Chloride-$AlCl_3$ Melts", *J. Phys. Chem.*, (1992) 96, 3828-3833.

6. Gray, J.L., and Maciel, G.E., "Aluminum-27 Nuclear Magnetic Resonance Study of the Room-Temperature Melt $AlCl_3$/n-Butylpyridinium Chloride", *J. Am. Chem. Soc.*, 1981, 103, 7147-7151.

7. W. D. Chandler and K. E. Johnson, "Thermodynamic Calculations for Reactions Involving Hydrogen Halide Polymers, Ions, and Lewis Acid Adducts. 3. Systems Constituted from Al^{3+}, H^+ and Cl^-", *Inorg. Chem.* (1999), 38, 2050-6.

8. Angueira, E. J., and Mark G. White, "Ionic liquid structure effect upon reactivity of toluene carbonylation: 1. Organic cation structure," *J. Mol. Catal. A: Chemical*, 238 (2005) 163-174.

9. Ohlin, C. A., Dyson, P.J., and Laurenczy, G., “Carbon monoxide solubility in ionic liquids: determination, prediction and relevance to hydroformylation”, *ChemComm*., **2004**, 1070-1.

10. Wang, Z., Heising, J.M., and Clearfield, A., “Sulfonated Microporous Organic-Inorganic Hybrids as Strong Bronsted Acids”, *J. Am. Chem. Soc*. (2003), 125, 10375-10383.

11. Xu, T.; Munson, E. J.; Haw, J. F., “Toward a Systematic Chemistry of Organic Reactions in Zeolites: In Situ NMR Studies of Ketones”, *J. Am. Chem. Soc.* **1994**, *116*, 1962-1972.

CHAPTER VI

RESEARCH SUMMARY AND RECOMENDATIONS

The arene carbonylation reactions are important pathways to the synthesis of aryl aldehydes. Aldehydes are desirable as functional groups since they can be easily oxidized to acids, as in terephthalic acid. There is a continuing interest in the subject of arene carbonylation, especially in strong acids and environmentally benign alternatives are sought to HF/BF_3 and to $AlCl_3$ as conversion agents. Ionic liquids offer a powerful solvent for useful conversion agents such as aluminum chloride. The IL's permit $AlCl_3$ to be used at lower HCl partial pressures than with other solvents.

The Al^{3+} species in acidic chloroaluminate IL's interact with HCl gas to form protons and chloroaluminate species that can harbor the product aldehydes. The superior reactivity demonstrated by acidic, chloroaluminate IL's is probably due to their enhanced solvation power for HCl and CO.

Simple equilibrium thermodynamics were used to identify the species in the IL, super acidic Brønsted ($ClHAl_2Cl_7^-$) and Lewis acidic ($Al_2Cl_7^-$) chloroaluminate anions that are responsible for the observed ultimate conversion of toluene to tolualdehyde. Modeling of the IL by semi-empirical methods showed that HCl could be placed in 3 different places in the IL and that the free energies of formation for these three structures were different. These different energies of formation may suggest that the mole fractions of the HCl residing in these different sites will be different. The H-Cl bond lengths were predicted to be different for the HCl in the different structures and we expect that the

acidity of the HCl proton to depend upon the bond length with the most acidic proton residing in the HCl with the longest bond length.

^{27}Al NMR predictions helped us to have a better idea of the aluminum speciation in the ionic liquids and possible chemical environment. More specifically, the modeling studies suggested the existence of an aluminum-containing species having a unique structure not previously reported in the literature: the anion pair, $AlCl_3AlCl_4^-$, which appears to show ^{27}Al-NMR chemical shifts that are different from the dimer or the monomer. However, the existence of an aluminum-containing species had been speculated by others (Gray and Maciel).

The ^{27}Al-NMR data of the IL before and after addition of HCl could be explained by a scheme that included this extra aluminum-containing species, which apparently participates in equilibrium with the anionic dimer $(Al_2Cl_7)^{-1}$ that has been reported in the literature. Only the anionic dimer is used in the reaction mechanism to initiate the carbonylation of toluene and to form an adduct with the product aldehyde thus lowering the free energy of the reaction so that high conversions can be realized. This equilibrium between the two dimeric, aluminum-containing species is controlled by the structure of the organic cation as influenced by the length of the R-group ligand. The kinetically controlled reactivity of this reaction apparently is related directly to the amount of the Brønsted super acid that was formed when HCl combines with the dimeric anion. The super acidity of the Brønsted species is the same when the Lewis acid is aluminum and for varying the R-group; however, IL's formed from $BMIM^+$ and MCl_3 show decreasing acid strengths as M is changed from Al to Ga to In, with the In IL being unreactive to arene carbonylation even though it shows activity towards some Friedel-Crafts alkylation

reactions. Highest activity correlated with highest acidity of Lewis acid partner: Al > Ga >> In. Group V metal chlorides are inactive.

The length of the R-group in a family of organic cations apparently plays an important role in the chemistry of toluene carbonylation reaction. The activity for the toluene carbonylation reaction demonstrated a systematic decrease as the chain length in the cation was increased. The predicted free energy of HCl absorption into the IL's was remarkably close to the observed free energy of absorption when one considers the absorption of HCl as structures 3.12-b and 3.12-c. Moreover, the H-Cl bond lengths were predicted to be different for the HCl in the different structures. In this work we showed that the variation in the reactivity as R was changed could not be correlated to the total amount of HCl absorbed in the ionic liquid since all of the IL's showed similar absorption amounts for HCl. The amount of CO dissolved in the IL's was apparently below the detection limit of the apparatus used here.

We can imagine some further work in this field of reactive ionic liquids. Some of these recommendations for this further research are narrow in scope and reflect our experience in completing this work. Other recommendations are much larger in scope and may include topics of research that will be needed for a "breakthrough" in the technology.

The narrowly focused recommendations include:

1) The use of a NMR with higher frequency for the ^{27}Al NMR experiments. This will provide higher resolution spectra that may allow us to see the different Al species that we believe exist in this system.

2) Lower detection limit for the volumetric apparatus used in CO absorption studies. This will allow us to reproduce what other researches had observed, therefore obtain a CO solubility pattern for our different IL's once the cation and anion were varied.
3) Higher pressure of ^{13}CO absorption studies using NMR. In our studies we could see ^{13}CO absorbed in the different IL's.
4) Dryer reagents. Reagents that have been thoroughly dried may help us to obtain more accurate reactivity data, even when no HCl was added and may help us to obtain more accurate numbers in the HCl total absorption studies, due to the fact that moisture created *in situ* HCl.

The successful completion of these research topics will make more complete the study that we have described here.

Other research efforts will be necessary before the ideas shown here can be applied to form a viable, commercially feasible technology for making aldehydes from arenes. For example, the present ionic liquids cannot be reused after the reaction has gone to completion. We show here some convincing evidence to suggest that the aldehyde product has formed a strong interaction with some part of the ionic liquid, perhaps the aluminum anion. It appears fruitful to consider synthesizing an ionic liquid from another group III-A metal chloride for which the $M_2Cl_7^-$ anion is derived from a weaker Lewis acid. The choice of this metal chloride must represent a balance between the minimum acidity necessary to form the Brønsted super acid upon contact with HCl and the maximum Lewis acidity to form an adduct with the aldehyde which then can be liberated upon mild heating in a vacuum. Our work shows that the Bronsted acidity

developed from the family of Group IIIA metal chlorides, Al, Ga, and In, decrease in accordance with the intrinsic Lewis acidity of the metal chloride. Whereas, Al was too strong of a Lewis acid to release the aldehyde and In was too weak of a Lewis acid to form a strong Brønsted acid upon application HCl, it appears that Ga demonstrated to be a weaker super acid and a weaker Lewis acid than Al. Moreover, we showed that the Bronsted acidity and reactivity of IL's derived from $AlCl_3$ could be tuned by changing the R-group in the dialkylimidazolium cation. Therefore, one may optimize the apparent acidity of these IL's so as to obtain the high acidity required for the conversion of substrate but form an aldehyde-IL complex where separation of product from the IL can be achieved by heating in vacuum. One remaining study to explore these ideas could be the titration of IL's derived from $GaCl_3$/3-R-1-Me-imidazolium chloride with p-tolualdehyde to determine if heating the IL-adduct in vacuum can break the complex.